Proceedings of the First HKBU-CSD Postgraduate Research Symposium (PG Day)

Xiaolong Jin and Jianliang Xu (Eds.)

Technical Report COMP-05-002

Department of Computer Science
Hong Kong Baptist University

January, 2005

FOREWORD

In order to enhance the research atmosphere and share research ideas among the postgraduate students, the Department of Computer Science at Hong Kong Baptist University starts to hold the HKBU-CSD Postgraduate Research Symposium (PG Day) from Spring 2005. The PG Day will be held biannually in the months of January and July each year.

Each postgraduate student (either MPhil or PhD) of the Department is mandatory to have a presentation on his/her research progress during the semester at the PG Day. Each presentation will be given 30 minutes including a question and answer session. The presentation of each student will be evaluated by his/her thesis committee. Each postgraduate student is also required to submit an extended abstract on his/her research progress, which is to be archived through a departmental technical report. A postgraduate student is required to attend all the postgraduate presentations. The faculty members in the Department will also attend the sessions relevant to their research areas.

The first PG Day was held on January 10, 2005. It received a total of 16 submissions from our PhD and MPhil students. The program of the first PG Day contains five sessions of presentations. It covers the following research topics:

- Autonomous Agents and Multi-Agent Systems
- Information Systems
- Knowledge Grids
- Machine Learning
- Mobile Positioning Systems
- Networking and Communication
- Pattern Recognition
- Sensor Data Management
- Wavelet and Its Applications
- Web Intelligence

The proceedings of the first PG Day will be published as a departmental technical report numbered COMP-05-002.

The successful organization of the first PG Day would not be possible without the help from many individuals and organizations. We would like to thank our Head, Prof. Jiming Liu, who proposed the idea of the PG Day and provided with us continuous support. We give our gratitude to the PG Coordinator, Dr. Yiu-Ming Cheung, also for his support. Special thanks go to the organizing committee members (Xiaolong Jin, Jian Huang, and Chung Kei Yeung). We would also like to thank our departmental secretaries (Claudia Chui and Sandy Lor) as well as our departmental technicians (Leah Poon, S. Y. Leung, K. M. So, Johnson Chow, L. L. Kwok, Tan Wong, and M. W. Yam) for their logistic and technical support. Thanks also to Mr. Ho Fai Wong, who made and maintained a wonderful homepage for the PG Day.

January 2005

Xiaolong Jin
Jianliang Xu

PG DAY PROGRAM

January 10 Monday, 2005		
Time	**Sessions**	
09:30-09:40	**Welcome** Prof. Jiming Liu, Head of Computer Science Department (LMC 514)	
09:40-09:50	**Opening Address** Prof. Rick W. K. Wong, Dean of Science (LMC 514)	
09:50-10:00	**Break**	
Venue	LMC 514	LMC 512
10:00-11:30	Session A1: (Chair: Kam Chau Chan) ***Agent and Machine Learning***	
	■ *Toward A Community of Machine Learners Through Learning Online Communities of Practice* Zhili Wu ■ *Towards Characterizing Complex Behavior in a Self-Organizing Multi-Agent System* Bingcheng Hu ■ *How to Win the Multi-Agent Competition in a Dynamic Environment with the Minority Game Strategies?* Tingting Wang	
11:30-11:45	Break	
11:45-13:15	Session A2: (Chair: Zhili Wu) ***Web Intelligence and Data Mining***	
	■ *Watermarking 3D Mesh Models for Authentication* Haotian Wu ■ *Towards Solving Large-scale POMDP Problems Using The Multi-Agent Approach* Xin Li ■ *Learning Global Models Based on Distributed Data Abstractions* Xiaofeng Zhang	
13:15-14:30	Lunch	
14:30-16:00	Session A3: (Chair: Man Kin Chu) ***Networking***	Session B3: (Chair: Bingcheng Hu) ***Pattern Recognition and Information Systems***
	■ *Data Dissemination in Wireless Sensor Networks* Minji Wu ■ *Upgrading Unicast All-Optical Networks for Multicast Communication* Kam Chau Chan ■ *Maintaining Temporal Consistency of Real Time Data in Broadcast Environments* Chui Ying Hui	■ *Worldviews Retrieval through Ontological Worldviews Model* Chung Kei Yeung ■ *Corner Detection for Object Recognition by Using Wavelet Transform* Lu Sun ■ *A Novel Algorithm for Improving the Generalization Capability of Kernel-based LDA Methods* Jian Huang ■ *Handwriting-based Writer Identification* Zhenyu He
16:00-16:20	Break	
16:20-17:50	Session A4: (Chair: Chui Ying Hui) ***Mobile Positioning Systems***	
	■ *A New Approach for Locating Mobile Stations under the Statistical Directional Propagation Model* Man Kin Chu ■ *Wireless LAN Positioning with Mobile Devices in a Library Environment* Hak Lim Wong ■ *Locating Mobile Station with Ellipse Propagation Model Based on the GSM Networks* Junyang Zhou	

LIST OF PARTICIPANTS

Student Name	Degree	Year	Supervisor Co-Supervisor	Research Committee Members
Kam Chau Chan	PhD	3	Yiu-Wing Leung Chok-Man Lam	Kee-Yin Ng Kwok-Wai Cheung
Jian Huang	PhD	3	Pong-Chi Yuen Yuan-Yan Tang	Chun Hung Li Jiming Liu
Lu Sun	PhD	2	Yuan-Yan Tang Pong-Chi Yuen	Chun Hung Li Jianliang Xu
Zhenyu He	PhD	2	Yuan-Yan Tang Jianliang Xu	Chok-Man Lam Bin Fang
Junyang Zhou	PhD	2	Kee-Yin Ng Jianliang Xu	Chun-Hung Li Jiming Liu
Xiaofeng Zhang	PhD	2	Kwok Wai Cheung Jiming Liu	Yiu-Ming Cheung Chun-Hung Li
Xin Li	PhD	1	Kwok-Wai Cheung Jiming Liu	Yiu-Ming Cheung Chun-Hung Li
Haotian Wu	PhD	1	Yiu-Ming Cheung Jiming Liu	Chun-Hung Li Jianliang Xu
Zhili Wu	PhD	1	Chun-Hung Li Jiming Liu	Kwok-Wai Cheung Yuan-Yan Tang
Man Kin Chu	MPhil	2	Kee-Yin Ng Chun-Hung Li	Jiming Liu Karl Leung
Hak Lim Wong	MPhil	2	Kee-Yin Ng Chun-Hung Li	Jiming Liu Karl Leung
Tingting Wang	MPhil	2	Jiming Liu Yuan-Yan Tang	Kwok-Wai Cheung Chun-Hung Li
Bingcheng Hu	MPhil	2	Jiming Liu Yuan-Yan Tang	Kwok-Wai Cheung Chun-Hung Li
Chung Kei Yeung	MPhil	2	Lai-Chung Chan Kwok-Wai Cheung	Kwok-Wai Cheung Chi-Kuen Wong
Minji Wu	MPhil	1	Jianliang Xu Xiaowen Chu	Jiming Liu Kee-Yin Ng
Chiu Ying Hui	MPhil	1	Kee-Yin Ng Jianliang Xu	Kwok-Wai Cheung Chun-Hung Li

TABLE OF CONTENTS

Session A4: Mobile Positioning Systems

Towards Characterizing Complex Behavior in a Self-Organizing Multi-Agent System

Bingcheng Hu

Abstract

In this paper, we show our current work on our Non Self Organizing Multi Agent System (NonSOMAS) and Self Organizing Multi Agent System (SOMAS). Through experiments and analysis, we investigate how Self-Organized Criticality (SOC) phenomena arise in SOMAS rather than in NonSOMAS. Furthermore, we compare the order of agent performance in the two systems and explain its implications.

1 Introduction

In the past year, we have carried out some research on the relationship between agent's local behavior and global characteristics of a multi-agent RoboNBA system [3] [4]. We have obtained some interesting results, however, our previous work did not include one thing: our research findings should be directly generalized to wider domains rather than RoboNBA and RoboCup [2]. Therefore, we plan to adopt new simulation models, which can be generalized to other research areas more easily. Specifically, we will address the problem of how to induce and explain the complex behavior in an MAS simulation model.

With the proposed simulation models, we will investigate the following problems in the paper:

- Under what conditions will an MAS exhibit SOC phenomena?
- How to evaluate the order of an MAS? Is it consistent with the properties of self organization process?

2 Experiments

In order to study the problems mentioned in Section 1, we have designed three sets of experiments and their associated measurements.

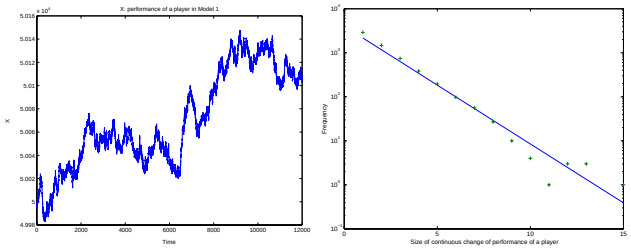

(a) Dynamics of performance of a player in NonSOMAS (x axis: performance, y axis: time).

(b) Distribution of performance avalanche (x axis: size of performance avalanche, y axis: frequency): an exponential distribution.

Figure 1. Experiment 1: Dynamics and some regularities of player performance in NonSOMAS.

2.1 Experiment 1

This experiment is carried out to examine the dynamics generated by NonSOMAS. Figure 1 is a typical output for intensive experiments. Figure 1 (a) illustrates the performance of the player as a function of time. From Figure 1 (b), we can see that the performance avalanche follows an exponential distribution, which indicates that a random variable is dominating the dynamics. Let the fixed probability for an increase in performance be p and then the probability for a corresponding decrease will be $1-p$. So the probability for a n step continuous increase or decrease will be $(1-p)p^n$ or $p(1-p)^n$, respectively, given changes are independent of one another. Note we use 5000 for the initial value of α and it is compared with $rand(10000)$. Therefore, the probabilities to increase or decrease the performance are equally 0.5 and the probabilities for a n step increase or decrease are 0.5^{n+1}. Consequently, the performance avalanche follows an exponential distribution if the random variable dominates the dynamics and proper initial values are used.

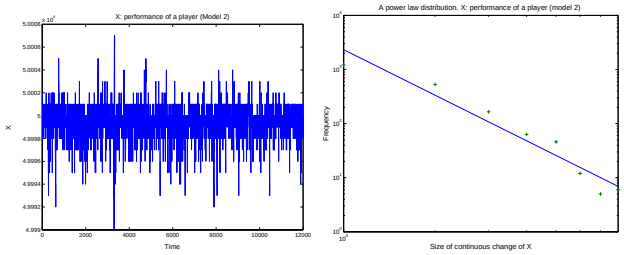

(a) Dynamics of performance of a player in SOMAS (x axis: performance, y axis: time).

(b) Distribution of performance avalanche (x axis: size of performance avalanche, y axis: frequency): a power law distribution.

Figure 2. Experiment 1: Dynamics and some regularities of player performance in SOMAS.

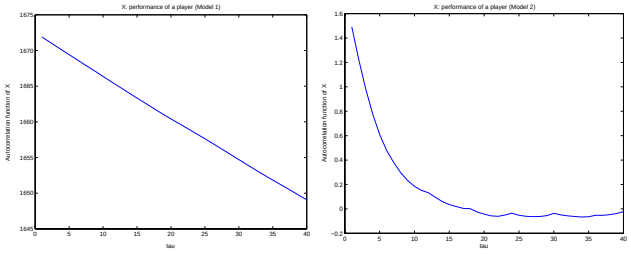

(a) Autocorrelation as a function of τ on performance of a player in NonSOMAS (x axis: τ, y axis: autocorrelation function).

(b) Autocorrelation as a function of τ on performance of a player in SOMAS (x axis: τ, y axis: autocorrelation function).

Figure 3. Comparison on the speed of autocorrelation function decay for player performance as τ increases.

2.2 Experiment 2

This experiment is carried out based on SOMAS. Through comparison on Experiment 1 and Experiment 2, we try to have some basic understanding on the Self Organized Criticality phenomena appearing in SOMAS.

Figure 2 is a typical output for intensive experiments. Figure 2 (a) illustrates the performance of a player as a function of time. From Figure 2 (b), we can see that the performance avalanche follows a power law distribution, which is significantly different from the exponential distribution we observed in Experiment 1. This result is quite robust since it appears under different conditions. For example, we use a wide range of k values in $Y(x, y)$ function, and the power law distribution is still there. We are quite confident at the moment the dynamics is not dominated by a random variable otherwise an exponential distribution will appear. What are the underlying mechanisms that generate this power law distribution? We would like to refer to SOC proposed by Bak [1] to explain the underlying mechanisms: under particular conditions, the system organizes by driving itself slowly and eventually it comes to a critical point, where it exhibits complex behavior, such as power law distribution (scale free in space). However, Bak did not point out specific conditions under which SOC would appear.

For our general competitive multi agent model, SOMAS, we consider the SOC phenomena appearing in it is due to the following reasons:

1. Critical interactions between players are important. In NonSOMAS, there is no critical interaction between players and their behavior is relatively ordered and predictable. On the other hand, in SOMAS, there are a total of ten players interacting together. Thus player behavior is relatively harder to predict and thus less ordered. From Figure 3, we can observe the remarkable difference between the order of player performance in the two models. From Figure 3 (a), we can see that the autocorrelation function value is decreasing quite slowly for NonSOMAS. However, in Figure 3 (b), there is an exponential decay as τ increases, which indicates lower order and predictability for player performance in SOMAS.

2. A higher level organization, team morale (M) in SOMAS, is essential. Due to the existence of team morale and its collective interactions with player performances through functions G, O, and P, we have a collective design of the model rather than more traditional ones, such as top-down or bottom-up design. Thanks to this collective design and backward causation embedded inside it, complex behavior of the model becomes possible [6][7]. Figure 4 illustrates a typical dynamics for team morale. From Figure 4 (b), interestingly, we can observe a power law distribution on the team morale avalanche. Furthermore, we can observe a slow decay in Figure 4 (c).

In summary, we can observe SOC phenomena in both low-level (performance) and high-level (team morale) aggregation in SOMAS. Furthermore, thanks to the collective design, the SOC phenomena exhibit by decreasing the order on the lower-level aggregation and preserving relatively high order on the higher-level aggregation in the model. This result is consistent with the properties of self-organization process [5].

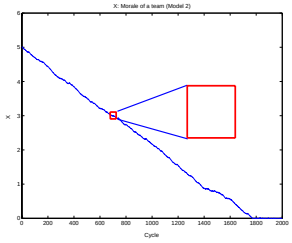

(a) Dynamics of morale of a team (x axis: morale, x unit is 0.005, y axis: attack cycle). The red rectangle is enlarged in Figure 4 (b)

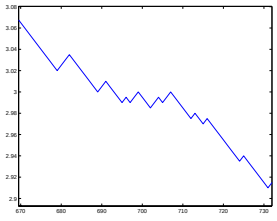

(b) A sub plot of Figure 4 (a) (x axis: morale [670-730], y axis: attack cycle [2.90-3.08]).

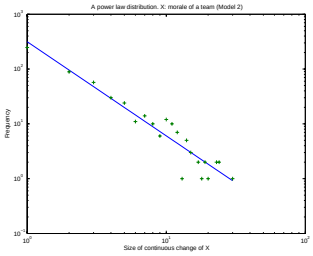

(c) Distribution of morale avalanche of a team (x axis: size of morale avalanche, y axis: frequency): a power law distribution.

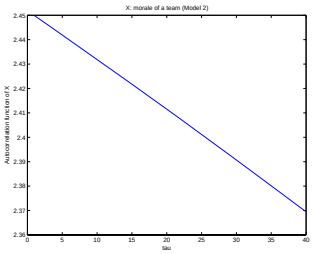

(d) Autocorrelation as a function of τ on team morale in SOMAS. (x axis: τ, y axis: autocorrelation function)

Figure 4. Experiment 2: Dynamics and some regularities of morale of a team in SOMAS.

3 Conclusions

In this paper, we illustrated two multi agent systems, NonSOMAS and SOMAS, which aim at modeling competitive scenarios of MAS. Based on the two models, we carried out three experiments. Comparing and analyzing the experimental results, we had some basic understanding on the Self-Organized Criticality phenomena that occurred in SOMAS. We discovered that the avalanche of player performance and team morale followed a power law distribution.

References

[1] P. Bak. *How Nature Works*. Springer-Verlag, 1996.

[2] M. Chen, K. Dorer, E. Foroughi, F. Heintz, Z. X. Huang, S. Kapetanakis, K. Kostiadis, J. Kummeneje, J. Murray, I. Noda, O. Obst, P. Riley, T. Steffens, Y. Wang, and X. Yin. *RoboCup server manual*. RoboCup Federation, February 2003.

[3] B. Hu, J. Liu, and X. Jin. From local behaviors to global performance in a multi-agent robonba system. In *IEEE/WIC/ACM Intelligent Agent Technology (IAT'04)*, pages 309–314, Beijing, 2004.

[4] B. Hu, J. Liu, and X. Jin. Multi-agent robonba simulation: From local behaviors to global characteristics. *Special Issue: Agent-Directed Simulation of the Simulation: Transactions of the Society for Modeling and Simulation International, to appear*, 2005.

[5] H. Parunak and S. Brueckner. Entropy and self-organization in multi-agent systems. In *International Conference on Autonomous Agents*, 2001.

[6] H. Parunak, S. Brueckner, M. Fleischer, and J. Odell. Co-x: Defining what agents do together. Workshop on Team and Coalition Formation, AAMAS'02, Bologna, Italy.

[7] R. Sawyer. Simulating emergence and downward causation in small groups. In: S. Moss and P. Davidsson (Eds.) Multi-Agent-based Simulation. Second International Workshop, MABS, 2000.

Towards A Community of Machine Learners Through Learning Online Communities of Practice

Zhili Wu

Abstract

Tasks in the context of learning interaction networks, like the study of information dynamics of the WWW, Email communication and online communities, or the study of how to improve them, pose challenges to machine learning. To handle such tasks, we intend to propose a community of machine learners (CoL), which is an ensemble of machine learners interconnected through proper interactions. Our research is conducted with two reciprocal modes: 1) Proposing machine learning models to online communities, to get better insights from the collective practices of community participants; 2) Through the learning of community effects as in 1), to propose a community of machine learners, which by interconnecting machine learners through a much social way, can then be used to fulfill the tasks that originate from relational and interactive networks. And we conducted preparatory studies on data gathered from Chinese Bulletin Board Systems and an online algorithm competition platform, to show the feasibility of further exploring the topics of learning community data and constructing a community of machine learners.

1 Introduction

With the assumption that artificial intelligence is indeed intelligent, that is, (an instance of) an algorithm can be taken as a learner not always dully controlled by, but compatible with human learners, the development of machine learning can then be traced back to the process of mimicking human learning. For example, the pattern recognition of human, such as the prediction based on none or several known samples, has been modelled into supervised learning, unsupervised learning and their hybrid [9] in machine learning, with the simplification that the inputs perceived by machine learners are often represented in a vector (and quantifiable) form. However, learning tasks in the context of interaction networks, like the study of information dynamics of the WWW, Email communication, virtual communities and the issues of how to improve them, pose challenges to conventional machine learning algorithms that are originally proposed to deal with simplified pattern recognition tasks with inputs constructed as (numerical) vectors. To comply such tasks usually arising from collective and interactive actions of human beings, it is essential to pay enough attentions to the interactive relations of tasks, and to build machine learners modelling the interactions. Moreover, such tasks again provide machine learning with imitable learning instances, and thus leave the discussion on constructing a network or community of machine learners open.

However, human learning in a social or interactive setting, though seeming to be useful and effective, has many underlying principles unknown, and migrating machine learners to be social is even more difficult. To name a few, some difficulties and challenges lie in: 1) the dynamics of social learning, with many factors on which unknown, is it feasible to build a society/community of machine learners by simply mimicking the still perplexing social ecology? Would it be more realistic to just focus on understanding and improving the current social learning? 2) the sociability of machine learners. It is still in doubt that social concepts, particularly the concept of community, can be applied to the machine learning domain which is not made of organisms, but solely mechanical components; 3) the relevance to computer science, that is to ask whether it is too early for computer science research to enter the field originally managed by social scientists, though with different perspectives and objectives. 4) the usefulness of such a socialized machine learners. Is it possible to compete or outperform a single learner constructed from the whole dataset, or an ensemble of learners by Bagging or Boosting, or other types of distributed learning?

This paper will first give some justifications on above difficulities, and discuss how we plan to avoid them with carefully selected approaches. This paper then briefly summaries some preparatory works on constructing a community of learners. The research is conducted with two reciprocal modes: 1) We analyze some characteristics of Chinese Bulletin Board Systems participated by university students. We show they comply observations and conclusions in common topology studies, like the ubiquitous power law

distribution. And we intend to capture the process of reputation formation and show that a combined learning approach demonstrates improved accuracies in separating different classes of posts in the BBS community. 2) We then discuss a case study on the phenomena of gathering community efforts to solve Matlab competition tasks.

2 Justification

2.1 Community and Community of Practice: Going Virtual

Among many social concepts related to human interactions, like network, committee, pool, ensemble and community, we are particularly interested in community, and more specifically, the online community which is supported by computer-mediated communication (CMC) of participants in the Internet. Nevertheless, we admit there are no serious gap among them before we have defined them in an exact way, which, however, is less possible because some of them are actually overlapped and contained by others.

It is still essential to make the concept of community as clear as possible, as in this research we will refer to community as an a definition applicable to both human learners and machine learners, under the assumption that machine learners, as instantiated from machine learning algorithms, are actually compatible with human learners, which by design are capable of interacting with a pool of others, and eventually contributing to forming a community.

It has been persistently argued that human beings learn in a social way, with interaction being an important factor. And a consequence of which is the formation of communities [16], and networks. Early researches have even shown many types of them are formed for very specific functions, or for the scenarios of situated learning with a co-located setting, which derives the concept of community of practice (COP) [8], or other counterparts like community of circumstance, interest, position and purpose.

However, community learning has gradually changed as the Internet becomes pervasive, since communication through which becomes convenient and information through which is accumulated rapidly [14]. Nowadays actions of human, through computer-mediated communication (CMC) empowered by the Internet, using less identifiable avatars or online IDs, make the communities more and more global, large in information throughput, heterogenous in members, complicated in purpose, and overall, versatile in functions.

Though there is defense that very specific and tightly interacted communities like traditional COP can not be clearly identified in the distractive cyber-space [15, 18], warm discussion on general virtual communities and new proposals on loosely combined online communities of practice can been easily seen [4]. It actually has been believed some principles and philosophy for COP are still valid but more should be discovered to reveal their ever-evolving dynamics arising from the rapid growth of technology and the amount of participation [20]. Such natures have also made improvement to them be of great utilization meanings at the application level [23, 2]. While the large amount of data generated within and between communities, has also enabled the analyses more qualitative, systematic and statistically convincing.

2.2 Relevance to Computer Science

By designing, our study is expected to be relevant and can contribute to the Computer Science.

For the learning of community data we focus on at the first stage of our research, it is to apply machine learning methods and tools to modelling community practices of participants, and it has two folds of significance: One, it can help us further understand the dynamics of the communities, particularly some social factors like fitness, trust within the virtual communities supported by real persons behind. Second, through computerized processing and analysis on community data, we can provide solutions to upgrading or improving the communities, so as to enhance participants' using experiences and facilitate their interactions.

For the construction of a community of machine learners, we believe that it will also have positive meanings for Computer Science, particularly for the field of ML, or AI. The field of machine learning has achieved great advancement from the analogy and imitation to human learning. This encourages us to stick with the strategy of conceptualizing the human interactions and then implementing them into a machine learning based framework. Since over the continuing course that human learning is going online and virtual, the machine learning methods have proved to be useful for understanding and improving the ongoing transformation of human learning, together with the factor that combining learners have been reported to be able to outperform a single learner, we thus feel the effort to construct such a community of learners is worthwhile.

2.3 Related Study and Uniqueness

For literatures on constructing a generative community of machine learners, few can be reported. This, of course, remains to us the issue of defending whether it is a feasible topic at all.

However, some related works can still be reviewed [1]. For the COP, and Virtual COP, as the concrete social objects we

[1] Please refer to http://www.comp.hkbu.edu.hk/∼vincent cop for more links to related references

want to depend on, there is a very long and diversified history of research on it. Many of them are seen to be quantitative and have captured some essences of online communities. Moreover, since the COP study has been drawn tight relations with other types of social learning research like the E-commerce on the WWW, Email, file sharing and instant messaging networks, and even more general topology studies widely dealt with, it makes us confident that the existing and future research outcomes can help us obtaining in-depth insight into the collective involvement of community participants. As for more thorough analysis, we focus on monitoring, gathering, processing data of online communities existing in Chinese society. And we also emphasize the approach of relying on machine learning methods to learn community data.

The issue that a combination of learners can outperform a single learner has often been discussed, especially for tasks with large scale data, or the case that the single machine learning algorithm does not fit for the task well either due to its weakness or bad parameter tuning. The usual techniques are ensemble including boosting [17], bagging [6] and bite [5], distributed learning [13, 19, 12, 7], and even distributed artificial intelligence like Distributed Problem Solving (DPS) and Multiagent Systems (MAS) [3, 22]. However, the characteristics of our approach are interactively combining algorithms, through the analogy of the communications in a real community, and secondly, we intend to focus on the combination of machine learners that are usually systematically devised for solving concrete learning tasks, and finally, our research concentrates on the tasks arising from data gathered from online communities that have less been handled by nowadays machine learning and data mining.

3 Preparatory Experimental Studies

3.1 Machine Learning on Virtual Community of Practice

We performed analyses on data gathered from the Zhongshan University BBS (ZSU-BBS) and the mainland China student BBS at HKBU (ISM-BBS). The ZSU-BBS is one of the most actively participated university BBSs in the Southern China. Because it is supported by a system which has been generally adopted in China's universities and colleges, and it also implements the exchange channel for communicating with other BBSs, it becomes one of our startup but expandable choices for studying the phenomena and effect of online communities. The ISM-BBS is used for other considerations: though it does not support a forwarding schema seamlessly communicating with other BBSs, and it just have board settings limitedly compatible with others, and is rather small in terms of the total participants and the daily posts, it is a BBS that the author is familiar with. By knowing its historical development and the offline interactions of its participants, the analysis of communities mapped to real persons and viewed from a long period can be conducted.

Some simple statistics on gathered data clearly indicate a BBS has small world properties, and demonstrates some observations on power-law distribution [21] commonly reported in some network studies. For example, as rules of thumb, 20% high frequency Chinese words weigh 80% of the total word count, and highly productive authors contribute 80% of the total posts. But same as the exclusion of stop words in obtaining a more meaningful word count, authors highly productive or active might not deserve their ranks that are solely based on simple counts of posts, residual time or page clicks, we hereby suggest synthesizing post content quantified by the bag of Chinese words, and the post's popularity measured by the number of follow-up posts to get a more realistic user (and/or post) ranking, based on a matrix decomposition method similar to the PageRank approach which is originally devised for ranking webpages in the Internet. This approach is consistent with the intuitive fact that really influential authors win their reputation through high-quality posts that are also interesting to other influential authors, and could be extended to providing a prior or afterward evaluation for combining a set of machine learners at the second stage of our study on constructing the community of machine learners.

Another aspect of learning on community data so far considered is to find the classes and clusters within or between communities. An experimental study we have done is to classify posts into two types to reveal their separation of being from two different boards. The formulation is simple, but induces many consequent utilizations and further motivations. For communities of any type, either be real persons or their pseudo-images or purely artificial machine learners, the task of finding groups from them has multiple folds of significance. For the special object to be classified (here the BBS data), its unique characteristic is its networked topologies, which has not been paid enough attention to. We hereby propose a simple combination strategy for data construction and learning ensemble, we show including topological and interaction relations to data representations and learning algorithms improves the classification accuracy, which either show topological data needs well designed learning algorithms to boost the performance on them, and conversely, it tells that topology itself subsumes information, if mined properly, proves to be useful, which indirectly hints that the feasibility of combining learners through a interactively growing community.

3.2 A Case Study of Problem Solving Through Community Effort

To have some understanding into collective works accomplished in real communities, we choose the MATLAB programming contest as a case study of the power of aggregating learners in a social way.

The MATLAB is an excellent platform for scientific computing, simulation and algorithm prototyping. Besides, it has a contest event [11, 10] hold twice per year, with a (usual combinatorial) problem given each time. Through an online interface, participants are encouraged to submit their own algorithms, or conduct tweak on existing submissions contributed by others. Measured by the performance determined by the degree of solving the task and the time consumed, the one making the largest leap or the most accumulated improvement, or achieving the best final score are appraised. Participants usually utilize hybrid competition strategies, like insolatedly developing own algorithms, actively tweaking top ranked solutions and getting help by posing questions to other submitters. This contest has been drawn relations with open source software development, and the Wikipedia [1], and even been seen to share some characteristics with Distributed Problem Solving(DPS).

We compile part of successful submissions in two such contests, the Gerrymandering and furniture contests [2]. By constructing the network of submission relations based on explicit reference and implicit measure of code similarity, plus the inferred community of submitters who are mutually impacted, we can verify the pattern of innovation as discussed in [10] is a zig-zag way, while the collective power of the community can also be clearly noticed though several top users contribute a lot, and the evolution path of the learning algorithms also presents some simple patterns similar to the ensemble and combination of machine learners differentiated by roles. It thus hints us the effort of combining learning algorithms into a community form is worth being further explored.

4. Conclusion

This extended abstract mainly discusses the motivation to the topic of constructing a community of machine learners, and provides some literature reviews and justification, as well as some startup experimental studies.

For this study still at its early stage, we have only pinpointed the general issues of learning the data with the involvement of human interactions, and proposed a rather general objective of constructing machine learners based on learning and mimicking the online communities of real persons, and been collecting and processing community data, as well as experimentally testing them. Results currently obtained verified that online communities, though overloaded by information and less organized, are learnable, subsume collective power, and call for further understanding and improvement to them.

And the presentation accompanied with the extended abstract will demonstrate in more detail the experimental results on learning BBS data and analyzing the open and online MATLAB programming arena, together with the introduction to more related studies, difficulties and further issues.

[2] http://www.mathworks.com/contest/furniture/home.html

References

[1] Wikipedia. http://wikipedia.org/.

[2] U. D. A. Stephanie and E. Stephen. Virtual communities of practice as learning networks. In *BYU Research Report*, 2003.

[3] A. H. Bond and L. Gasser. An analysis of problems and research in dai. *Readings in Distributed Artificial Intelligence*, pages 3–35, 1988.

[4] P. H. C. Kimble. Communities of practice: Going virtual. In *Knowledge Management and Business Model Innovation*, 2001.

[5] N. V. Chawla, L. O. Hall, K. W. Bowyer, and W. P. Kegelmeyer. Learning ensembles from bites: A scalable and accurate approach. *J. Mach. Learn. Res.*, 5:421–451, 2004.

[6] N. V. Chawla, T. E. Moore, L. O. Hall, K. W. Bowyer, W. P. Kegelmeyer, and C. Springer. Distributed learning with bagging-like performance. *Pattern Recogn. Lett.*, 24(1-3):455–471, 2003.

[7] B. Cox. Evolving a distributed learning community. http://virtualschool.edu/cox/pub/EDLC.

[8] W. E. *Communities of Practice: Learning, Meaning, and Identity*. Cambridge University Press, 1998.

[9] A. Gammerman, V. Vovk, and V. Vapnik. Learning by transduction. In *Uncertainty in Artificial Intelligence*, pages 148–155, 1998.

[10] N. Gulley. Patterns of innovation: a web-based matlab programming contest. In *CHI '01: CHI '01 extended abstracts on Human factors in computing systems*, pages 337–338. ACM Press, 2001.

[11] N. Gulley. In praise of tweaking: a wiki-like programming contest. *interactions*, 11(3):18–23, 2004.

[12] L. Hall, K. Bowyer, W. Kegelmeyer, T. Moore, and C. Chao. Distributed learning on very large data sets, 2000.

[13] J. Hollan, E. Hutchins, and D. Kirsh. Distributed cognition: toward a new foundation for human-computer interaction research. *ACM Trans. Comput.-Hum. Interact.*, 7(2):174–196, 2000.

[14] A. Kavanaugh. The impact of the internet on community involvement: A network analysis approach. In *Telecommunications Policy Research Conference*, 1999.

[15] C. Kimble and P. Hildreth. Communities of practice: Going one step too far? In *Proceedings 9e colloque de l'AIM, Evry, France, May 2004*, 2004.

[16] J. Lave and W. E. *Situated Learning: Legitimate Peripheral Participation*. Cambridge University Press, 1991.

[17] A. Lazarevic and Z. Obradovic. Boosting algorithms for parallel and distributed learning. *Distrib. Parallel Databases*, 11(2):203–229, 2002.

[18] C. Lueg. Where is the action in virtual communities of practice? In *Proceedings of the workshop Communication and Cooperation in Knowledge Communities at the German Conference on Computer-Supported Cooperative Work (D-CSCW)*, 2000.

[19] S. McConnell and D. B. Skillicorn. Building predictors from vertically distributed data. In *CASCON '04: Proceedings of the 2004 conference of the Centre for Advanced Studies on Collaborative research*, pages 150–162. IBM Press, 2004.

[20] A. Pentland. Learning communities - understanding information flow in human networks. *BT Technology Journal*, 22(4):62–70, 2004.

[21] G. Siganos, M. Faloutsos, P. Faloutsos, and C. Faloutsos. Power laws and the as-level internet topology. *IEEE/ACM Trans. Netw.*, 11(4):514–524, 2003.

[22] P. Stone and M. Veloso. Multiagent systems: A survey from a machine learning perspective. *Auton. Robots*, 8(3):345–383, 2000.

[23] K. Tracey, C. Penn, and C. J. H. Fowler. Developing an infrastructure to support communities of learning. *BT Technology Journal*, 17(1):98–110, 1999.

How to Win the Multi-Agent Competition in a Dynamic Environment with the Minority Game Strategies?

Tingting Wang

Abstract

A team-based competitive environment is a complex multi-agent environment, in which agents are required to coordinate with each other not only to enhance their collective behavior, but also to compete with the other team. We aim to model the dynamic competitive environment, and further provide our strategy for assisting a team to be winner in competing with other teams in this environment. The Minority Game (MG), as widely used in modeling financial marketing problems, can enhance the collective behavior of a group of agents in a competitive environment. In our work, we simulate most common coordination behaviors in a competitive environment and design a strategy inspired by MG, then find out the typical situation in which this MG strategy works.

1 Introduction

1.1 Motivation

In distributed multi-agent systems, agents need to cooperate to enhance their collective behavior. Agents in such systems have limited sensing range and uncertainty about their surroundings. They have to work together in a team with an appropriate strategies to optimally fulfill their tasks, as well as compete with other teams. The challenge of the environment that these agents locate lies that the situation dynamically and rapidly changes, agents need to decide their respective actions based on real-time feedback. They also have bounded rationality and limited resources.

We aim to model the above characteristics of the dynamic competitive environment, and further provide our strategy for assisting a team to be winner in competing with other teams in this dynamic environment. The strategy is a collection of decisions made by agents when facing with various situations. The agent make a decision by selecting an action from a set of possible actions.

In our work, we develop a simple grid-like environment named *TGRID* to simplify a real competitive environment, which embodies various coordinations among agents and omits the detail skills of a single agent. Using this simplified environment, we simulate most common coordination behaviors in a competitive environment and try to find out the strategy that helps a team of agents stand uphand in competitions.

In *TGRID*, a number of targets are generated and need to be catched by different teams of agents. The competition is embodied by the limited number of targets. The teams with different strategies compete with each other in order to catch more targets. The dynamic generation of the targets and the various moving routes of the targets make the conditions change dynamically. Then, we can examine different strategies under different conditions, and find out the specific condition which is suitable to apply a specific strategy.

The Minority Game (MG), proposed by Challet and Zhang [1], is a game theory for studying cooperation and competition of agents given limited resources. Agents playing MG do not interact directly with each other. They achieve their implicit collective behavior through an information sharing mechanism. Scientists have made some modifications and proposed several variants of MG, such as evolutionary MG [3], multiple choice MG [2].

MG is a strategy to enhance the collective behavior of a group of agents in a competitive environment. By relating the *alternatives* of players in MG to the strategy of agents in a competitive environment, we can design a MG inspired strategy in a competitive multi-agent system, and then examine whether or not MG works in this environment and under what conditions MG works. Also, we aim to examine how the inherent parameters of MG influence the performance of the MG strategy.

1.2 Problem Statement

Here we elaborate the above mentioned issues into the following detailed problems:

1. How can we develop a common environment to enable coordination behaviors among competitive agents?

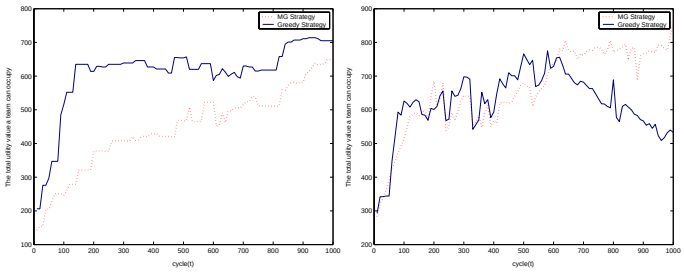

(a) (b)

Figure 1. The total utility value of the cells occupied by each team. (a) Target is moving in a linear motion. (b)Target is moving in a curved motion.

2. How can we formulate an MG-inspired method, i.e., the MG strategy, in this environment?
3. Whether or not the MG strategy in (1) is effective? If yes, in what condition it is effective?
4. Whether the parameters of MG influence the performance of the MG strategy? If yes, how can we characterize this influence?

2 Experiments

The target in the competitive environment may be static or moving in various fashions. Our experiments will try to answer, whether or not the MG strategy can help a team do effective role assignments in these competitive situations.

The results are drawn in Figure 1 and 2.

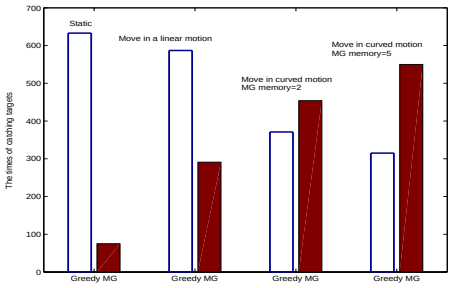

Figure 2. The times that each team catches the targets.

The above observations point out that the nonlinear motion of targets influence the effectiveness of the MG strategy. The MG strategy is efficient in a rapidly changing environment, that is, the environment with targets in nonlinear motion.

However, the MG strategy is not suitable for all kind of nonlinear situations. When the swing of the motion of the target is larger than a special threshold, the team that uses the MG strategy catches the target more often. Also, too high frequency is near random motion, while too low is similar to linear motion. Both of these two extreme weaken the predict ability of the MG strategy.

3 Conclusion

In our work, we designed a grid environment *TGRID* to simulate the coordinate behaviors among agents. We observed that, the MG strategy is not always effective. Its performance depends on the motion of the targets. When targets are static or move in a linear motion, the MG strategy is not quite effective than the greedy strategy. However, if the targets move in a nonlinear motion, i.e., the complexity of the motion is higher than a linear motion, the MG strategy can help agents do effective action selection to occupy good positions and catch more targets. We also change the swing and frequency of the motion and observe that, the swing, the frequency and the size of *TGRID* limit the effectiveness of the MG strategy.

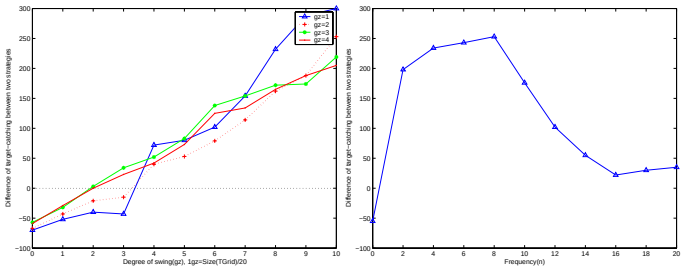

(a) (b)

Figure 3. (a)The difference of target-catching between two strategies when the target moves in $n * sin(4x)$. (b)The difference of target-catching between two strategies when the target moves in $30 * sin(n * x)$.

References

[1] D. Challet and Y.-C. Zhang. Emergence of cooperation and organization in an evolutionary game. *Physica A*, 246(3-4):407–418, 1997.

[2] L. Ein-Dor, R. Metzler, I. Kanter, and W. Kinzel. Multi-choices minority game. *Physical Review E*, 63(066103), 2001.

[3] S. Hod and E. Nakar. Self-segregation vs. clustering in the evolutionary minority game. *Physical Review Letters*, 88(238702), May 2002.

Watermarking 3D Mesh Models for Authentication

Hao-Tian Wu

Abstract

In this paper, the watermarking techniques for 3D models are reviewed and a new fragile watermarking method is proposed to authenticate 3D mesh models. In the proposed method, a sequence of data bits is adaptively embedded into the mesh based on the global characteristics of the mesh model, and the hidden information can be blindly retrieved from the watermarked mesh model using a key. Compared to the existing algorithms, the proposed one has the following advantages: (1) the embedded watermark is invariant to affine transformation while sensitive to other operations; (2) the embedding strength can be controlled to the extent that even a trivial tampering with the watermarked mesh would lead the hidden watermark to change. Unauthorized modifications on mesh models can be detected and estimated.

1 Introduction

While the prevalence of network facilitates people's acquirement and distribution of multimedia works, it also challenges the protection of digital works' copyrights. As a potential technique for copyright protection of digital works, digital watermarking for multimedia data (e.g., digital images, video and audio streams, 3D models) has been proposed and arduously studied in the literature.

In general, "watermarking" comprises an encoding process and a decoding process. The former generates a watermarked object by encoding a mount of information namely watermark into a cover object, whereas the latter is to retrieve information from the watermarked object according to the embedding algorithm. Recently, watermarking 3D objects, such as 3D polygonal meshes and various 3D geometric CAD data, has received much attention in the community and considerable progress has been made.

In the literature[3-21], a variety of watermarking algorithms have been proposed to embed watermarks into 3D models, mainly 3D polygonal meshes. For instance, the algorithms in [5-14] embed the watermarks by modifying the geometry of the 3D meshes, such as the vertex coordinates and surface normal distribution, and so forth. They have shown the robustness against some operations to which 3D models are routinely subjected, e.g., affine transformation and mesh simplification. Furthermore, some algorithm (e.g., see [12,13]) modify the mesh topology, i.e., the connectivity, to embed the watermarks which is robust against geometrical operations, but weak to topological modifications. Additionally, some works in [14,22] have used the appearance attributes associated with 3D mesh models to embed the watermarks. In the paper [15], data embedding algorithms for NURBS and other types of parametric curves and faces are also proposed.

To enhance the robustness of watermarking systems, some frequency methods have been recently proposed. In [17,18], an algorithm that employs multi-resolution wavelet decomposition of polygonal mesh models is presented. In [19], an informed watermarking algorithm that constructs a set of scalar basis functions over the mesh vertices is proposed and the watermark is embedded into the "low frequency" of the polygonal meshes. In [20], Guskov's multi-resolution signal processing method [26] is adopted and a 3D non-uniform relaxation operator is used to construct a Burt-Adelson pyramid [27] to embed watermark information into a suitable coarser mesh. Mesh spectral analysis techniques [25] are also employed to transform the original meshes to the frequency domain and the watermark information is embedded into the low frequency of the meshes, as shown in [16,21].

Nevertheless, few fragile watermarking algorithms [3,4,23] have been proposed to authenticate the originality and integrity of 3D models. Actually, the first fragile watermarking of 3D objects for verification purpose was addressed by Yeo and Yeung in [4], as a 3D version of the approach proposed for 2D image watermarking. In the daily use, 3D mesh models are routinely subjected to affine transformations, such as translation, rotation and uniformly scaling. These operations are reversible and will not degrade the value of 3D mesh models in most cases. The sensitivity of the approach in [4] to affine transformations limits its power for verification of 3D models.

In this paper, we shall present a new fragile watermarking approach to authenticating 3D mesh models. In our approach, the encoding process is adaptive to both geometry and topology of the original mesh model to produce the wa-

termarked mesh model. The proposed approach is based on the global characteristics of the mesh models while the mesh topology is unchanged. Compared to the method in [4], our approach makes the embedded watermark invariant to translation, rotation and uniformly scaling, but sensitive to other geometrical or topological operations. The strength of the watermarked information can be controlled to the extent that even a trivial modification on the watermarked mesh model would lead the watermark signal to change.

2 The Proposed Approach

We perform our watermarking process on meshes, which are considered as the "lowest common denominator" of surface representations. It is easy to convert other representations of 3D models to meshes. We aim to authenticate both geometry and topology of the mesh model, i.e., both the connectivity and vertex positions need to be verified not having been modified. Our approach extends an implementation of quantization index modulation (QIM) [1] called dither quantization [2] to mesh watermarking.

2.1 The Encoding Process

To extend dither quantization to mesh watermarking, we choose the quantization step adaptive to the mesh geometry. The watermarking process is based on the global characteristics of 3D mesh models, mainly including the centroid position and the largest dimension of the mesh model. Suppose $V = \{v_1, \cdots, v_m\}$ is the set of vertex positions in V^3, the centroid position v_c of the mesh model is defined by

$$v_c = \frac{1}{m}\sum_{i=1}^{m} v_i. \tag{1}$$

The Euclidean distance d_i between a given vertex with the position v_i and the centroid of the mesh model is given by

$$d_i = \sqrt{(v_{ix} - v_{cx})^2 + (v_{iy} - v_{cy})^2 + (v_{iz} - v_{cz})^2}, \tag{2}$$

where v_{ix}, v_{iy} and v_{iz} are the coordinates of v_i on $X-axis$, $Y-axis$ and $Z-axis$, respectively. Using (2), we can find out the furthest vertex with the position v_d to the mesh centroid. The corresponding distance D is then denoted as

$$D = \sqrt{(v_{dx} - v_{cx})^2 + (v_{dy} - v_{cy})^2 + (v_{dz} - v_{cz})^2}. \tag{3}$$

We refer to the distance D as the largest dimension of the mesh model. Then the quantization step S is chosen as

$$S = D/N, \tag{4}$$

where N is a specified value. The distance from a given face to the mesh centroid is defined as the Euclidean distance from the centroid of the face to that of mesh geometry. Furthermore, the centroid position v_{ic} of a given face f_i with u edges is obtained using the following formula:

$$v_{ic} = \frac{1}{u}\sum_{j=1}^{u} v_{ij}, \tag{5}$$

where $v_{ij}, j \in \{1, 2, \cdots, u\}$ is the vertex position in the face f_i. The distance d_{fi} from the face f_i to the mesh centroid can be calculated using

$$d_{fi} = \sqrt{(v_{icx} - v_{cx})^2 + (v_{icy} - v_{cy})^2 + (v_{icz} - v_{cz})^2}. \tag{6}$$

Subsequently, we obtain the integer quotient Q_i and the remainder R_i by

$$Q_i = d_{fi}/S, \tag{7}$$

$$R_i = d_{fi}\%S. \tag{8}$$

To embed one bit value $w(i)$, we modify the centroid position of face f_i so that Q_i is an even value for the bit value 0, or an odd value for 1. In order to make $Q_i\%2 = w(i)$ always hold meanwhile reducing the false-alarm probability, we adjust the distance d_{fi} by the following way

$$d'_{fi} = \begin{cases} Q_i \times S + S/2 & \text{if } Q_i\%2 = w(i) \\ Q_i \times S - S/2 & \text{if } Q_i\%2 = \overline{w(i)} \ \&\ R_i < S/2 \\ Q_i \times S + 3S/2 & \text{if } Q_i\%2 = \overline{w(i)} \ \&\ R_i \geq S/2 \end{cases}, \tag{9}$$

where v'_{ic} is the centroid position of the face f_i after the modulation and d'_{fi} is the distance from v'_{ic} to v_c. The resulting d'_{fi} is used to adjust the position v_{is} of the selected vertex in the face f_i, supposing the face f_i consists of u vertices with the centroid position v_{ic}. Consequently, we have

$$v'_{is} = (v_c + (v_{ic} - v_c) \times \frac{d'_{fi}}{d_{fi}}) \times u - \sum_{j=1, j\neq s}^{u} v_{ij}, \tag{10}$$

where v_{ij} refers to the vertex position in the face f_i, and v'_{is} is the position of the selected vertex after the adjustment.

The detailed procedure to embed the watermark information is as follows: At first, all vertices of the original mesh are unmarked and the position of mesh centroid can be obtained by (1). Then, the furthest vertex to the centroid is found using (2) and its corresponding distance to the mesh centroid is calculated using (3). Since the largest dimension D of the mesh model should not be changed, the furthest vertex is marked and its position will not be modified. The quantization step S can be chosen by specifying the value of N in (4). Using a key, we scramble the index I of faces to obtain the scrambled index I', which we will follow in

the watermark embedding process. Before one bit of the watermark information is embedded by adjusting the distance from a face to the mesh centroid, all vertices in the face should be checked and only the unmarked vertices are selected. If there is at least one unmarked vertex in a face f_i, the face is qualified to carry one bit information and only one unmarked vertex is selected. The distance from the face to the mesh centroid is calculated by (6) and adjusted by (7-9) according to the bit value of the watermark. Since the largest dimension of the mesh model must be maintained in the encoding process, if the modified distance exceeds it, twice of the quantization step should be subtracted from it so that the embedded bit value is kept. Then, the position of the selected vertex is modified using (10), whereby the face centroid is moved to the desired position. After this operation, all vertices in the face f_i will be marked. If there is no unmarked vertex in a face, it implies that the face's candidate for embedding watermark information is not qualified and the checking mechanism will skip to the next face indexed by I' until all the watermark information is embedded.

The above embedding process inevitably introduces the distortion of the mesh geometry as some of the vertex coordinates are changed. In the encoding process, not all faces can be used to embed the watermark information. Otherwise, the position of the original mesh centroid will be lost. A small portion of the vertices are needed to restore it after the embedding process. We refer to this process as the centroid restoration process, which modifies the coordinates of the unmarked vertices in the last faces indexed by I' to compensate the error introduced by the embedding process. In our experiments, the percent of vertices used for the restoration operation is no more than 0.5%.

Supposing there are M vertex positions have been adjusted in the embedding process, the centroid restoration process begins with the calculation of the introduced error by

$$E = \sum_{j=1}^{M} v'_j - \sum_{j=1}^{M} v_j, \tag{11}$$

where v_j and v'_j are the vertex positions before and after the embedding process, respectively. To ensure that the distance from the mesh centroid to the adjusted vertex will not exceed D, the positions of the unmarked vertices are adjusted in the following way:

Step 1: The admissible adjusting radius r_j of an unmarked vertex with the position v_j is calculated by

$$r_j = D - \sqrt{(v_{cx} - v_{jx})^2 + (v_{cy} - v_{jy})^2 + (v_{cz} - v_{jz})^2}; \tag{12}$$

Step 2: The value of r_j is used to weight the adjusting vector of each unmarked vertex to ensure that the vertex will not be moved outside its admissible range. The individual adjusting weight e_j can be obtained by

$$e_j = E \cdot \frac{r_j}{\sum_{k=1}^{m-M} r_k}, \tag{13}$$

where $m - M$ is the number of the vertices used in the centroid restoration process.

Step 3: The corresponding adjusting weight is subtracted from v_j to restore the position of the mesh centroid by

$$v'_j = v_j - e_j, \tag{14}$$

where v'_j represents the vertex position after the adjustment and v_j the unmarked vertex position.

The encoding process ends as the position of the mesh centroid is restored.

2.2 The Authentication Process

In the authentication process, only the value of parameter N, the key K and the original watermark W are needed to authenticate the integrity of mesh geometry.

Similar to the encoding process, all the vertices of the original mesh are unmarked initially. The centroid position v'_c of the suspect mesh model can be obtained by (1), which should equal to the centroid position v_c of the original mesh. Then, the furthest vertex to the centroid is found using (2) and its corresponding distance D' is calculated by (3), which should equal to the largest dimension D of the original mesh model. The quantization step is calculated by

$$S' = D'/N \tag{15}$$

with the provided parameter N. Since the furthest vertex is marked before the embedding process, it should also be marked before the extraction process. Subsequently, the face index I in the mesh is scrambled using the key K to produce the scrambled index I'. Before calculating the centroid position of a given face, the marks of its vertices should be checked. If there is at least one unmarked vertex in a face f'_i, the face will be qualified to extract the embedded bit information and its centroid position v'_{ic} will be calculated using (5). Then, the distance D_{fi} from the face f'_i to the mesh centroid can be calculated by

$$D_{fi} = \sqrt{(v'_{icx} - v'_{cx})^2 + (v'_{icy} - v'_{cy})^2 + (v'_{icz} - v'_{cz})^2}, \tag{16}$$

and the integer quotient Q'_i can be obtained by

$$Q'_i = D_{fi}/S'. \tag{17}$$

The bit information $w'(i)$ can be extracted by

$$w'(i) = Q'_i \% 2. \tag{18}$$

After this operation, all the vertices in the face f_i' will be marked. If there is no unmarked vertex in a face, no information is extracted and the authentication mechanism will automatically skip to the next face indexed by I'. Since we know the original watermark W , the extraction process will cease once the number of the extracted bits matches the number of the embedded bits.

After the extraction process, the extracted watermark W' is compared with the original watermark W using the following cross-correlation function, supposing their lengths are both identical to L:

$$NC = \frac{1}{L}\sum_{i=1}^{L} I(w'(i), w(i)), \tag{19}$$

with

$$I(w'(i), w(i)) = \begin{cases} 1 & \text{if } w'(i) = w(i) \\ 0 & \text{otherwise} \end{cases}, \tag{20}$$

where NC refers to the normalized cross-correlation value between the original and the extracted watermarks. If the watermarked mesh geometry is intact, the NC value will be 1; otherwise, it will be less than 1. If there is no correlation between the original watermark and the extracted watermark, the NC value will be about 0. We claim the mesh geometry as being tampered if the resulting NC value from (19) is less than 1.

3 Experimental Results

We have tested the proposed approach on several mesh models listed in Table 1 and a 2D binary image is chosen as the watermark. Figure 2 illustrates the original mesh models and their watermarked versions. The capacities of the models used in our experiments are also listed in Table 1, given that 0.25% vertices are used for the centroid restoration process.

Table 1. The mesh models used in the experiments

Models	Vertices	Faces	Capacity(bits)
dog	7158	13176	5563
wolf	7232	13992	5938
raptor	8171	14568	7544
horse	9988	18363	7594
cat	10361	19098	8018
lion	16652	32096	14460

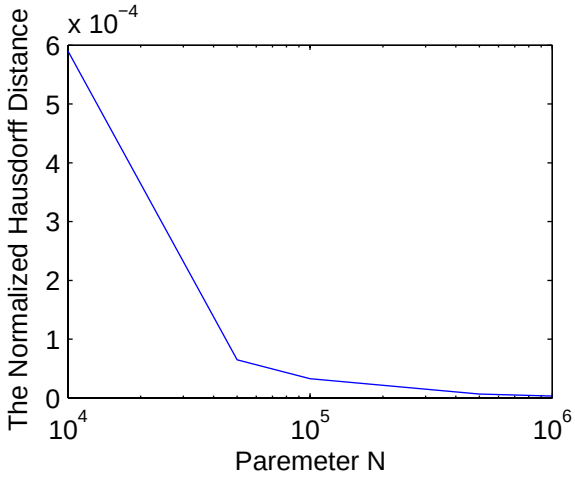

Figure 1. The normalized Hausdorff Distance subject to the parameter N

To evaluate the imperceptibility of the proposed algorithm, we used the normalized Hausdorff Distance between the original mesh model and the watermarked mesh model to measure the distortion introduced by the encoding process, upon the fact that the topology of the mesh models has not been changed during the watermarking process. The resulting distance was normalized by the largest dimension D of the mesh. Figure 1 describes the amount of the distortion subject to the parameter of N, given that the percent of vertices used for the centroid restoration process is about 0.25%. From the experimental results, it can be seen that the introduced distortion on mesh model decreases rapidly as the parameter N increases.

In the experiments, the watermarked mesh models went through the affine transformation (including translation, rotation and uniformly scaling), changing the positions of two vertices oppositely (respectively by adding the vectors $\{2S, 2S, 2S\}$ and $\{-2S, -2S, -2S\}$), modifying one vertex position by adding the vector $\{\frac{mD}{2N}, \frac{mD}{2N}, \frac{mD}{2N}\}$, reducing one face from the mesh, and adding the noise signal $\{n_x, n_y, n_z\}$ to all the vertex positions with n_x, n_y and n_z are uniformly distributed within the interval $[-S, S]$, respectively. The mesh models after these operations are also listed in Figure 2. We extract the watermark from the processed mesh models with and without the key K and calculate the normalized cross-correlation value between the extracted and the original watermarks using (19). The experimental results are listed in the Table 2.

Table 2. The NC values between the original and extracted watermarks ($N = 1000000$)

Models	affine transformations	changing two vertex positions oppositely	modifying one vertex position	reducing one face	adding noise on all vertex positions	extracting without the key
dog	1.0000	0.9992	0.3196	0.0215	0.6721	0.0200
wolf	1.0000	0.9993	0.4344	0.0132	0.5934	0.0029
raptor	1.0000	0.9997	0.3695	0.1245	0.6972	0.0225
horse	1.0000	0.9994	0.1671	0.0137	0.4661	-0.0102
cat	1.0000	0.9992	0.3963	0.0737	0.7072	0.0103
lion	1.0000	0.9995	0.4539	0.1729	0.6363	-0.0088

4 Concluding Remarks and Future Work

In this paper, we have proposed a new fragile watermarking method for 3D mesh models to detect unauthorized tampering. The proposed method applies to all the mesh models without any restriction. The experimental results have demonstrated that the proposed method is able to imperceptibly and adaptively embed a number of information into the mesh model. And the embedded watermark can be blindly extracted from the watermarked mesh model and detect the unauthorized tampering with the mesh model. In our method, the distortion introduced by the encoding process is quite small and can be controlled to a predefined range. Compared with the work in [4], the embedded watermark by our approach is invariant to affine transformation, including translation, rotation and uniformly scaling, but sensitive to other operations that alters the mesh model.

In the proposed method, the capacity of the mesh model to carry the watermark information is dependent on its vertex number. The number of data bits that can be hidden in the mesh cannot exceed the number of the vertices, since modifying one vertex position can only embed one bit information and there always exist vertices whose positions have not been modified during the watermark embedding process. One improvement of the proposed approach is to increase the capacity of the mesh models to carry the watermark information. With more watermark information is embedded in the mesh model, the watermarked mesh model will be more sensitive to unauthorized modifications.

In the encoding process, the original mesh model has been modified to hide the watermark information, so it is desirable to recover it from its watermarked version in the case that the original model is not available. Reversibility is an enhanced feature of 3D watermarking system because it compensates the distortion of mesh model introduced by the encoding process. Hence, developing the reversible version of the proposed approach is the other target for research.

Since the proposed method is conducted in spatial domain, how to authenticate the mesh models in the frequency domain is another challenging topic.

References

[1] B. Chen and G.W.Wornell, "Quantization index modulation: A class of provably good methods for digital watermarking and information embedding," *IEEE Trans. Inform. Theory*, vol. 47, pp. 1423-1443, May 2001.

[2] B. Chen and G.W.Wornell, "Digital watermarking and information embedding using dither modulation," *IEEE Second Workshop on Multimedia Signal Processing*, pp. 273-278, 1998.

[3] B.-L. Yeo and M. M. Yeung, "Watermarking 3-D objects for verification," *IEEE Comput. Graph. Applicat.*, pp. 36-45, Jan./Feb. 1999.

[4] M. M. Yeung and B.-L. Yeo, "Fragile watermarking of three dimensional objects," *Proc. 1998 Int'l Conf. Image Processing, ICIP98*, volume 2, pp. 442-446. IEEE Computer Society, 1998.

[5] Z. Q. Yu, H. H. S. Ip and L. F. Kwork, "A robust watermarking scheme for 3D triangle mesh models," *Pattern Recognition*, Vol. 36, pp. 2603-2614(12), 2003.

[6] O. Benedens, "Watermarking of 3-D polygon based models with robustness against mesh simplification," *Proc. SPIE: Security Watermarking Multimedia Contents*, pp. 329-340, 1999.

[7] O. Benedens, "Geometry-based watermarking of 3-D models," *IEEE Comput. Graph., Special Issue on Image Security*, pp. 46-55, Jan./Feb. 1999.

[8] O. Benedens, "Two high capacity methods for embedding public watermarks into 3-D polygonal models," *Proc. Multimedia Security Workshop ACM Multimedia*, pp. 95-99, 1999.

[9] O. Benedens and C. Busch, "Toward blind detection of robust watermarks in polygonal models," *Proc. EUROGRAPHICS Comput. Graph. Forum*, vol. 19, pp. C199-C208, 2000.

[10] M. G. Wagner, "Robust watermarking of polygonal meshes," *Proc.Geometric Modeling Processing*, pp. 201-208, Hong Kong, Apr. 2001.

[11] F. Cayre and B. Macq, "Data hiding on 3-D triangle meshes," *IEEE Trans. Signal. Processing*, vol. 51, pp. 939-949 (4), 2003.

[12] R. Ohbuchi, H. Masuda and M. Aono, "Watermarking Three-Dimensional Polygonal Models," *Proceedings of the ACM Multimedia*, pp. 261-272, Seattle, 1997.

[13] R. Ohbuchi, H. Masuda and M. Aono, "Watermarking Three-Dimensional Polygonal Models Through Geometric and Topological Modifications," *IEEE J. Select. Areas Commun.*, vol. 16, pp. 551-560, Apr. 1998.

[14] R. Ohbuchi, H. Masuda and M. Aono, "Geometrical and Non-geometrical Targets for Data Embedding in Three-Dimensional Polygonal Models," *Computer Communications*, vol. 21, pp. 1344-1354, Elsevier, 1998.

[15] R. Ohbuchi, H. Masuda and M. Aono, "A shape-preserving data embedding algorithm for NURBS curves and surfaces," *Proc. Comput. Graph. Int.*, June 4-11, 1999.

[16] R. Ohbuchi, S. Takahashi, T. Miyasawa and A. Mukaiyama, "Watermarking 3-D polygonal meshes in the mesh spectral domain," *Proc.Graphics Interface*, pp. 9-17, Ottawa, ON, Canada, June 2001.

[17] H. Date, S. Kanai and T. Kishinami, "Digital watermarking for 3-D polygonal model based on wavelet transform," *Proc. ASME Des. Eng. Techn. Conf.*, Sept. 12-15, 1999.

[18] S. Kanai, H. Date and T. Kishinami, "Digital watermarking for 3-D polygons using multiresolution wavelet decomposition," *Proc. Sixth Int.Workshop Geometric Modeling: Fundamentals Applicat.*, Sept. 7-9, 1998.

[19] E. Praun, H. Hoppe and A. Finkelstein, "Robust mesh watermarking," *Proc. SIGGRAPH*, pp. 69-76, 1999.

[20] Kangkang Yin, Zhigeng Pan, Jiaoying Shi and David Zhang, "Robust mesh watermarking based on multiresolution processing," *Computers & Graphics*, vol. 25, pp. 409-420, 2001.

[21] F. Cayre, P. Rondao-Alface, F. Schmitt, B. Macq and H. Maitre, "Application of Spectral Decomposition to Compression and Watermarking of 3D Triangle Mesh Geometry," *Signal Processing: Image Communications*, vol. 18, pp.309-319 (4), 2003.

[22] Liangjun Zhang, Ruofeng Tong, Feiqi Su and Jinxiang Dong, "A Mesh Watermarking Approach for Appearance Attributes," *Pacific Conference on Computer Graphics and Applications*, pp. 450-451, Beijing, 2002.

[23] Hsueh-Yi Lin, Hong-yuan Mark Liao, Chun-Shien Lu and Ja-Chen Lin, "Fragile watermarking for authenticating 3-D polygonal meshes," *Proc. 16th IPPR Conf on CVGIP*, pp. 298-304, 2003

[24] H. Hoppe, T. DeRose, T. Duchamp, J. McDonald and W. Stuetzle, "Mesh optimization," *Computer Graphics (SIGGRAPH '93 Proceedings)*, pp.19-26, 1993.

[25] Z. Karni and C. Gotsman, "Spectral compression of mesh geometry," *Proc. SIGGRAPH*, pp. 279-286, 2000.

[26] I. Guskov, W. Sweldens and P. Schroeder, "Multiresolution signal processing for meshes," *Proc. SIGGRAPH*, pp. 325-334, 1999.

[27] P. J. Burt and E. H. Adelson, "Laplacian pyramid as a compact image code," *IEEE Transactions on Communications*, pp. 532-540, 1983.

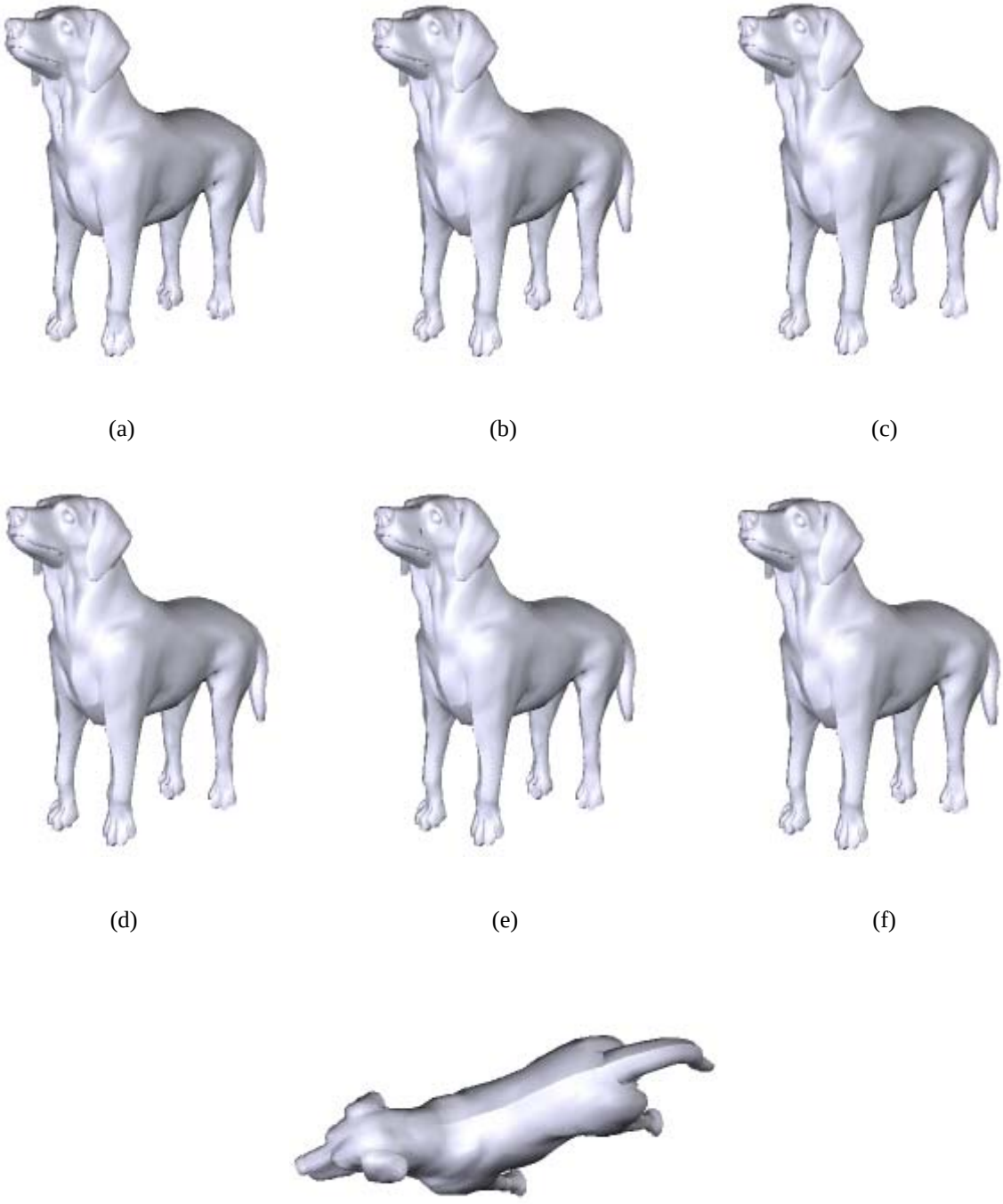

(a) (b) (c)

(d) (e) (f)

(g)

Figure 2. (a). The original mesh model "dog"; (b). The watermarked mesh model; (c). The watermarked mesh model after one vertex position modified; (d). The watermarked mesh model after two vertex position modified oppositely; (e). The watermarked mesh model after one face reduced; (f). The watermarked mesh model after adding noise; (g). The watermarked mesh model after affine transformations

Towards Solving Large-scale POMDP Problems Using The Multi-Agent Approach

LI Xin

Abstract

Markov decision process (MDP) is commonly used to model a stocahstic environment for supporting optimal decision making. However, solving a large-scale MDP problem under the partially observable condition (also known as POMDP) is known to be computationally intractable. This paper discusses the motivation of using the multi-agent approah to make the problem tractable and related research directions.

1 Introduction

Markov decision process (MDP) is commonly used to model a stochastic environment for supporting optimal decision making. An MDP model consists of a finite set of states, a set of corresponding state transition probabilities and a reward function. Solving an MDP problem means finding an optimal policy which maps each state to an action so as to achieve the best long-term reward. One of the most important assumptions in MDP is that the state of the environment is fully observable. This, however, is unfit to a lot of real-world problems. Partially observable Markov decision process (POMDP) generalizes MDP in which the decision process is based on incomplete information about the state. A POMDP model is essentially equivalent to that of MDP with the addition of a finite set of observations and a set of corresponding observation probabilities. The policy of a POMDP is now a mapping from histories of observations to actions.

2 Solving Large-scale POMDP Problems

2.1 Problem Complexity

Value iteration and policy iteration are two popular approaches for computing the optimal policy for solving MDP problems, with the complexity of $O(n^2)$ where n denotes the number of states. For POMDPs, the policy is defined over the *belief* state which can be taken as a probability distribution over the unobservable real states as an effective summary of the observation history. The belief state is updated based on the last action, the current observation, and the previous belief state using the Bayes rule. The policy of a POMDP is thus a mapping from a belief state to an action. The space of belief state is continuous. Obviously, the complexity of computing the optimal policy for a POMDP is much higher than that of an MDP. The best bound for obtaining the exact solution is doubly exponential in the horizon [4]. For large-scale POMDP problems, it is computationally infeasible even if the value function can been proven piecewise linear and convex (PWLC) over the internal state space [1].

2.2 Decomposition of POMDPs

In the literature, there exist a number of different methods for solving POMDP problems such as the witness algorithm [2], VDC algorithm [8], BFSC alogrithm [9] etc.. One promising direction is to decompose a POMDP into a collection of smaller POMDPs by exploring the structural modularization of the problem domain allowing much larger problems to be solved.

Hierarchical POMDP (HPOMDP) Decomposition has recently been proposed for decomposing a POMDP problem into a hierarchy of related POMDP models of reduced size. PolCA [7] is a representative example where the decomposition is resulting from the decomposobility of the action domain. The limitation of HPOMDP is that the decomposition is not fully automatic, where the hierarchy of actions is done by domain experts where corresponding experience and domain knowledge are needed. So this kind of hierarchical decomposition is domain specific. A generic methodology for the decomposition of POMDP problems remains to be an open research issue.

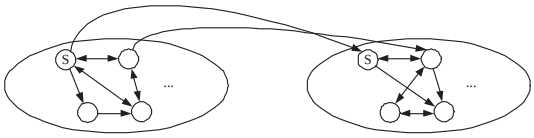

Figure 1. Partition Expected

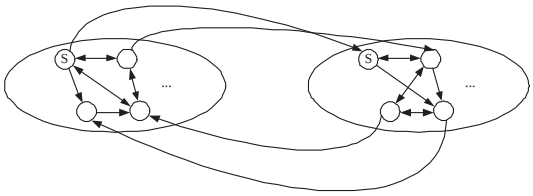

Figure 2. Minimal Cut Partition

3 Solving POMDP Problems Using A Multi-Agent Method

3.1 Towards Automatic Decomposition

As mentioned above, automatic problem decomposition for POMDPs is non-trivial. One possible way is to decompose a POMDP policy graph [1] into two or more sub-graphs. For simplicity, only the decomposition with two sub-graphs is discussed. If the decomposition can induce one set of cohesive states such that the states in the set cannot transit into the states of the remaining set (See Figure 1), a natural decomposition is resulted. In other words, the edges between the two set of states are unidirectional. For MDPs, the edges correspond to actions. For POMDPs, the edges correspond to the combination of actions and observations. The optimal policies of the sub-POMDPs form parts of the optimal policy of the overall POMDP. Unfortunately, many POMDPs cannot be partitioned into this form. The edges between the two set of states induced by a partition could have two directions (See Figure 2). An alternative is to find a minimal cut to reduce the number of the edges between the two sets of states as far as possible. We are currently investigating the different decomposition paradigms. Based on a particular decomposition, we can assume each sub-POMDP to be served by an agent. The communication and coordination of these agents with the neighborhood defined by the edges between the sets could be exploited to achieve an optimal policy for the whole POMDP. Note that the sub-POMDP problems cannot be solved independently as they are still interrelated.

3.2 The Multi-Agent Approach

Given a decomposition of a POMDP, how the multi agents should interact to get an overall policy is a critical research issue, even if all the important information and reward functions of the POMDP is known. Nash Equilibrium is an important concept commonly used in multi-agent learning [5] for solving decentralized MDP [3] /POMDP problems [6]. Our research agenda is to investigate how this paradigm can be applied to the decomposition of a MDP/POMDP problem. The basic idea is that every agent would conjecture other agents' behaviors and give the best response to other agents from its local view. A Nash equilibrium usually would not deduce the optimal policy. However, it should be able to guarantee a not too bad sub-optimal. We believe that similar ideas can also be used in our multi-agent method to solve a large-scale POMDP problems. In brief, one agent conjectures the *future* actions of some other agents to give the best response. It is analogous to cutting a sequential events into several parallel sub-events. Another possible direction to look at is whether the decomposition and the optimal policy computation can be integrated in the multi-agent framework. For instance, every agent can compete for its own set of actions from the original action set. The competition should at the same time consider how well the problem can be decomposed.

What being described so far assumes that the whole model of the decision process is known. That is, we have the perfect knowledge about the reward function, transition function and observation function. Solving the corresponding POMDP problems is an off-line process. It is also interested to see how the multi-agent approach can be extend to support online learning (e.g., Q-learning [10]) for POMDP under partial observation scenarios.

4 Summary

This paper addresses some research issues related to solving large-scale POMDP problems using the multi-agent perspective. In particular, automatic problem decomposition, integration of decomposition and policy computation in a multi-agent setting, and on-line learning are discussed. As MDPs and POMDPs provide a perfect framework for decision making in an uncertainty environment, we would also like to apply the proposed method to stochastic planning problems such as web service composition.

References

[1] POMDP Tutorial. http://www.cassandra.org/pomdp/tutorial/index.shtml.

[2] A.Cassandra. *Exact and approximate algorithms for partially observable Markov decision processes*. U.Brown, 1998.

[3] R. Becker, S. Zilberstein, V. Lesser, and C. V. Goldman. Transition-Independent Decentralized Markov Decision Processes. In *Proceedings of the Second International Joint Conference on Autonomous Agents and Multi Agent Systems*, pages 41–48, Melbourne, Australia, July 2003. ACM Press.

[4] D. Burago, M. de Rougemont, and A. Slissenko. On the complexity of partially observed Markov decision processes. *Theoretical Computer Science*, 157(2):161–183, 1996.

[5] M. P. W. Junling Hu. Nash q-learning for general-sum stochastic games. *Journal of Machine Learning Research*, 4:1039–1069, 2003.

[6] R. Nair, M. Tambe, M. Yokoo, D. Pynadath, and S. Marsella. Taming decentralized pomdps: Towards efficient policy computation for multiagent settings. 2003.

[7] J. Pineau and S. Thrun. An integrated approach to hierarchy and abstraction for pomdps. Technical Report CMU-RI-TR-02-21, Robotics Institute, Carnegie Mellon University, Pittsburgh, PA, August 2002.

[8] P. Poupart and C. Boutilier. Value-directed compression of pomdps. In S. T. S. Becker and K. Obermayer, editors, *Advances in Neural Information Processing Systems 15*, pages 1547–1554. MIT Press, Cambridge, MA, 2003.

[9] P. Poupart and C. Boutilier. Bounded finite state controllers. In S. Thrun, L. Saul, and B. Schölkopf, editors, *Advances in Neural Information Processing Systems 16*. MIT Press, Cambridge, MA, 2004.

[10] C. Watkins. *Learning from Delayed Rewards*. PhD thesis, Cambridge Univ., Cambridge England, 1989.

Learning Global Models Based on Distributed Data Abstractions

Xiaofeng Zhang

Abstract

Recently, there is an emerging need for distributed data mining techniques due to either computational or privacy related constraints. Achieving highly accurate data mining results and, at the same time, preserving individuals' privacy in a distributed environments becomes an increasingly important research issue. In this paper, we adopt a model-based approach for data abstraction, and subsequently global model learning. In particular, the Gaussian mixture model (GMM) is used as a flexible representation for each distributed data set. Instead of aggregating local data sets in a global server for mining, we propose to aggregate local GMM model parameters and a novel EM-like algorithm is proposed for learning a global GMM using solely local GMM parameters. Future research plan for further extending the proposed approach is also discussed.

1 Introduction

Most of the machine learning and data mining algorithms work with a rather basic assumption that all the training data can be pooled together in a centralized data repository. Recently, there exist a growing number of cases that the data have to be physically distributed due to some constraints. Examples include the data privacy concern in commercial enterprises where customers' private information are supposed not to be disclosed to other parties without their consent. Another example is mining individuals' incoming e-mails for some global patterns of junk mails, and sharing personal emails with others is a scenario which is almost impossible. Additional relevant examples including distributed medical data analysis, intrusion detection, data fusion in sensor networks, etc.[7]

The distributed mining problem concerned here is different from related fields like distributed query processing where the partition of the data sets is under the user's control and is often based on some criteria for facilitating the global objective. In our case, the local data sets cannot be partitioned purposedly which does happen in many real applications and calls for a lot of recent research efforts in distributed data mining [1].

1.1 Distributed Data Mining

A common methodology for distributed data analysis/mining is a two-stage one — first performing local data analysis and then combining the local results forming a global one. For example, in [10], a meta-learning process was proposed as an additional learning process for combining a set of locally learned classifiers (decision trees in particular). A related implementation has been realized under a Grid platform known as the Knowledge Grid [2]. In [7], Kargupta *et al.* proposed collective data mining where the distributed data possess different sets of features, each being considered as an orthogonal basis. The orthogonal bases are then combined to give the overall result. The scheme have been applied to learning Bayesian Networks for Web log analysis [4, 3].

One major limitation of this approach is that making local decision/analysis can result in information loss for global pattern discovery. One possible solution is to allow knowledge exchange. In [8], it has been shown that interleaving local model learning and model exchange steps can improve the accuracy of the global model. An alternative is to adopt a flexible representation for each local data set to minimize the chance of losing important local structural information. In this paper, we, inspired by [5, 9], take the second approach and adopt the Gaussian mixture model for local data abstraction.

The advantage of our approach is that by transferring only the local model parameters, data privacy and the level of data details (represented as the number of components) can now be controlled. The bandwidth requirement is also low. However, in order to support the proposed learning paradigm, algorithms for learning global models using a set of local models are needed.

2 Problem Formulation

Let t denote an observed data instance, θ_l denote the parameters of the l^{th} local model, θ_{lj} denote the j^{th} component's parameters of the l^{th} local model, α_j denote the

mixing proportion of the j^{th} component in the l^{th} local model, μ_j and σ_j denote the mean and standard deviation of the j^{th} component of the l^{th} local model respectively. The probability density function (pdf) of the l^{th} local model $p_{local}(t|\theta_l)$ with K_l components is given as,

$$p_{local}(t|\theta_l) = \sum_{j=1}^{K_l} \alpha_j p_j(t|\theta_{lj}) \quad (1)$$

$$\sum_{j=1}^{K_l} \alpha_j = 1$$

$$p_j(t) = \frac{1}{2\pi\sigma_j^2} \exp\{-\frac{(t-\mu_j)^2}{2\sigma_j^2}\}.$$

Assume that there are totally L distributed sources (i.e. L local GMMs). The corresponding model parameters $\{\theta_1, \theta_2, ..., \theta_L\}$ are sent to a global server to learn a global data model, which can be a generative model, such as GMM, a generative topographic mapping (GTM) model, etc. For simplicity, we only consider the Gaussian mixture model with M components as the global model with its pdf given as

$$p_{global}(t|\theta_g) = \sum_{k=1}^{M} \alpha_k p_k(t|\theta_k). \quad (2)$$

2.1 Learning Local Model Parameters

There are many research efforts on learning gaussian mixture model parameters via variants of the standard EM algorithm. Since learning the local GMMs is not the focus of this paper, we just follow the standard EM steps to acquire the local model parameters.

2.2 Learning Global Model Parameters

First, we assume that we can regenerate the global data samples from the local models for learning the global model. The corresponding complete log likelihood function is:

$$L_{comp} = lnP(t, z|\theta_g)$$

$$= \sum_{i=1}^{N}\sum_{k=1}^{M} I_{ik}[ln(\frac{1}{\sqrt{2\pi}\sigma_k}) - \frac{(t_i-\mu_k)^2}{2\sigma^2} + ln\alpha_k] \quad (3)$$

where I_{ik} is the indicator function for the j^{th} component of the global model generating the i^{th} data sample.
Then, the standard EM algorithm can be applied, with the E-step given as

$$R_{ik} = \frac{\alpha_k \exp\{-\frac{1}{2\sigma_k^2}(t_i-\mu_k)^2\}}{\sum_{j=1}^{M} \alpha_j \exp\{-\frac{1}{2\sigma_k^2}(t_i-\mu_j)^2\}} \quad (4)$$

and the M-step (for parameter re-estimation), given as

$$\mu_k = \frac{\sum_{i=1}^{N} R_{ik} t_i}{\sum_{i=1}^{N} R_{ik}} \quad (5)$$

$$\alpha_k = \frac{1}{N}\sum_{i=1}^{N} R_{ik} \quad (6)$$

$$\sigma_k^2 = \frac{\sum_{i=1}^{N} R_{ik}(t_i-\mu_k)^2}{\sum_{i=1}^{N} R_{ik}} \quad (7)$$

While regenerating the data using, say, the Monte Carlo Markov Chain sampling [6] is quite costly, we propose to learn directly from the local model parameters.
Assume that R_{lk} is now an indicator for a local component with the underlying data generated by a global component. That is, the likelihood of the subset of data generated by the k^{th} component of the global model is assumed to be approximated by that of the corresponding l^{th} local component being generated by the same component of the global model. Applying the EM algorithm again, we get the new M-steps as

$$\mu_k = \frac{\sum_{l=1}^{L} R_{lk}\mu_l}{\sum_{l=1}^{L} R_{lk}} \quad (8)$$

$$\alpha_k = \frac{1}{L}\sum_{l=1}^{L} R_{lk} \quad (9)$$

$$\sigma_k^2 = \frac{\sum_{l=1}^{L} R_{lk}(\sigma_l^2+\mu_l^2)}{\sum_{l=1}^{L} R_{lk}} - \mu_k^2 \quad (10)$$

To estimate R_{lk} (E-step), KL-divergence is used, resulting in

$$R_{lk} = \frac{\exp\{-D(P_{global}(t,z|\theta_k)||P_{local}(t,z|\theta_l))\}}{\sum_{k=1}^{M}\exp\{-D(P_{global}(t,z|\theta_k)||P_{localj}(t,z|\theta_{lj}))\}} \quad (11)$$

$$R_{lk} = \frac{\exp\{-ln\frac{\sigma_l}{\sigma_k} + \frac{(\sigma_k^2-\sigma_l^2)+(\mu_k-\mu_l)^2}{2\sigma_l^2}\}}{\sum_{k=1}^{M}\exp\{-ln\frac{\sigma_l}{\sigma_k} + \frac{(\sigma_k^2-\sigma_l^2)+(\mu_k-\mu_l)^2}{2\sigma_l^2}\}} \quad (12)$$

where $D(P||Q)$ denote the distance between two probabilistic models P and Q. We are currently performing experiments for validating the mathematical derivation.

3 Conclusion and Future Plan

In this paper, a novel EM-like algorithm is proposed for learning the global model based on solely local model parameters rather than data samples. We believe that what we proposed in this paper is a generic way to learn global models, where GMM is just one particular case. We will extend the result of this paper to learn a global GTM, with the plan

to formalize a more generalized way for global model learning using local data sets represented as GMMs. In addition, we will extend our approach to tackle privacy preserving data mining which is also a hot topic in recent years. Generally speaking, a more detailed model has less privacy, and vice versa. Thus, the granularity of the local models can be constructed based on individual's privacy concern. However, how to well quantify data privacy for regularizing the local clustering results remains to be an important research issue. Thirdly, if the global model precision can be estimated and found to be not satisfactory, active negotiation with the local data sources for improving the overall precision by compromising to some degree the local privacy settings at a minimum cost is another interesting research direction to look at.

References

[1] Distributed Data Mining Bibliography. http://www.csee.umbc.edu/~hillol/DDMBIB/ddmbib_html/index.html.

[2] M. Cannataro and D. Talia. The Knowledge Grid. *Communications of the ACM*, 46(1):89–93, January 2003.

[3] R. Chen and S. Krishnamoorthy. A New Algorithm for Learning Parameters of a Bayesian Network from Distributed Data. In *Proceedings of the 2002 IEEE International Conference on Data Mining (ICDM 2002)*, pages 585–588, Maebashi City, Japan, December 2002. IEEE Computer Society.

[4] R. Chen, S. Krishnamoorthy, and H. Kargupta. Distributed Web Mining using Bayesian Networks from Multiple Data Streams. In *Proceedings of the IEEE International Conference on Data Mining*, pages 281–288. IEEE Press, November 2001.

[5] J. Ghosh, A. Strehl, and S. Merugu. A Consensus Framework for Integrating Distributed Clusterings Under Limited Knowledge Sharing. In *Proceedings of NSF Workshop on Next Generation Data Mining*, pages 99–108, Baltimore, MD, November 2002.

[6] W. R. Gilks, S. Richardson, and D. J. Spiegelhalter. *Markov Chain Monte Carlo in Practice*. Chapman and Hall, London, 1996 (ISBN: 0-412-05551-1).
This book thoroughly summarizes the uses of MCMC in Bayesian analysis. It is a core book for Bayesian studies.

[7] H. Kargupta, B. Park, D. Hershberger, and E. Johnson. Collective Data Mining: A New Perspective Towards Distributed Data Mining. In H. Kargupta and P. Chan, editors, *Advances in Distributed and Parallel Knowledge Discovery*, pages 133–184. MIT/AAAI Press, 2000.

[8] C. Lam, X. Zhang, and W. Cheung. Mining Local Data Sources For Learning Global Cluster Models. In *Proceedings of IEEE/WIC/ACM International Conference on Web Intelligence (WI'04)*, pages 748–751, September 2004.

[9] S. Merugu and J. Ghosh. Privacy-preserving Distributed Clustering using Generative Models. In *The Third IEEE International Conference on Data Mining (ICDM'03)*, Melbourne, FL, November 2003.

[10] A. Prodromidis and P. Chan. Meta-learning in Distributed Data Mining Systems: Issues and Approaches. In H. Kargupta and P. Chan, editors, *Advances of Distributed Data Mining*. MIT/AAAI Press, 2000.

Data Dissemination in Wireless Sensor Networks

Minji WU

Abstract

This paper briefly reviews the research issues for wireless sensor networks. It also presents our ongoing work of monitoring top-k queries in a single-hop wireless sensor network. A data collection heuristic is proposed to balance the energy consumption of each sensor node and to extend the network lifetime. Preliminary experimental results show that the proposed heuristic outperforms a basic scheme. Directions for future research are also included.

1. Introduction

Recent advances in micro-electro-mechanism and wireless communication technologies have enabled the deployment of low-cost wireless sensor networks for a variety of applications that entail *in-situ* sensing (e.g., habitat monitoring). A wireless sensor network leverages the collaborative effort of a large number of sensor nodes to accomplish a certain mission. Powered by batteries, the sensor nodes are small in size. They make use of minimal computation facilities to measure some properties of physical environments and simple wireless interfaces to communicate with each other.

A variety of sensing tasks are possible with a wireless sensor network. Most of these tasks are related to ambient conditions, such as temperature, humidity, light, pressure, vehicular movement, soil makeup, noise level, presence or absence of a certain kind of objects.

In order to have a better understanding of wireless sensor networks (WSNs), we identify some special characteristics that differ from other networks. [1, 6]:

- **Application Specialization:** Thanks to the sensing, computing, and communication technologies, many different application scenarios become possible. However, it is not likely to develop a one-size-fits-all WSN that could be shared by different applications for different tasks. Rather, a WSN is typically deployed for a specific application.
- **Environment Interaction:** Since WSNs are designed to interact with the environment, their traffic characteristics are expected to be very different from traditional networks. A typical consequence is that a WSN may exhibit a very low data rate over a long period of time, but have very bursty traffic when something happens (e.g., a phenomenon is detected).
- **Energy Consumption:** This is a key difference between WSN and many other networks. Replacing/recharging batteries for sensor nodes is not only costly but also impossible in many situations (e.g., in a hard-to-reach area). Once the power supply on a portion of sensor nodes in depleted, the WSN may fail to carry on its mission. In order to prolong the lifetime of the whole system, we should make use of energy in an efficient yet balanced manner. Energy efficiency has been a research topic that many researchers focus their interests on.
- **Self Configurability:** WSNs should be able to self configure to connected networks. Often, a WSN is deployed in some critical area which may have radioactive or chemical conditions and human beings cannot easily reach. In these scenarios, self configurability is extremely important.
- **Simplicity:** Since sensor nodes are small and the energy is scarce, the operating and network software must be simple enough in order to make a long lifetime of the system.

2. A Brief Literature Review

There has been a large body of research on WSNs in the literature. In the following, we outline the research issues that have been actively pursued by the researchers.

- **Medium Access Control (MAC):** Medium access is an active research area for WSNs [12]. Generally, MAC deals with data transmission collisions, while in WSNs, MAC protocol also has to take into account the energy efficiency issue. The key question is how to ensure that the sensor nodes can stay in power-saving mode as long as possible while still being able to communicate without significant transmission collisions and delays.
- **Topology Control:** In traditional wired networks, every node (computer) is controlled by human; hence, it is easy to manage the network topology. However, a WSN is constructed of unattended sensor nodes. Even more, sensor nodes may face frequent failures, which make topology maintenance difficult. The main task of topology control in WSNs is to adjust transmission power of sensor nodes to configure their neighbors in order to maintain network connectivity [9].
- **Message Routing:** The network routing is another active research area. It shares some commonalities with ad hoc networking, but the more stringent requirements regarding scalability, energy

efficiency, and data centricness call for new solutions [6]. These above requirements make naming and addressing mechanisms in WSNs different from the traditional network protocols. Among the proposed WSN routing protocols, the Greedy Perimeter Stateless Routing (GPSR) [7] is probably the most popular protocol.

- **Data Dissemination:** Many data dissemination techniques have been proposed for sensor networks to explore in-network query processing, distributed data storage, and approximation techniques. One interesting approach is to treat the entire sensor network as a distributed database and to interact with it via SQL-like queries. Madden *et al*. [8] presented pull-based acquisitional query processing (ACQP), where the sensors control where, when, and how often the data are acquired and delivered to query processing operators. Ratnasamy *et al.* [10] proposed a distributed data-centric storage model: the sensor reading is pushed to the sensor node nearest to some geometric location hashed from a predefined key. Recent work has also started to study approximate queries that trade data quality for energy efficiency [4, 5]. The key here is how to allocate the error budget to the sensor nodes in the network.

3. Ongoing Work – Monitoring Top-*k* Queries

3.1. Problem and Objective

I have been working on monitoring top-*k* queries in wireless sensor networks in the past semester. A top-*k* query finds the *k* sensor nodes with the highest sensor readings in the network, e.g., a top-2 query "retrieving the two nodes (regions) with the highest temperature readings." Monitoring of top-*k* queries in distributed networks has been studied in the literature [2, 3]. However, the authors in [2, 3] did not consider energy and lifetime models. Thus, their proposed techniques are not directly applicable to energy-constrained wireless sensor networks. Different from [2, 3], our objective is to balance energy consumption at each sensor node and to extend the network lifetime.

As is known to all, the lifetime of a WSN is determined by the power supply of the sensor nodes. When a sensor node runs out of energy, its coverage is lost. The mission of a sensor application would not be able to continue if the coverage loss is remarkable. For simplicity, we assume here that when one node runs out of energy, the sensor network fails to carry on its mission. To prolong the network lifetime, we should make the energy consumption at each sensor node as balanced as possible.

3.2. Monitoring Approaches

Consider a single-hop wireless sensor network consisting of a base station and N sensor nodes. The sensor nodes report their sensed values to the base station, where top-*k* queries are monitored. A naïve scheme to monitor a top-*k* query is that all the sensor nodes periodically (e.g., at the sensing rate) send their readings to the base station, and the base station identifies the top k nodes for the query. Obviously, this scheme is not energy efficient due to excessive data update traffic.

To reduce the update traffic, the idea is to set a pair of boundaries (U_i, L_i) for each sensor node i. As long as the sensor reading at node i does not go beyond the range of (U_i, L_i), no update reporting is needed, thereby cutting down the network traffic. Specifically, assuming the initial sensor readings $(V_1, V_2, \ldots, V_N)$ are sorted in descending order, a boundary pair $(+\infty, L_1)$ is set to the node with the top reading, (U_i, L_i) to the nodes with the next top-k-1 readings, and a boundary pair $(U_{k+1}, -\infty)$ to the rest of the nodes. Upon acquiring a new sensor reading, the node i reports it to the base station only if the new value leaves the range of $(V_i + U_i, V_i - L_i)$. The base station, after receiving an updated reading from a node, replaces the node's old reading with the newly received reading; it also re-sorts all the data, calculates new boundary pairs for all nodes and, if a boundary pair for a node is updated, sends the new pair to the node.

The key of this approach is the setting of boundaries $(L_1, L_2, \ldots, L_k, U_2, U_3, \ldots, U_{k+1})$. We have to satisfy the following constraint for the setting:

$$L_i + U_{i+1} = V_i - V_{i+1} \quad (i = 1, 2, \ldots, k). \qquad (1)$$

The simplest boundary setting is *uniform* that evenly distributes the bound at the center point of the difference $V_i - V_{i+1}$. That is, for all $i = 1, 2, \ldots, k$, we set

$$L_i = U_{i+1} = (V_i - V_{i+1})/2.$$

However, the uniform boundary setting may not perform well as it does not take into account the reading changing patterns of the sensor nodes in the network. If the sensor readings from all nodes update following the same pattern, it is possible that the uniform setting can achieve a good performance, i.e., a long network lifetime. But, if on the contrary, the reading changing patterns differ dramatically among all the nodes, the uniform setting is not a good choice as it will result in imbalanced consumption of energy. We here develop a new algorithm taking advantage of the reading changing patterns in order to balance the energy consumption rates for the sensor nodes.

Suppose the average time of sensor node i changing the sensed value beyond Δ is known as $f_i(\Delta)$. Denote by C_i the energy cost of sending an update message from node i to the base station. Thus, given a boundary setting of Δ, the energy consumption rate at node i is given by $C_i / f_i(\Delta)$. To balance the energy consumption, we should choose each pair of L_i and U_{i+1} such that the energy consumption rates for nodes i and $i+1$ equal subject to constraint (1), i.e.,:

$$C_i / f_i(L_i) = C_{i+1} / f_{i+1}(U_{i+1}),$$
$$\text{s.t.} \quad L_i + U_{i+1} = V_i - V_{i+1}.$$

However, in reality we cannot know in advance how the sensor readings evolve dynamically. Thus, we devise a practical boundary setting scheme by assuming a commonly adopted random walk model. In the random walk model, the value changes in steps with an inter-step interval of l. It decreases or increases the current value by an amount of d at each step. From [11], we know that:

$$f(\delta) = (\frac{\delta}{d})^2 \cdot l \cdot$$

We let all sensor nodes measure the delta changes of their sensor readings at the same rate L. When sensor node i updates its reading to the base station, it will piggyback the measured average delta change, d_i. Hence, the optimization problem becomes to choose (L_i, U_{i+1}) such that:

$$C_i d_i^2 / L_i^2 L = C_{i+1} d_{i+1}^2 / U_{i+1}^2 L,$$
$$\text{s. t.} \quad L_i + U_{i+1} = V_i - V_{i+1}.$$

It is easy to see that the solution is:

$$\frac{L_i}{U_{i+1}} = \frac{d_i}{d_{i+1}} \sqrt{\frac{C_i}{C_{i+1}}}.$$

3.3. Preliminary Experimental Results

To evaluate the performance of the proposed data collection approach, we developed a simulator based on ns-2. We simulate a sensor network of 10 sensor nodes and 1 base station (see Figure 1 for the layout). The sensor nodes can operate in one of three modes: sending message, receiving message, and sleeping. These modes differ in energy consumption. The energy consumption for sending a message is determined by a cost function: $s \cdot (\alpha + \beta \cdot d^q)$, where s is the message size, α is a distance-independent term, β is the coefficient for a distance-dependent term, q is the component for the distance-dependent term, and d is the distance of message transfer. We set α = 50 nJ/b, β = 100 pJ/b/m^2, and q = 2 in the simulation. The energy consumption for receiving a message is given by $s \cdot \gamma$, where γ is set at 50 nJ/b. The power consumption in sleeping mode is set at 0.016 mW. The intitial energy budget at each sensor node was set at 0.01 Joule.

The readings of each sensor node change following a random walk model. At each step, the reading changes by an amount (called *step size*) which is randomly assigned from a configurable range [-Δ, Δ]. Table 1 lists the data change profiles used in the experiments. In the UU profile, all sensor nodes follow the same random walk model, while in the UH, HU and HH profiles, the sensor nodes differ in step size and inter-step interval.

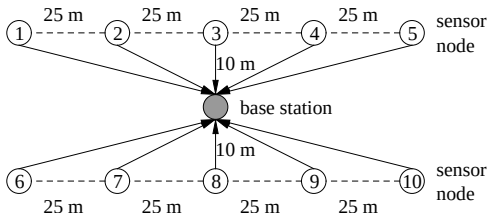

Figure 1: Sensor Network Layout

Table 1: Data Change Profiles

Pattern	Step Size (Δ)	Inter-Step Interval
HU	Sensors 1-2: 10	All sensors: 0.2 sec
	Sensors 3-10: 2	
UU	All sensors: 2	All sensors: 0.2 sec
UH	All sensors: 2	Sensors 1-5: 0.2 sec
		Sensors 6-10:1.0 sec
HH	Sensors 1-2: 10	Sensors 1-5: 0.2 sec
	Sensors 3-10: 2	Sensors 6-10: 1.0 sec

We measured the network lifetime, i.e., the time when the first node runs out of energy, over 10 simulation runs. We compare the proposed data collection approach against the basic approach with a uniform boundary setting (described in Section 3.2). As shown in Figure 1, the proposed approach extends the network lifetime over the uniform scheme by 5.81% - 30.29% on average. It can be seen that the improvement is much more significant for the profiles with heterogeneous inter-step intervals.

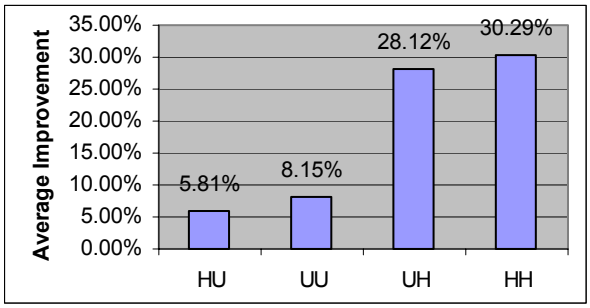

Figure 2: Performance Comparison

3.4. Future Work

For future work, we are going to elaborate the proposed approach by further incorporating the factor of sensor node's residual energy and evaluate it using some real trace data. We also plan to investigate the boundary setting methods under multiple queries and/or multi-hop networks, in which the setting of boundaries for each node becomes more complicated. Monitoring of error-bounded approximate top-k queries is another interesting research topic to pursue.

Reference

[1] I. F. Akylildiz, W. Su, Y. Sankasubramaniam, and E. Cayirci. Wireless Sensor Networks: A Survey.

Computer Networks, 38: 393-422, 2002.
[2] B. Babcock and C. Olston. Distributed Top-K Monitoring. In *Proc. ACM SIGMOD*, 2003.
[3] P. Cao and Z. Wang. Efficient Top-K Query Calculation in Distributed Networks. In *Proc. PODC*, 2004.
[4] A. Deligiannakis, Y. Kotidis, and N. Roussopoulos. Hierarchical In-Network Data Aggregation with Quality Guarantees. In *Proc. EDBT*, 2004.
[5] Q. Han, S. Mehrotra, and N. Venkatasubramanian. Energy Efficient Data Collection in Distributed Sensor Environments. In *Proc. IEEE ICDCS*, 2004.
[6] H. Karl and A. Willig. A Short Survey of Wireless Sensor Networks. Technical Report, Technical University Berlin, 2003.
[7] B. Karp and H. T. Kung. GPSR: Greedy Perimeter Stateless Routing for Wireless Networks. In *Proc. ACM Mobicom*, 2000.
[8] S. R. Madden, M. J. Franklin, J. M. Hellerstein, and W. Hong. The Design of an Acquisitional Query Processor for Sensor Networks. In *ACM SIGMOD*, 2003.
[9] J. Pan, Y. Hou, L. Cai, Y. Shi, and S. Shen. Topology Control for Wireless Sensor Networks. In *Proc. ACM MobiCom,* 2003.
[10] S. Ratnasamy, B. Karp, S. Shenker, D. Estrin, R. Govindan, L. Yin, and F. Yu. Data-Centric Storage in Sensornets with GHT, A Geographic Hash Table. *ACM/Kluwer MONET*, 8(4), 2003.
[11] J. Xu and Y. Tang. EASE: An Energy-Efficient In-Network Storage Scheme for Object Tracking in Sensor Networks. Technical Report, Hong Kong Baptist University, 2004.
[12] W. Ye, J. Heidemann, and D. Estrin. An Energy-Efficient MAC Protocol for Wireless Sensor Networks. In *Proc. IEEE Infocom*, 2002.

Upgrading Unicast All-Optical Networks for Multicast Communication

Tony Kam-Chau Chan

Abstract

We identify the problem of upgrading existing unicast all-optical networks to support multicast communication. In upgrading, it is necessary to modify the node architecture so that the resulting nodes can support point-to-multipoint optical switching. In modification, it is desirable to retain and use the existing node components while adding a small number of components, so that the cost of upgrading can be kept small. We propose three designs to fulfill these goals: (i) the pre-splitting design *adds splitting modules before the existing optical switches to split the incoming optical signals for point-to-multipoint optical switching, (ii) the* post-splitting design *adds splitting modules after the existing optical switches, and (iii) the* pre/post-splitting design *adds splitting modules before and after the existing optical switches. We demonstrate that each design is most effective for certain traffic patterns.*

1. Introduction

Optical networks with wavelength division multiplexing superimpose signals at different wavelengths to extend the bandwidth of optical fibers. If signals between source and destination remain in optical domain, the networks are referred to as all-optical networks.

Signals in all-optical networks are transmitted through *lightpaths*. A lightpath is a point-to-point all-optical channel on a particular wavelength along the fibers between source and destination. In point-to-multipoint communication, the concept of lightpath is generalized into *light-tree* [1] which is an all-optical multicast tree with single source and multiple destinations.

There are many attractive features of light-trees [4]. Through the light-trees, multicasting at optical layer can effectively be implemented to support many bandwidth-intensive multicasting applications, such as HDTV (high-definition television), video conferencing, and video-on-demand services. Incorporating light-tree concept into network design can reduce the requirement of transceivers and make more efficient use of network bandwidth [1], [4], [5].

Light-trees can be realized by employing *light splitters*, which can split input into multiple output signals. Optical cross-connects (OXCs) with light splitting ability are referred to as *multicast-capable* OXCs (MC-OXCs). To implement multicasting at optical layer, MC-OXCs must be employed at the nodes (or some nodes).

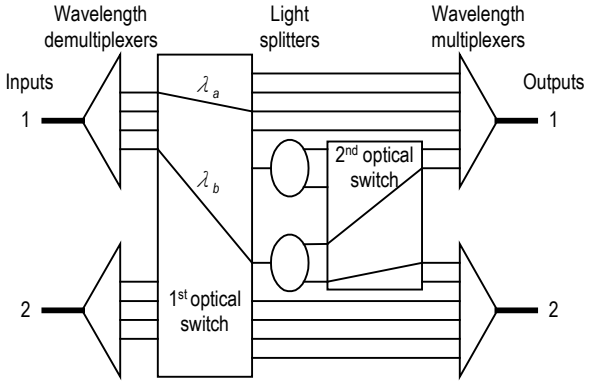

Fig. 1. 2x2 Multicast-capable wavelength-routing switch [1]**.**

There are three existing designs of MC-OXC. Fig. 1 shows a 2×2 MC-OXC[1] [1] which can support 4 wavelength channels per fiber. Signals with splitting requirement [see λ_b in Fig. 1] are directed to light splitters and switched at the second switch. Signals without splitting requirement [see λ_a in Fig. 1] are switched directly at the first switch. Another design [2] uses split-and-delivery (SaD) switches to construct MC-OXCs [see Fig. 2 & 3]. An $N\times N$ SaD switch consists of N light splitters, N^2 optical gates, and N^2 1×2 switches. Each input signal is split into N outputs and the desired outputs are selected through the optical gates and the 1×2 switches. This design can support multiple point-to-multipoint switching sessions at the same wavelength. However, it suffers from excessive power loss because all inputs must be split into N output signals regardless of their types (multicast or unicast). Hence, a power-efficient design is proposed in [3]. The main idea is to share the light splitters. Fig. 4 shows an $N\times N$ SaD switch with splitter sharing which consists of one light splitter, N optical gates, and N 1×2 switches. The shared light splitter will only split signals with splitting requirement. Since this SaD switch contains one light splitter, this design can only support one point-to-multipoint switching session per wavelength channels.

To provide multicasting at optical layer, we can either construct a new all-optical network with MC-OXCs or upgrade an existing all-optical network to support multicast services. In constructing a new network, we can choose any of the three existing design

[1] In [1], they call this MC-OXC as multicast-capable wavelength-routing switch.

[1]-[3] as the node architecture. In upgrading, the existing node architecture must be modified to support

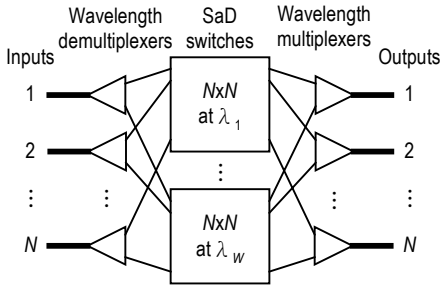

Fig. 2. *N*×*N* MC-OXC based on SaD switch architecture [2]**, *W* wavelengths.**

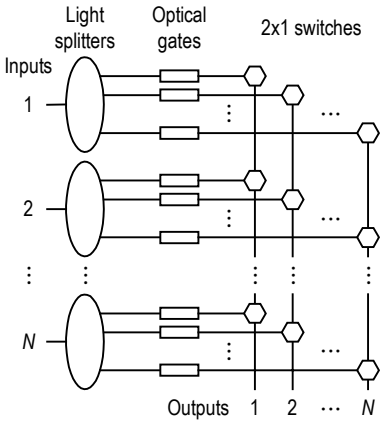

Fig. 3. *N*×*N* SaD switch [2]**.**

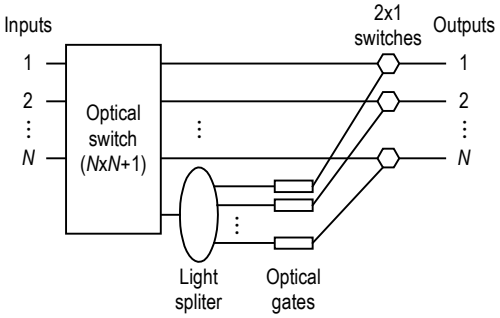

Fig. 4. *N*x*N* SaD switch with splitter sharing [3].

point-to-multipoint optical switching. During the modification, it is desirable to retain and use the existing node components while adding a small number of components, so that the cost of upgrading can be kept small. However, for the best of our knowledge, we find no existing design concerns about upgrading existing node architecture to support point-to-multipoint optical switching. For instance, we consider the node architecture as shown in Fig. 5. There are W $N\times N$ optical switches which are responsible for switching signals of the N incoming/outgoing fibers at different wavelength channels (λ_1, λ_2, …, λ_W). If the node is modified by any of the three existing designs [1]-[3], all existing optical switches must be replaced because none of the designs requires $N\times N$ optical switches. Consequently, we cannot keep upgrading cost small by using the three existing designs.

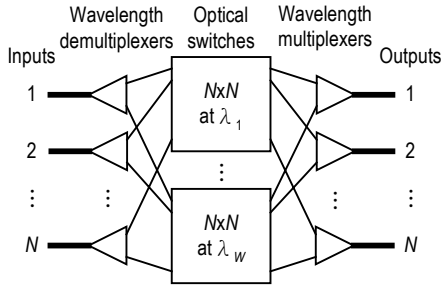

Fig. 5 Existing node architecture of unicast all-optical network.

In this paper, we identify the problem of upgrading existing unicast all-optical networks to support multicast communication. To keep upgrading cost small, we propose two splitting modules, named pre-splitting and post-splitting, which can work with existing optical switches to support point-to-multipoint optical switching. Based on the splitting modules, three designs are proposed. Each design is most effective for certain traffic patterns.

The rest of the paper is organized as follows. Section 2 describes the two splitting modules and the three designs. Section 3 describes how the three designs are applied in all-optical multi-fiber networks. Future work is presented in Section 4 and the paper is concluded in Section 5.

2. Upgrading Designs for Single-Fiber Networks

We refer to the node architecture of unicast all-optical networks as shown in Fig. 5. To modify it, we propose two splitting modules named pre-splitting and post-splitting, which can provide light splitting functionality and work with the existing optical switches to support point-to-multipoint optical switching. Based on the splitting modules, we propose three designs which are described as follows.

2.1. Pre-splitting Design

In pre-splitting design, we add pre-splitting modules before the existing optical switches [see Fig. 6]. Pre-splitting modules can be fabricated to support different degree of splitting. An $N\times N$ d-degree pre-splitting module consists of N light splitters, dN optical gates, and N light combiners. The light combiners, like the splitters, are passive devices which can combine multiple inputs into one output signal. The optical gates are active (expensive) devices which control signals to the combiners and dominate the cost of the splitting modules.

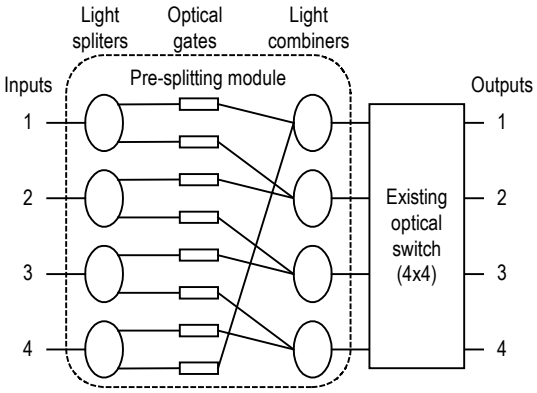

Fig. 6 4x4 2-degree pre-splitting module.

Fig. 6 shows an example of how a 4×4 2-degree pre-splitting module works with a 4×4 optical switch. Through the splitting modules, each input is split to *d* signals and the signals are selected by the optical gates so that at most one signal goes through each combiner. Finally, the signals are switched at the existing optical switch. Hence, point-to-multipoint optical switching is achieved.

To keep upgrading cost small, *d* must be small. Though the splitting ability is more restricted at small *d*, many multicast tree could still be found even for each node supporting 2 degree of splitting [6]. Hence, this design would be more cost-effective at *d* ranging from 2 to 3.

2.2. Post-splitting Design

In post-splitting design, we add post-splitting modules after the existing optical switches [see Fig. 7]. Post-splitting modules can be fabricated to contain certain ports, named *splitting-capable* (SC) ports, which have light splitting ability. An *N*×*N* post-splitting module with *s* SC ports consists of *s* light splitters, *sN* optical gates, and *N* light combiners. The optical gates attached to each splitter are responsible for controlling signals to the desired outputs. Like pre-splitting module, the optical gates are active devices which dominate the cost of the splitting modules.

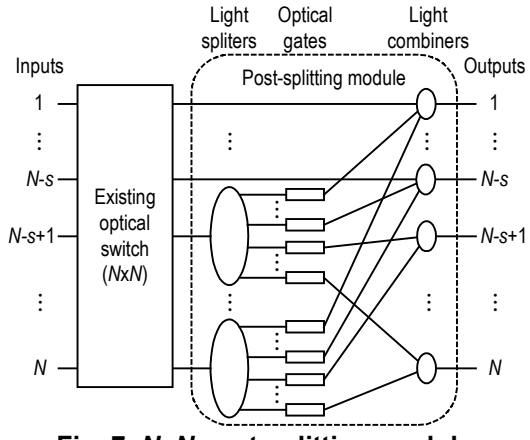

Fig. 7. *N*x*N* post-splitting module.

Fig. 7 shows how an *N*×*N* post-splitting module works with an *N*×*N* optical switch. When signals require splitting, the existing optical switch will direct the signals to the SC ports (ports *N*-*s*+1 to *N*) in which signals are split and delivered to the desired outputs. Point-to-point signals destined for outputs 1 to *N*-*s* are switched directly at the existing optical switch, while those destined for outputs *N*-*s*+1 to *N* would be switched through any of the SC ports. Each combiner must be kept at most one signal passing through it.

To keep upgrading cost small, *s* must be small. We expect that this design would be more cost-effective at *s* ranging from 1 to 2.

2.3. Pre/post-splitting Design

In pre/post-splitting design, we add both pre-splitting and post-splitting modules to the existing optical switches as shown in Fig. 8. This design takes benefits of both pre-splitting and post-splitting designs. Both splitting modules can cooperate with each other to provide better multicast services. When splitting request cannot be realized at pre-splitting modules, it may be served through the post-splitting modules. For instance, Fig. 8 shows a 4×4 optical switch which is modified by a 4×4 2-degree pre-splitting module and a 4×4 post-splitting module with 1 SC port. Unlike pre-splitting design, this design can support unrestricted degree of splitting through the post-splitting module. Besides, if signal from input 1 is occupying two output ports of the pre-splitting module, signal from input 2 (or 4) can still be split through the post-splitting module [see Fig. 8].

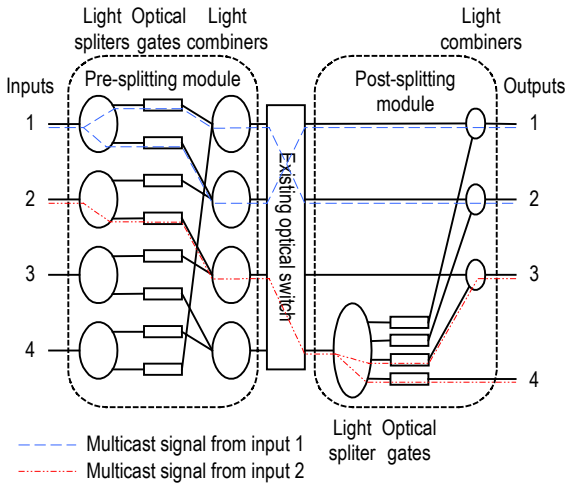

Fig. 8. 4x4 pre/post-splitting module.

2.4. Discussion and Comparison

We consider the light splitting ability of pre-splitting and post-splitting modules. All input ports of pre-splitting modules have light splitting ability, while

only certain SC ports of post-splitting modules have the light splitting ability. Hence, we expect that pre-splitting design can support more multicast sessions than the post-splitting design. However, as post-splitting module can provide unrestricted degree of light splitting, post-splitting design would be more favorable for multicast sessions with many destination nodes.

Pre/post-splitting design takes benefits of both pre-splitting and post-splitting design. We expect that pre/post-splitting design would be more adaptable to various traffic patterns. However, the upgrading cost of pre/post-splitting design would be comparatively higher than the other two designs because two splitting modules must be added in modifying each existing optical switch.

Table 1 summarizes the comparison of the three designs.

Table 1.
Comparison of pre-splitting, post-splitting, and pre/post-splitting designs (apply to both single-fiber and multi-fiber networks).

Designs	No. of multicast sessions that can be supported	Types of multicast sessions that can be supported	Upgrading cost
Pre-splitting	Large	Session with few destination nodes	Low
Post-splitting	Moderate	Session with many destination nodes	Low
Pre/post-splitting	Very large	All sessions with any destination nodes	Moderate

3. Upgrading Designs for Multi-fiber Networks

We consider the node architecture of all-optical multi-fiber networks as shown in Fig. 9. There are L incoming/outgoing links, each link has F fibers and each fiber can support W channels at wavelength λ_1, λ_2, …, λ_W. W $LF\times LF$ optical switches are required. In modifying the node to support point-to-multipoint optical switching, we can flexibly apply the two proposed splitting modules. The three corresponding designs are described as follows.

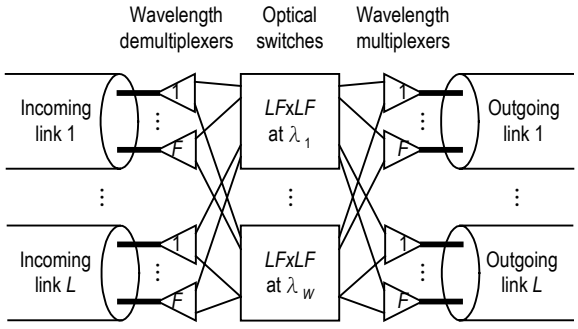

Fig. 9. Node architecture of all-optical multi-fiber networks.

3.1. Pre-splitting Design

When signals are transmitted between two connected nodes in multi-fiber networks, we can select any available fiber from the connected link for the transmission. Similarly, if the signals are multicast signals, we can select certain fibers which are connected to light splitters for the transmission. Hence, in modifying the nodes of multi-fiber networks to support point-to-multipoint optical switching, it is not necessary to make all inputs support light splitting. Referring to the node architecture as shown in Fig. 9, we can modify the $LF\times LF$ optical switches by $L\times L$ pre-splitting modules as shown in Fig. 10. Each splitting module may support different degree of splitting.

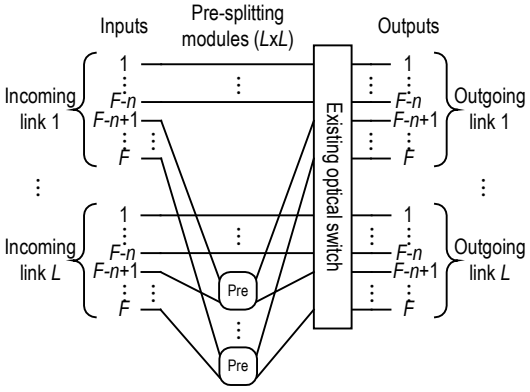

Fig. 10. Connection of *n* pre-splitting modules to an existing optical switch in all-optical multi-fiber networks.

Depends on the network requirements, we can gradually increase multicasting capacity of the nodes by increasing the pre-splitting modules. For instance, as the network, initially, requires supporting a few multicast sessions, we can modify the nodes by adding one pre-splitting module to each existing optical switch. When the network requires more multicasting capacity, we can add more pre-splitting modules as in Fig. 10. Hence, progressive upgrade could be achieved.

3.2. Post-splitting Design

When a multicast signal is transmitted through a particular node, the degree of splitting is unlikely more than the connected links of the node no mater the node is on a single-fiber or multi-fiber network. Hence, in modifying the node architecture as shown in Fig. 9, it may not necessary to split and deliver multicast signals to all outgoing fibers. The degree of splitting equals L would be adequate in many situations. Consequently, we can modify the $LF\times LF$ optical switches by $L\times L$ post-splitting modules as shown in Fig. 11.

Like pre-splitting design, we can gradually increase multicasting capacity of the nodes by increasing the post-splitting modules. Progressive upgrade could also be achieved.

3.3. Pre/post-splitting Design

Like pre/post-splitting design in single-fiber networks, we can use both pre-splitting and post-splitting modules to modify the nodes of multi-fiber networks. Fig. 12 shows how the $LF \times LF$ optical switches are modified by a number of $L \times L$ pre-splitting and $L \times L$ post-splitting modules. Similarly, progressive upgrade could also be achieved by adding different number of splitting modules.

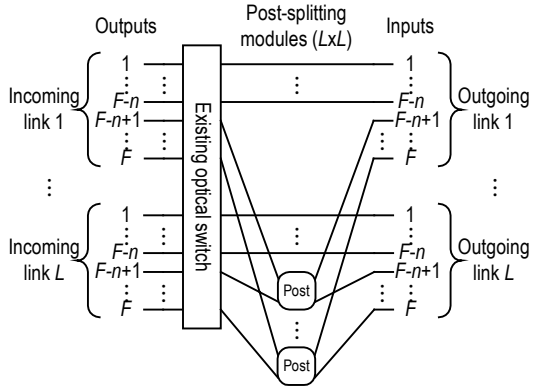

Fig. 11. Connection of *n* post-splitting modules to an existing optical switch in all-optical multi-fiber networks.

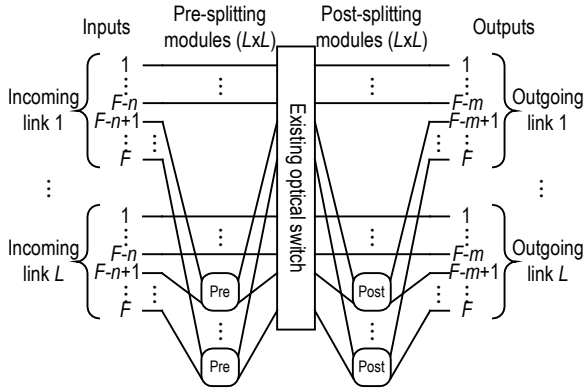

Fig. 12. Connection of *n* post-splitting and *m* post-splitting modules to an existing optical switch in all-optical multi-fiber networks.

3.4. Discussion and Comparison

The comparison of the three designs in Table 1 is still applied to the three corresponding designs in this section because all designs employ the splitting modules in similar way. One major difference in modifying the nodes of multi-fiber networks is that all the three corresponding designs can support progressive upgrade. Progressive upgrade allows fast deployment of services because little investment can make unicast all-optical networks support multicast communication.

4. Future Work

To evaluate our proposed designs, we will perform simulation experiments.

5. Conclusions

In this paper, we identified the problem in upgrading unicast all-optical networks to support multicast communication. We proposed two splitting modules, named pre-splitting and post-splitting, which can provide light splitting functionality and work with the existing optical switches to support point-to-multipoint optical switching. As all existing optical switches can be retained and used, the upgrading cost can be kept small. Based on the splitting modules, we proposed three designs named pre-splitting, post-splitting, and pre/post-splitting. Each design is most effective for certain traffic patterns. In all-optical multi-fiber networks, the splitting modules can work flexibly with the existing optical switches to achieve progressive upgrade.

6. References

[1] L. H. Sahasrabuddhe and B. Mukherjee, "Light-tree: optical multicasting for improved performance in wavelength-routed networks," *IEEE Commun. Mag.*, pp. 67-73, Feb. 1999.

[2] W. S. Hu and Q. J. Zeng, "Multicasting optical cross connects employing splitter-and-delivery switch," *IEEE Photonics Tech. Lett.*, vol. 10, pp. 970-972, Jul 1998.

[3] M. Ali and J. S. Deogun, "Power-efficient design of multicast wavelength-routed networks," *IEEE J. Select. Areas Commun.*, vol 18, no. 10, pp. 1852-1862, Oct. 2000.

[4] G. N. Rouskas, "Optical layer multicast: rationale, building blocks, and challenges," *IEEE Network*, pp. 60-65, Jan/Feb. 2003.

[5] R. Malli, X. Zhang, and C. Qiao, "Benefit of multicasting in all-optical networks," in *Proc. SPIE*, vol. 3531, pp. 209-220, Nov. 1998

[6] F. Bauer and A. Varma, "Degree-constrained multicasting in point-to-point networks," in *Proc. INFOCOM'95*, pp. 369-376, 1995.

Maintaining Temporal Consistency of Real Time Data in Broadcast Environments

Hui Chui Ying

Abstract

Many new mobile computing applications have real-time properties and requirements. the values of the data items are highly dynamic and the transactions generated from mobile clients may associate with a deadline constraint on their completion time. In this report, we first study a protocol based on timestamp ordering that can show significant performance improvement in reducing the number of unnecessary transaction restarts such that the timeliness of mobile transactions can be enhanced. We then study a broadcast method that provide consistent data items to mobile transactions in addition to minimizing data access delay.

1 Introduction

Nowadays, millions of users are carrying some kind of portable computing devices that use a wireless interface to access the worldwide information network for business or personal use. In most of the existing mobile computing applications, such as information dispersal systems for stock prices and sensor data, there are time constraints for both transactions and data [3]. This means data will become invalid as time passes. At the same time, real-time transactions must read temporally consistent data in order to generate correct results . Hence, transactions must complete their executions by their deadlines, and the data they read must be sufficiently fresh.

Temporal consistency of data can be defined in terms of the age of the data and the dispersion of ages among data. The age of a data object describes how up-to-date its value is. The dispersion of two data objects is the difference between their ages. Data objects are temporally consistent if their ages and dispersions are sufficiently small to meet the requirement of the application. In addition, the temporal constraints of data can be described by the data deadline. Data deadline tells when the validity of a data object will expire. For a transaction to commit and generate correct results, both the transaction deadline and data deadline must be satisfied. Temporal consistency is difficult to maintain in broadcast environments [1]. In broadcast environments, it takes a longer time for the most recent data versions to reach at the mobile clients and the mobile clients also need to wait for the broadcast of the requested data objects. Therefore, it may be more difficult for transactions to commit before the validity of their data objects expires.

2 The BCC-TI protocol

The basic idea of the BCC-TI protocol is to dynamically adjust the position of the ROTs in the current serialization order by recording a timestamp interval associated with each active ROT [4]. Each ROT has a timestamp interval. Data conflict is checked by the shut out of timestamp interval. Whenever a ROT reads a data object from the broadcast disk, the lower bound of the timestamp interval will be adjusted to reflect the serialization order induced between it and the committed update transactions that have written the data object. If the write timestamp (WTS) of the data object is greater than the lower bound, the lower bound will be set to this WTS. If the timestamp interval shuts out, i.e. lower bound$\geq$upper bound, a non-serializable execution performed by the ROT is detected and the ROT will be restarted.

To check the data conflict with respect to the server transactions committed in previous broadcast cycle, ROT needs to be checked against the control information broadcast at the beginning of each broadcast cycle. The control information in the current broadcast cycle stores the information of the data objects, which are updated during previous broadcast cycle. To determine whether a ROT has introduced a non-serializable execution with respect to the committed update transactions, mobile clients need to adjust the upper bound of the timestamp interval. If the updated write timestamp (WTS) of the data object, which has been read by the ROT, is smaller than the upper bound, the upper bound will be set to this WTS. This adjustment implies that the recent write operation of the data object does not affect the old value read by the ROT in previous broadcast cycles. If the timestamp interval shuts out, i.e. lower bound$\geq$upper

bound, a non-serializable execution performed by the ROT is detected and the ROT will be restarted.

3 Multi-versions data broadcast

Multi-versions data broadcast (MV) can provide consistent data items to mobile transactions in addition to minimizing data access delay. In MV, the database maintains multiple versions for a data item. Updates on data items are batched together until the end of a broadcast cycle. Each newly created data version is assigned a version number, which indicates at which cycle-end it is generated. The server broadcasts previous versions of a data item together with the last committed version of the data item at the last broadcast cycle.

If a mobile transaction wants to access a data item, it will get the latest version for its first read operation from broadcast cycle. The subsequent read operations of the transaction will read data items with the same version number as the first one. By allowing a transaction to read an older version of a data item, data consistency can be ensured at the expense of currency as a mobile transaction is allowed to access old version of a data item.

References

[1] Acharya, S., Alonso, R., Franklin, M. and Zdonik, S. Broadcast disks: data management for asymmetric communication environments. In *Proceedings of the 1995 ACM SIGMOD international conference on management of data*, pages 199–210, San Jose, California, USA, 1995.

[2] Haritsa, J. R., Carey, M. J. and Livny, M. On being optimistic about real-time constraints. In *Proceedings of the ninth ACM SIGACT-SIGMOD-SIGART symposium on principles of database systems*, pages 331–343, Nashville, Tennessee, USA, 1990.

[3] Lam, K. Y., Chan, Edward and Au, Mei-Wai. Broadcast of Consistent Data to Read-Only Transactions from Mobile Clients. In *Proceedings of 2nd IEEE Workshop on Mobile Computing Systems and Applications*, New Orleans, February 1999.

[4] Lee, V. C. S., Lam, K. W., and Son, S.H. Concurrency Control Using Timestamp Ordering in Broadcast Environments. *The Computer Journal*, 45(4):410–422, 2002.

Worldviews Retrieval through Ontological Worldviews Model

Chung Kei Yeung

Abstract

Soft Systems Methodology (SSM) is a soft systems approach to solve the ill-defined problems. However, in this methodology, the discovery of worldviews and formation of system boundary have not been mentioned in details. Therefore, we propose to use the ontological worldviews model to discover the worldviews and boundary. The model aims to exploit the hierarchical structure of a tree to maintain the decomposition and structure relationships of the real world. The resulting hierarchical structure of ontological worldviews model can provide an overview which describes the structure, boundary, objectives and tasks of the system. The information can facilitate the subsequent development stages.

1. Introduction

SSM [12] uses a soft systems approach. It focuses on problem solving, particularly of ill-defined problems. It emphasizes on modeling the human activity system, since it believes that people have a considerable effect on the solution design of a system [7]. For example, hotel management is one of the systems modeled by SSM [6]. In order to define the system holistically, rich pictures are drawn and the different worldviews are structured by root definition using CATWOE. After that, the desired situations are then compared to the actual situation and the cultural feasibility is studied. If the changes are considered desirable and feasible, the corrective changes can take place. The desired operations based on the conceptual models are defined. Input or output analyses of operation for information requirements definition are then performed for subsequent data modeling.

SSM aims to understand the existence of reality since it concerns on learning and studying on the system. Actually, its aims can be accomplished by using ontology. As stated by Smith [14], ontology as the science of what is, of the kinds and structures of objects, properties, events, process, and relations in every area of reality. The identification and clarification of being and existences are done based on investigating their kinds, natures and relations. It is important for SSM to achieve its aims of investigating and understanding of the system.

However, the SSM still has some deficiencies that prevent it from thorough investigating and understanding of the system. These deficiencies are systematic worldviews retrieval and boundary formation which will be explained in details. In order to enhance the SSM, we have proposed the ontological worldviews model for worldviews retrieval, and given an illustration to show how it works.

2. The deficiency of Worldviews Discovery in SSM

2.1. Systematic Worldviews Retrieval

The idea of worldview originally comes from the SSM [1, 2, 3]. The SSM is used in human activity systems in which the participants have different requirements, viewpoints and perceptions on the same issue. These elements lead to the emerging of the worldviews. The worldviews can be retrieved through the rich pictures and expressed by using root definitions. However, the use of rich pictures cannot retrieve the worldviews systematically such that the relationships between the worldviews cannot show clearly. As a result, it is difficult to know whether there is any missing worldviews.

Petri Nets has been used as a tool to identify the relationships of worldviews. Lamp [8] has applied this skill to retrieve the related worldviews by referring to the clients involved and linking the worldviews together by their common properties in the conceptual model. However, by using this approach, the emergent properties may be hidden since the worldviews are considered as compartments. Besides, the decomposition and structure of the real world cannot be shown as it lacks of the concept of worldviews and sub-worldviews. These features are important for representing the existence of a real system [17, 18], we have to reserve and express them in the worldviews and conceptual model.

Besides, the relationships of the worldviews are better formed in the worldviews level instead of conceptual

model. By discovering all the relationships in worldviews level, the completeness and correlation of the worldviews can be examined first. This can reduce the cost and workload of handling the undiscovered worldviews in the later stages. The worldviews and their relationships can also provide an overview of the system which describes the aims and the tasks that the system performs. Therefore, systematic worldviews retrieval is essential to retrieve the worldviews and their relationships with respect to the decomposition and structure of the real world.

2.2. Boundary Formation

Organizations are the systems which have coherent purposes and goals [9]. Applying the same theory, system is the components which have coherent purposes and goals. The integration of different components concerning each other forms a boundary [5]. Inside the same boundary, the components are inter-related by the purposes and goals. Besides, the limit of the system can be defined.

However, the SSM do not emphasize on identifying a boundary. The rich picture is the tool that is for modeling all the entities and activities that are related to each other in a system. It tries to take all worldviews into consideration to avoid missing any worldviews for the system. The resulting model then forms the boundary. However, all worldviews in the rich picture are not necessary to achieve the coherent purposes and goals. As a result, some redundant worldviews which do not lie on the coherent goals may also be included. The redundant worldviews affect the system analysis in the later development stage, such as redundant components, extra development time and cost.

The importance of forming the boundary is already stated in the Systems Thinking [11]. The defining the boundary is not only depended on the developers, but also the participants of the system. By collecting the related worldviews and withdraw the unrelated one, the boundary is formed. Córdoba, Midgley & Torres [5] stated that in order to resolve the conflicts on boundary, privilege could be given to one boundary at the expense of the others.
The boundary can also be got by participants' interaction, such as debating about the situation of the system [4]. This will cause the continuous discussion and modification on the boundary is called boundary critique [5].

Whether the components or worldviews should be included in the boundary is a hot topic for discussion. Robinson & Wilson [13] concerns about the totality and concreteness. They though that everything is interconnected. Therefore, it is necessary to have a look beyond the boundary and integration. On the other hand, Levins [10] suggested that it is impossible to investigate the whole system. The system should be investigated only a part. However, if necessary, the boundary can be extended to provide more explanation and interconnection to clear the doubt about the boundary. Ulrich [15] suggested considering the not well-understood parts as a part of the system, in order to increase the confident in understanding and handling the system situation. Later, this scholar also suggested the Critical Systems Heuristics for boundary judgment [16].

The formation of boundary is an important issue in systems development. We have to define explicit steps for boundary formation in SSM to provide a coherent framework for the subsequence development stages.

3. Worldviews Retrieval through Ontological Worldviews Model

In order to achieve the systematic worldviews retrieval and boundary formation, we have developed an ontological worldviews model. The model consists of hierarchical structure which can decompose the worldviews with respect to the structure of the real world. Therefore, there are worldviews and sub-worldviews. The model is a tree structure that consists of parent-child or inherent relationships which can facilitate us to check their correlation, completeness and dependence for a system. By using the model, we can distinguish the worldviews from others without difficulties.

For the users, they may want to investigate into part of the system only. It is not efficient to use the rich picture to find out the related participants and worldviews since some unrelated objects would also be got. Rich picture is only useful when we want to understand the cause and effect relationship of the worldviews. Therefore, it can let to understand the reason of worldviews appearance. We decide to use the global objectives as the root worldview. The root worldview represents the objectives of the system. The root worldview is then analyzed and searched for any related sub-worldviews. The sub-worldviews can be discovered through the transformation processes, actors and clients. The transformation processes indicate the operations that the task performs while the actors and clients represent the actors or the owners of the sub-tasks or sub-worldviews. Based on the parent's worldview and transformation processes, we have to find out how the actors and clients will be affected. As a result, we can retrieve the sub-worldviews of the parent worldview.

The worldviews discovery processes can process for each sub-worldviews recursively until all the related sub-worldviews are found. The resulting root worldview and sub-worldviews form the hierarchy that shows the inherent and dependence relationship. The method we applied in this systematic worldviews retrieval is a top-down method, that is, we first define the global objects and tasks, and then further break them down into components to get more details. By using this method, we can have a deeper understanding on the participant's worldviews, retaining the emergent properties, decomposition and structure of the real world through the hierarchical structure. The boundary of the system can also be got, as all the functions of the system are oriented to the hierarchy. Since the hierarchical structure is described by ontology, we use ontological worldviews model to describe the resulting structure.

In order to identify different groups of worldviews and their decompositions, we use a numbering system as shown in Figure 1. For the Level 1 sub-worldviews of root worldview, one digit starts from one is used to numbering the sub-worldviews. For the level 2 sub-worldviews, the first several digits should be inherent from their parents and plus one more digit starting from one. By using this numbering, we can use the digits, exclusive the last digit, to identify them from different groups and level of worldviews. It is notified that it is meaningful if and only if the parent has at least two children.

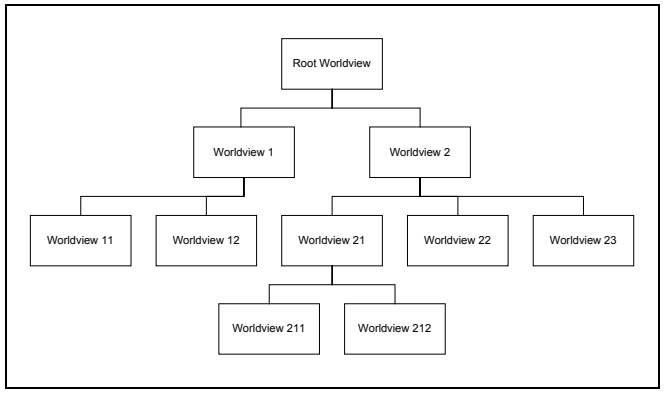

Figure 1. The hierarchy of worldviews with numbering system.

4. Illustration of Worldviews Retrieval

For each worldview, we use the root definition with CATWOE analysis to describe the worldview. Besides, the performance measures, which capture the owners' expectation, should also specify which could be used as one of the criteria to determine the requirements of the owners. Besides, the performance measures are also useful components to determine the emergent properties, which will be described it's handling in next section.

The worldviews retrieval will be explained by using the Student Residence Halls (SRH) of Hong Kong Baptist University. The participants in the SRH have different worldviews on the room assignment. They want to find the best solution to assign the rooms to students. We will use their worldviews to demonstrate how their worldviews can be retrieved systematically through the ontological worldviews model. The resulting hierarchy is shown in Figure 2.

Root Worldview (Rooms Occupation) Definition: A SRH owned system, which under the environment constraints of the performance of the rooms assignment efficiency, transforms the empty rooms in the halls to be occupied rooms, which is carried out by the SRH Staff, in order to fill the room with students who need a place to live in and the staff who need consistent room assignment information.

Performance Measures: 1. Increase the working efficiency of room assignment. 2. Reduce the workload of the SRH staff. 3. Assign the students to the right room.

From the root worldview, we have to brainstorm and discuss who will be affected and how their objectives created. After gathering the information, we have to group the similar objectives together and form a sub-worldview. This results in several sub-worldviews with more explicit and well-defined objectives.

Worldview 1 (Rooms Management) Definition: A SRH owned system, which under the environment constraints of the efficiency to manage the rooms, transforms the rooms status to consistent rooms information, which is carried out by the SRH Staff, in order to made up the rooms information in the view of staff who need consistent rooms information.

Performance Measures: 1. Make the rooms information consistent.

Worldview 2 (Student Information Management) Definition: A SRH owned system, which under the environment constraints of keeping the most updated student information, transforms the students personal details to consistent and update students information, which is carried out by the SRH staff and students, in

order to get the update students information in the view of staff who need consistent students information.

Performance Measures: 1. Get the most updated students information.
Worldview 3 (Rooms Assignment) Definition: A students and staff owned system, which under the environment constraints of satisfying the requirements of students and staff, transforms the students and rooms information to the rooms assignment result, which is carried out by the SRH Staff and students, in order to fill the room with students who need a place to live in and the staff who need to assign the students to their rooms.

Performance Measures: 1. Rent is minimum (for students). 2. Achieve a maximum profit (for staff).

For the worldview 3, it can further break down into 2 sub-worldviews, so that deeper descriptions can be got to describe the more specific objectives and tasks.

Worldview 31 (Rooms Choosing) Definition: A students owned system, which under the environment constraints of satisfying the requirements of students, transforms the students expectations to actual results, which is carried out by students themselves, in order to satisfy the students who want to live in their dream rooms.

Performance Measures: 1. Choose the dream room.

Worldview 32 (Rooms Assigning) Definition: A staff owned system, which under the environment constraints of satisfying the requirements of staff and students, transforms the students expectation to official result, which is carried out by the SRH staff, in order to satisfy the students who want to live in their dream rooms.

Performance Measures: 1. Want to best fit the room to students to reduce the rate of room change afterwards.

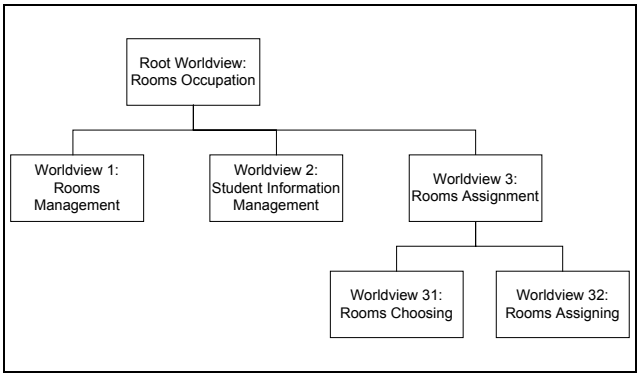

Figure 2. The resulting hierarchy of the illustration.

5. Conclusion

After the systematic worldviews retrieval, we can get the worldviews with CATWOE definitions and performance measures. The emergent properties, decomposition and structure of the real world can be retained through the hierarchical structure. Besides, the overview and boundary of the system can provide the objectives and the tasks the system performs. As a result, an overview and basic requirements with coherent framework can be provided for the later system development stage.

6. References

[1] Checkland, P. (1981). Systems Thinking, Systems Practice. Chichester: Wiley.

[2] Checkland, P. and Holwell, S. (1998) Information, Systems and Information Systems: Making Sense of The Field, Chichester, UK: John Wiley.

[3] Checkland, P., & Scholes, J. (1990). Soft Systems Methodology In Action. John Wiley and Sons.

[4] Córdoba, J. (2003). Enhancing critical reflection in planning information systems: Two strategies. Critical Management Studies Conference (CMS), Lancaster, July 2003.

[5] Córdoba, J., Midgley, G. & Torres, D. (2000). Planning by concern: A critical systems thinking approach for information systems (IS) planning and its application in a 'developing' country. British Academy of Management Annual Conference, Edinburgh, September 2000.

[6] Ingram, H. (2000) Using Soft Systems Methodology to Manage Hotels: A Case Study. Managing Service Quality, Vol.10 Issue.1, pp. 6-10.

[7] Jones, L., Peters, G. (1972). Production Systems Modeling and the Production Environment. The Open University Press, Milton Keynes, pp. 76-98.

[8] Lamp, J. W. (1998). Using Petri Nets to Model Weltanschauung Alternatives in Soft Systems Methodology. Proceedings of the Third Australian Conference on Requirements Engineering, pp. 91 - 100.

[9] Lehaney, B. & Clarke, S. (1997). Critical Approaches to Information Systems Development: Some Practical Implicaitions, Systems for Susyainability: People, Organizations and

Environments, proceedings of the 5th International Conference of the United Kingdom Systems Society, Milton Keynes, Edited by F.Stowell, Ison, R., Holloway, R., Jackson, S and McRobb, S, Plenum, London, pp. 333 - 337.

[10] Levins, R. (1998). Dialectics and systems theory. Science and Society 63(3), pp. 375 – 399.

[11] Lewis, P. J. (1994). Information Systems Development: Systems Thinking in the Field of Information-Systems. Pitman, London.

[12] Patching, D. (1990). Practical Soft Systems Analysis. Pitman, London.

[13] Robinson, B. & Wilson, F. (2002). Soft Systems Methodology and Dialectics in an information environment: a case study of the Battle of Britain, Systems Research and Behavioral Science 19: pp. 1 - 14.

[14] Smith, B. (2001). Formal Ontology and Information Systems, New York: ACM Press.

[15] Ulrich, W. (1987). Critical heuristics of social systems design. In Critical Systems Thinking: Directed Readings, Flood RL, Jackson MC (eds). Wiley: Chichester, pp. 103–115.

[16] Ulrich, W. (2003). A Brief Introduction to "Critical Systems Thinking for Professionals and Citizens". http://www.geocities.com/csh_home/cst_brief.html

[17] Wand, Y. & Weber, R. (1993). An ontological model of an information system. IEEE Transactions on Software Engineering, 16, pp. 1282 - 1292.

[18] Wand, Y., & Weber, R. (1993). On the Ontological Expressiveness of Information Systems Analysis and Design Grammars. Journal of Information Systems, pp. 217–237.

Corner Detection for Object Recognition by Using Wavelet Transform

Lu Sun

Abstract

We propose a novel scheme for corner detection algorithm using wavelet transform. The development of the method depends on a new wavelet function which is designed specifically for corner features. We know that corner points have high curvature on the contour. Our method can utilize both the information of the local extrema and modulus of transform results to detect corners and arcs effectively. Experimental results show that the proposed algorithm has good performance.

1. Introduction

Generally, corner points, which have high curvature on the contour, are very useful descriptive feature. Such corner points contain important information about the shape of an object.

Most existing corner detectors are single-scale algorithms that work well if the object has similar size features. However, most objects consist of multiple size features. Hence, they may either miss significant corners or detect false corners. To overcome this drawback, multiscale detection of corners is needed. Although there are some algorithms that detect corners by using positions of curvature extrema at multiple scales, it is time consuming because of the large number of scales required for operation. In addition, some false corners (arcs) are still detected. Therefore, it is desirable to develop a new multiscale algorithm that is more effective and more computationally efficient. To attain this goal, more useful information must be extracted from multiple scales.

In recent years, the wavelet transform (WT) became an active area of research for multiscale signal analysis. It has been described as a "mathematic microscope" because it can be used to study the local behavior of a function or a measure by integrating the information contained in multiple scales. Corners are local features, and hence, the WT appears to be very attractive for achieving this goal.

In this correspondence, we propose a new multiscale corner detection algorithm using WT. In the algorithm, a three-scale WT on contour orientation is first performed. Utilizing both the information of the local extrema and modulus of transform results, corners and arcs are detected. The orientation ramp width serves as a good indicator of the corner that can be determined by the ratio of the transformed modulus.

The experimental results have shown that our detector has good performance on corner detection. These results also demonstrate that our detector is more efficient in computation because the fewer number of scales are required and the fast implementation of the adopted wavelet transform is applied.

2. New Wavelet Function

Let $f \in L^2(R^2)$ be an image. Its continuous wavelet transform (CST) with respect to the fixed wavelet ψ and scale s>0, $W_s f(x,y)$ is defined by

$$W_s f(x,y) := (f * \psi_s)(x,y) = \iint_{R^2} f(u,v) \frac{1}{s^2} \psi(\frac{x-u}{s} - \frac{y-v}{s}) dudv,$$

where * denotes the convolution operator in $L^2(R^2)$ and $\psi_s(u,v)$ the dilation of $\psi(u,v)$ denoted by the scale factor s as follows: $\psi_s(u,v) := \frac{1}{s^2}\psi(\frac{u}{s},\frac{v}{s})$. For a general theory of the scale wavelet transform, it can be found in [1]. Here two wavelets are derived from the partial derivative of $\theta(x,y): \psi^1(x,y) := \frac{\partial}{\partial x}\theta(x,y)$ and $\psi^2(x,y) := \frac{\partial}{\partial x}\theta(x,y).$ Let us denote $\theta_s(x,y) := \frac{1}{s^2}\theta(\frac{x}{x},\frac{y}{s})$. Their scale wavelet transforms can be written as

$$W_1^i f(x,y) = (f * \psi_s^1)(x,y)$$
$$= s\frac{\partial}{\partial x}(f * \theta_s)(x,y), W_s^2 f(x,y) \quad \text{.....(1)}$$
$$= (f * \psi_s^2)(x,y) = s\frac{\partial}{\partial y}(f * \theta_s)(x,y)$$

Its corresponding modulus and gradient of wavelet transform are defined respectively as follows:

$$|\nabla W_s f(x,y)| := \sqrt{|W_s^1 f(x,y)|^2 + |W_s^2 f(x,y)|^2} \quad \text{,.....(2)}$$

$$Af(s,x,y) := \arg\tan(\frac{W^2 f(s,x,y)}{W^1 f(s,x,y)}) \quad \text{.....(3)}$$

To detect the corners of contour of image, the following odd function, which is designed specifically for computing the modulus maxima, is considered as wavelet function

$$\varphi(t)=\begin{cases}0, t\in[1,\infty)\\ \varphi_3(t), t\in[3/4,1)\\ \varphi_2(t)+\varphi_3(t), t\in[1/4,3/4)\\ \varphi_1(t)+\varphi_2(t)+\varphi_3(t), t\in[0,1/4)\end{cases} \quad \text{.....(4)}$$

where,

$$\varphi_1(t)=-\frac{2}{\pi}(-8t\ln\frac{1+\sqrt{1-16t^2}}{4t}+\frac{1}{2t}\sqrt{1-16t^2}),$$

$$\varphi_2(t)=-\frac{2}{\pi}(8t\ln\frac{3+\sqrt{9-16t^2}}{4t}-\frac{3}{2t}\sqrt{9-16t^2}), \quad \text{..... .....(5)}$$

$$\varphi_3(t)=-\frac{2}{\pi}(-4t\ln\frac{1+\sqrt{1-t^2}}{t}+\frac{4}{t}\sqrt{1-t^2})$$

Apparently, the function $\phi(x):=f_0^x\psi(u)du$ is an even function with compactly supported on [-1 1], and $\phi'(x)=\psi(x)$ holds as well. Accordingly, for two dimension case, it is easy to see that the smoothness function $\theta(x,y)$, which is defined by $\theta(x,y):=\phi(\sqrt{x^2+y^2})$, is the reasonable choice. Correspondingly, the 2-D wavelet functions are given by

$$\begin{cases}\psi^1(x,y):=\frac{\partial}{\partial x}\theta(x,y)=\phi'(\sqrt{x^2+y^2})\frac{x}{\sqrt{x^2+y^2}}\\ \psi^2(x,y):=\frac{\partial}{\partial y}\theta(x,y)=\phi'(\sqrt{x^2+y^2})\frac{y}{\sqrt{x^2+y^2}}\end{cases} \quad \text{.....(6)}$$

3. Algorithm and detection steps

3.1. Smoothed corner and arc

Let C(t)=(X(t),Y(t)),represent a regular planar curve where t is the arc length. The orientation is defined as

$$\phi(t)=\tan^{-1}((dY/dt)/(dX/dt)) \quad \text{.....(7)}$$

If the orientation at point P_i is defined by simply replacing the derivative above by the first difference, the orientation resolution is only $\frac{\pi}{4}$, To improve the orientation resolution, the orientation at point is defined as

$$\phi(i)=\tan^{-1}((Y_{i+q}-Y_{i-q})/(X_{i+q}-X_{i-q})) \quad \text{.....(8)}$$

In this correspondence, q was chosen to be three. This choice causes the orientation profile of a corner to become a ramp-like profile instead of a step with a variation interval equal to the smoothing length SL=2q+1=7.Strictly speaking, the smoothed corner orientation profile is nonlinear. However, because it is either strictly monotonic decreasing or increasing and the width of variation interval is small, it can be closely approximated by a ramp. As to an arc, the smoothed orientation at P_i is equivalent to calculating the tangential angle at P_i that varies linearly along the arc. Therefore, the smoothed arc orientation profile is still a ramp with a variation interval equal to l+SL-1, where l is the length of the arc. From above, we know that the smoothed orientation profiles of both the corner and arc are ramps, and the only difference between them is the ramp width.

The determination of the parameter q depends on two conflicting factors, namely, the orientation resolution and the corner discrimination ability. The larger the q , the higher the orientation resolution, however, the poorer the discrimination ability. It is because that the double corner may possible be merged if the corner separation is less than the smoothing length SL. The proper choice under these conditions is to select the smallest q value that can provide acceptable orientation resolution. Because the orientation resolution is not acceptable when q<3,q=3 is selected.

3.2. Corner Detection Steps

The corner detection algorithm is summarized in the following steps:

1.The bounding contour of a shape is firstly extracted by using a boundary extractor. There are six different edge-finding methods in Matlab. We use the Canny method to find edges of image. The Canny method finds edges by looking for local maxima of the gradient of image. The gradient is calculated using the derivative of a Gaussian filter. The method uses two thresholds, to detect strong and weak edges, and includes the weak edges in the output only if they are connected to strong edges. This method is therefore less likely than the others to be "fooled" by noise, and more likely to detect true weak edges.

2.According to the definition in this equation $\phi(i)=\tan^{-1}((Y_{i+q}-Y_{i-q})/(X_{i+q}-X_{i-q}))$ the smoothed orientation function of this contour $\phi(i)$ is acquired.

3.WT is performed for $\phi(i)$ at three scales. The WT equation used in our research is below:

$$
\begin{aligned}
W_s f(k) &= \int_{-\infty}^{\infty} f(t)\varphi_s(k-t)dt \\
&= \sum_{l\in Z}\int_{l-1}^{l} f(l)\varphi_s(k-t)dt \\
&= \sum_{l\in Z} f(l)\Big[\int_{-\infty}^{l}\varphi_s(k-t)dt - \int_{-\infty}^{l-1}\varphi_s(k-t)dt\Big] \\
&= \sum_{l\in Z} f(l)\Big[\int_{(k-l)/s}^{\infty}\varphi(t)dt - \int_{(k-l+1)/s}^{\infty}\varphi(t)dt\Big] \\
&= \sum_{l\in Z} f(l)\int_{(k-l)/s}^{\infty}\varphi(t)dt - \sum_{l\in Z} f(l+1)\int_{(k-l)/s}^{\infty}\varphi(t)dt \\
&= \sum_{l\in Z}\ [f(l)-f(l+1)]\varphi_{k-l}^{s},
\end{aligned}
$$

where, $\varphi_{k-l}^{s}=\int_{\frac{k-l}{s}}^{\infty}\varphi(t)dt$

$\varphi(t)$,I have introduced at the second part. Please refer to the equation (4)&(5).The results $W\phi(s,i)$, s=$2^1,2^2,2^3$ are stored in 1-D array.

4. The modulus maxima of $W\phi(s,i)$ at three consecutive scales, which indicate the appearance of a corner, are detected.

4. Experimental Results

Three bmp-format images were used to test the performance of my detector.

Figure 1. Capital A

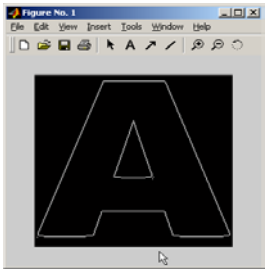

Figure 2. Edge of "A"

Fig. 1 shows the shapes of Capital A and the extracted contours of Capital A is shown in Fig. 2.Using the orientation Equation (8), We get figure 3 below

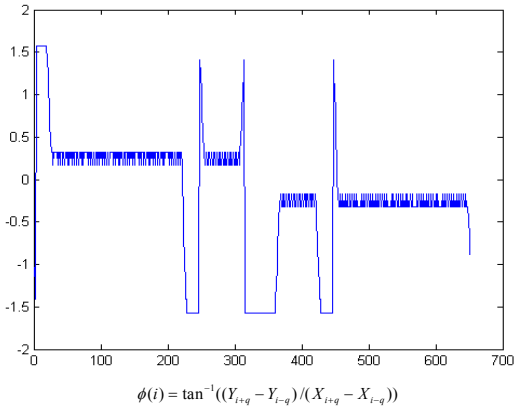

Fig 3 shows the orientation at each point

Using the four steps of corner detection, we get Fig. 4.and Fig 5. In Fig 4 , Such points which have max values in neighbour field are high possibly corner points.

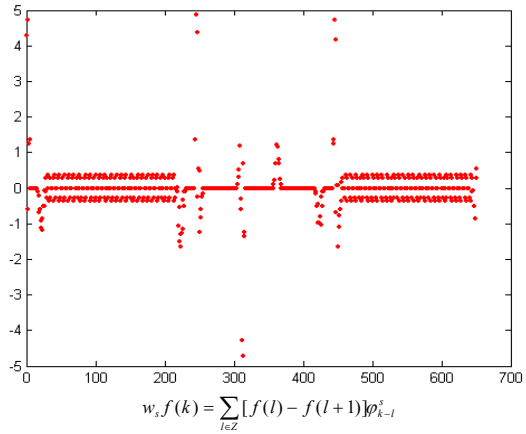

Fig 4

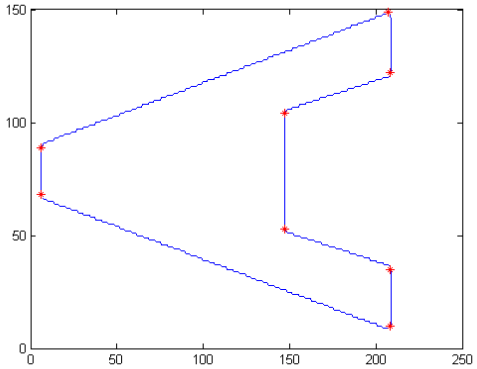

Fig 5

Fig 5 proves that the proposed detector can effectively discriminate corners from arcs.

In the second experiment, we use our algorithm to detect more complex shape of object. Fig. 6 shows the extracted contour of a key.

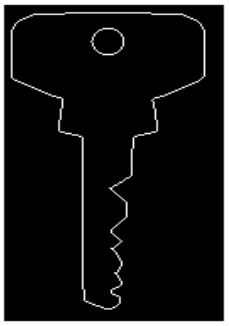

Fig 6

Fig. 7 and Fig. 8 respectively show the orientation and the WT value at each point. Fig. 9 shows the experimental result.

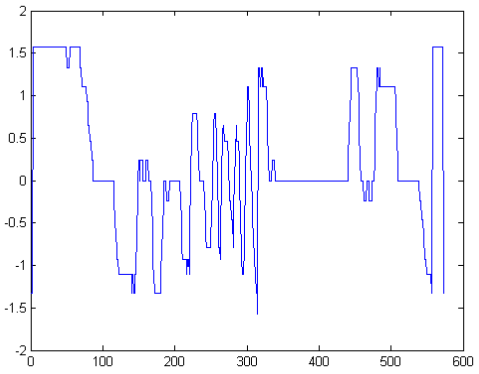

Fig 7

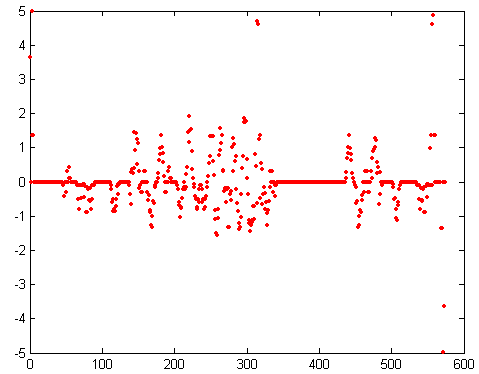

Fig 8

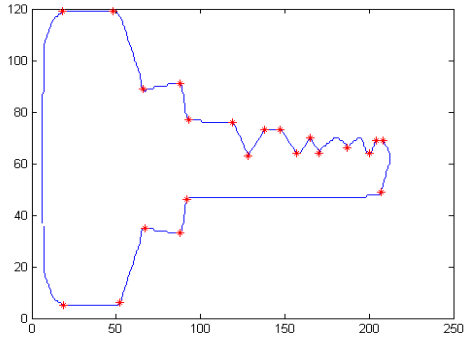

Fig 9

The third experiment based on the same algorithm shows the results of corner detection. We noticed that a few corners are neglected but most corners are successfully detected. Actually, we have made many experiments on objects with different and complex shapes. More than 90% corner points can be successfully detected.

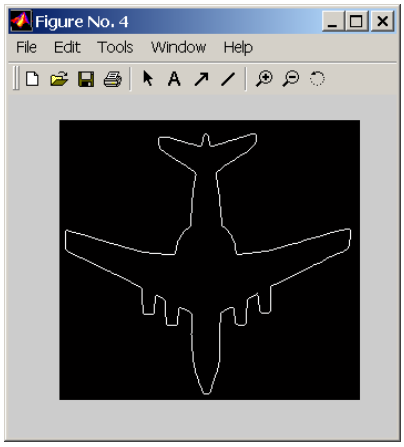

Fig 10 edge of a plane

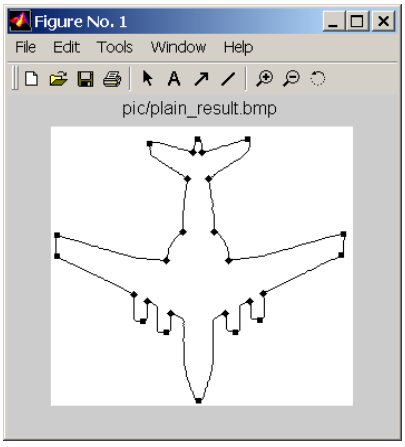

Fig 11 the result of experiment

5. Conclusions

Some desirable characteristics of wavelet transform with our constructed wavelet function are presented. Our method can utilize both the information of the local extrema and modulus of transform results to detect corners and arcs effectively. Experimental results show that the proposed algorithm has good performance.

6. References

[1] S.Mallat.Wavelet Tour of Signal Processing. Academic Press, San Diego, US, 1998

[2] A.Rosenfeld and E.Johnston, "Angle detection on digital curves," IEEE Trans. Comput., vol.22 , pp. 875-878,1973

[3] H.L.Beus and S. S. H. Tiu, "An improved corner detection algorithm based on chain-coded plane curves," Patt. Recogn., vol.20,pp. 291-296,1987

[4] Jiann-Shu Lee,Yung-Nien Sun, and "Chin-Hsing Chen, Multiscale Corner Detection by Using Wavelet Transform"

[5] P.Meer,E.S. Baugher, and A.Rosenfeld, "Extraction of trend lines and extrema from multiscale curves," Patt. Recogn.,vol.21,no.3,pp.217-226,1988

[6] F.Attneave, "Some informational aspects of visual perception," Psychol. Rev., vol.61, pp. 183-193,1954

[7] A.Rattarangsi and R.T.Chin, "Scale-based detection of corners of planar curves," IEEE Trans. Patt.Anal.Machine Intell., vol. 14, pp. 430-448,1992

A Novel Algorithm for Improving the Generalization Capability of Kernel-based LDA Methods

Jian HUANG

Abstract

*Kernel approach has been proposed to solve classification problem with complex distributions by mapping the input space to higher dimensional feature space. Applying kernel trick on Linear Discriminant Analysis (*LDA*) algorithm, some kernel-based* LDA *algorithms have been developed and applied on face recognition in the last five years. The experimental results show that, in general, kernel-based* LDA *methods outperform* LDA *methods. However, one of the crucial factors in kernel-based* LDA *approach is that how to increase the generalization capability of the kernel-based learning methods. The generalization capability means that, after a kernel-based* LDA *algorithm "learns" the distribution of the different classes by a set of training samples, how well the algorithm will be performed with testing sample outside the training set. In order to solve this problem, this paper proposes to adopt the concept of eigenvalue stability bound and develop an optimal kernel parameter estimation (*OKPE*) algorithm. The proposed OKPE algorithm is then applied to two current kernel-based LDA methods, namely* Kernel Subspace-LDA *and* Kernel Direct-LDA. *Experimental results show that after applying the OKPE algorithm, the generalization capability of the two methods are improved and the recognition performance are also improved.*

Keywords: Kernel LDA, Generalization Capability, Kernel parameters and Face Recognition

1 Introduction

Face recognition research has been started in the late 70's and becomes one of the active and exciting research areas in computer science and information technology since 1990 [1, 2]. Many face recognition algorithms/systems have been developed in the last decade. Among various approaches, appearance-based method, in general, gives a promising result. *Linear Discriminant Analysis* (*LDA*) is the most popular methods in appearance-based approach for face recognition. Their superior performances have been reported in many literatures in the last decade [3, 4]. General speaking, *LDA*-based face recognition algorithm gives a satisfactory result under controlled conditions and many of the face image variations, such as facial expressions and small occlusion, can be handled. However, the performance is not satisfactory under some variations, such as illumination and pose. To solve such complicated image variations, kernel trick has been introduced into *LDA* algorithm. The basic idea is to nonlinearly map the input data from input space to higher dimensional feature space, and then perform *LDA* in the feature space. By performing this nonlinear mapping, we hope that the complex distribution becomes linearly separable in feature space. The basic concept of Kernel-based *LDA* is defined as follwos.

Suppose $\phi : \mathbf{R}^d \to F^{df}, x \to \phi(x)$, be a nonlinear mapping from input space $\mathbf{R}$ to a high dimensional feature space F. Consider a C-class problem in feature space, the total set of all classes is represented by $\mathcal{C} = \{\mathcal{C}_1, \mathcal{C}_2, \ldots, \mathcal{C}_C\}$, the jth class $\mathcal{C}_j$ contains N_j samples, $j = 1, 2, \ldots, C$. Let N be the total number of training samples, i.e. $N = \sum_{j=1}^{C} N_j$. Let j-th sample of $\mathcal{C}_i$ be x_j^i . S_w,S_b and S_t can be formulated in feature space F as follows

$$\begin{aligned} S_w &= \sum_{i=1}^{C}\sum_{j=1}^{N_i}(\frac{1}{\sqrt{N}}(\phi(x_j^i) - m_i))(\frac{1}{\sqrt{N}}(\phi(x_j^i) - m_i))^T \\ &= \Phi_w \Phi_w^T \\ S_b &= \sum_{i=1}^{C}(\sqrt{\frac{N_i}{N}}(m_i - m))(\sqrt{\frac{N_i}{N}}(m_i - m))^T \\ &= \Phi_b \Phi_b^T \end{aligned}$$

$$\begin{aligned} S_t &= \sum_{i=1}^{C}\sum_{j=1}^{N_i}(\frac{1}{\sqrt{N}}(\phi(x_j^i) - m))(\frac{1}{\sqrt{N}}(\phi(x_j^i) - m))^T \\ &= \Phi_t \Phi_t^T \end{aligned}$$

Then the kernel-based *LDA* is given by solving the following eigenvalue problem:

$$W = arg\max_W \frac{tr\left(W^T S_b W\right)}{tr\left(W^T S_w W\right)} \tag{1}$$

Recently, many kernel-based *LDA* methods have been developed and applied in face recognition. All the superior performance reported in literatures shows that Kernel-based *LDA* method is a good and feasible approach to solve the illumination and pose problems in face recognition technology. However, the critical problem for assessing the performance of Kernel-based *LDA* method is its generalization capability. Good kernel-based learning method should have stable performance not only on training data but also on testing data. So how to generalize well from training data to testing data is a crucial problem to be considered in kernel-based learning method. In kernel-based *LDA* method, the value of kernel parameters will seriously influence the distribution of the mapped feature vectors in higher dimensional feature space and so kernel parameters are crucial to the generalization performance of Kernel-based *LDA* method. In view of this, we propose an algorithm to automatically tuning the kernel parameters while control the eigenvalue stability to improve the generalization capability of Kernel-based *LDA* method.

The rest of this paper is organized as follows. The proposed algorithm is described detaily in Section 2. In section 3, we briefly describe how to apply our proposed algorithm on existing Kernel-based *LDA* methods. The experimental results are discussed in section 4. Finally, conclusions of this paper are given in Section 5.

2 Proposed Algorithm

We have mentioned that the value of kernel parameters will seriously influence the distribution of the mapped feature vectors in higher dimensional feature space and so kernel parameters are crucial to the generalization capability of Kernel-based *LDA* method. In this paper, we adopt the popular *Gaussian RBF* kernel which is defined as

$$k(x,y) = \exp\left(-\sum_i \frac{(x_i - y_i)^2}{2\theta_i^2}\right) \qquad (2)$$

The *RBF* kernel function consists of scale factors θ_i, which are the kernel parameters that we are going to estimate. The number of parameters may equal to the dimension of the input data. Existing kernel-based *LDA* methods consider $\theta = \theta_1 = \theta_2 = \ldots = \theta_d$ and manually select the best value for θ.

In estimating the kernel parameters, they cannot be too large (e.g. $\theta \to \infty$) nor too small (e.g. $\theta \to 0$) as both situations will give a poor generalization capability on Kernel-based methods. The determination of the kernel parameter is required and is crucial to the generalization performance of Kernel-based methods. When $\theta \to \infty$, all training data points in the input space will be mapped to a single point in the feature space. On these mapped feature points, $Trace(Sb)$ and $Trace(Sw)$ both tend to zero. So applying *LDA* method on such kind of mapped feature points certainly cannot give a good generalization performance. However, when θ decreases from ∞ toward 0, training data points of the same class will cluster to an individual single point in the feature space and training data points belongs to difference classes will be more and more apart from each others accordingly. When $\theta \to 0$, on these mapped feature points, the ratio $\frac{Trace(Sb)}{Trace(Sw)}$ tends to ∞. From the classification point of view, these training data points are well separated after the kernel mapping. The *LDA* projection matrix being generated from such kind of mapped feature points certainly can give good classification results on training data points. However, for a testing data outside of the training set, it may not be able to distinguish them correctly due to "*overfitting*" [5]. In this situation, Kernel *LDA* method cannot be generalized well from training data set to testing data set. From the above discussions, both too large and too small kernel parameters should be avoided. To find the proper value for kernel parameters, the straightforward strategy is to search the whole parameter space and find the best value(s). But this procedure is very time consuming and intractable when the number of parameters exceeds two [6].

In 2002, Mika [7] proposed an eigenvalue stability bound to measure the stability of the principle component analysis. Here, we propose to use the eigenvalue stability bound to measure the generalization capability of Kernel-base *LDA* method. Based on this eigenvalue stability measurement, we propose the *OKPE* algorithm to automatically tuning multiple kernel parameters for Kernel-based *LDA* method. Instead of minimizing the estimation of the generalization error, we propose to maximize an objective function which explicitly depends on kernel parameters and the eigenvalue stability bound is proposed to control the generalization capability of Kernel-base *LDA* method. The objective function we used here is the Maximum Margin Criterion [8]. To have a clear understanding on eigenvalue stability bound, we need the following theorem[7] for discussion.

Theorem 1 [7]: Assume that $\mathcal{X} = \{x_1, ..., x_M\} \subset \mathcal{R}^N$ is generated according to some unkonwn but fixed distribution P and that $\|x - E(X)\| \leq R < \infty$ for all $x \sim P$. Let $C_{\mathcal{X}}$ and $\mathbf{m}_{\mathcal{X}}$ be the covariance matrix and mean estimates from $\mathcal{X}$ and let $C_{(\mathcal{X}\setminus x_i)\cup x}$, $\mathbf{m}_{(\mathcal{X}\setminus x_i)\cup x}$ be the covariance and mean estimated from $\mathcal{X}$ with the *i*-th element replaced by x. Then for any $\mathcal{I} \subset \{1, ..., N\}$ and $i = 1, ..., N$:

$$\left|\sum_{j\in\mathcal{I}} \left[\lambda_j(C_{\mathcal{X}}) - \lambda_j(C_{(\mathcal{X}\setminus x_i)\cup x})\right]\right| \leq \frac{8R^2}{M-2} \qquad (3)$$

(please refer to [7] for detailed proof.)

From theorem 1, we can see that the term $\frac{8R^2}{M-2}$ measures

how much the eigenvalue will be changed after replacing one of training vectors from outside training set. So if the term $\frac{8R^2}{M-2}$ is small, it means that under such distribution P, the eigenvalues of the covariance matrix are less sensitive on the training data set. In other words, we can say that the kernel-based learning algorithm is less sensitive on training data set. In turn, the algorithm will be generalized well from training data set to testing data set. When the number of training samples M are fixed, we can use the bound R in (3) to measure the stability.

From the above discussion, we should choose proper kernel parameters that maximize the objective function while guarantee the good generalization capability in which the bound R cannot be exceeded a threshold.

Based on the above analysis, the detailed procedure of our proposed optimized kernel parameter estimation method is described as follows.

Step 1: Given threshold R^0, step size ρ^0, initialize iteration counter $k = 0$ and kernel parameter set $\theta = (\theta_1, \theta_2, \ldots, \theta_{N_\theta})$ with initial values $\theta^0 = (\theta_1^0, \theta_2^0, \ldots, \theta_{N_\theta}^0)$, where N_θ is the number of kernel parameters to be used in *RBF* kernel function.

Step 2: Based on Kernel-based *LDA* method, find the projection matrix:

$$W^0 = \arg\max_W J(W) = \arg\max_W \frac{W^T S_b W}{W^T S_w W}$$

Step 3: Construct the objective function using the Maximum Margin Criterion:

$$F(W) = tr\left(W^T S_b W - W^T S_w W\right)$$

Step 4: Updates the parameter set θ by a gradient step such that the objective function is maximized as follows

- Compute the gradient D_θ^k to get the search direction which maximizes the objective function

$$D_\theta^k = \left(\frac{\partial F}{\partial \theta_1}, \frac{\partial F}{\partial \theta_2}, .., \frac{\partial F}{\partial \theta_{N_\theta}}\right)$$

- Compute the bound R using $R = max\|y_i - E(Y)\|, i = 1, 2, .., N$, where N is the number of training samples, $y_i = {W^0}^T \phi(x_i), i = 1, 2, \ldots, N$ is the projected sample vector using Kernel-based *LDA* method. If $R > R^0$, then go to step 5.

- Compute the unit vector $\hat{D}_\theta^k$ of the gradient vector D_θ^k

$$\hat{D}_\theta^k = \frac{D_\theta^k}{\|D_\theta^k\|}$$

- Let $\theta = \theta + \rho^0 \hat{D}_\theta^k$ and $k = k + 1$, Go to step 2.

Step 5: Terminate and output results

For the initial value of the kernel parameters, we select the mean of distance of all the training vectors as follows,

$$\theta_1^0 = \theta_2^0 = \ldots = \theta_{N_\theta}^0 = \frac{1}{(N \cdot (N-1))} \cdot \sum_{i,j=1}^{N} \|x_i - x_j\|^2 = \overline{\theta}^0 \tag{4}$$

and the initial step size ρ^0 is set to $\frac{\overline{\theta}^0}{100}$ in our experiments.

3 Applying *OKPE* algorithm on existing Kernel-based *LDA* method

In this section, we will apply the proposed *OKPE* algorithm on two existing kernel-based *LDA* methods, namely *Kernel Subspace-LDA* (*KSLDA*) [9] and *Kernel Direct-LDA* (*KDDA*) [10].

3.1 Applying *OKPE* algorithm on *Kernel Subspace-LDA*

Based on the derivation of *KSLDA* [9] method, the projection matrix W is selected in the sub-null space of S_w. That means the term $tr\left(W^T S_w W\right)$ is equal to zero. So the objective function $F(W)$ can be reformulated as follows,

$$\begin{aligned} F(W) &= tr\left(W^T S_b W\right) \\ &= tr\left(G^T \Phi_t^T \Phi_b \Phi_b^T \Phi_t^T G\right) \\ &= tr\left(G^T P P^T G\right) \end{aligned} \tag{5}$$

where $G = V'' A$ and G is determined by *KSLDA* method, $P = \Phi_t^T \Phi_b$ is a $N \times C$ matrix (please refer to [9] for detailed derivation on G and P) and can be expressed in terms of kernel matrix K as:

$$P = K \cdot \Lambda_{NC} - K \cdot I_{NC} - 1_{NN} \cdot K \cdot \Delta_{NC} + 1_{NN} \cdot K \cdot \Gamma_{NC} \tag{6}$$

where $\Lambda_{NC} = \text{diag}\left([\Lambda_{N_1}, \Lambda_{N_2}, .., \Lambda_{N_c}\right]$ is a $N \times C$ block diagonal matrix, and Λ_{N_i} is a $N_i \times 1$ matrix with all terms equal to $\frac{1}{N\sqrt{N_i}}$. I_{NC} is a $N \times C$ matrix with each element of i-th column equal to $\frac{\sqrt{N_i}}{N^2}$. 1_{NN} is a $N \times N$ matrix with all terms equal to one. $\Delta_{NC} = \text{diag}\left[\Delta_{N_1}, \Delta_{N_2}, .., \Delta_{N_c}\right]$ is a $N \times C$ block diagonal matrix, and Δ_{N_i} is a $N_i \times 1$ matrix

with all terms equal to $\frac{1}{N^2\sqrt{N_i}}$. Γ_{NC} is a $N \times C$ matrix with each element of i-th column equal to $\frac{\sqrt{N_i}}{N^3}$.

So the objective function $F(W)$ can be described as an explicit function of kernel parameters. When initial values of kernel parameters θ^0 are given, to maximize the objective function, we need to find the search direction to update kernel parameters θ^0. To get the search direction, we need to compute the gradient of $F(W)$ with respect to kernel parameters θ.

We denote the partial differentiate of the kernel matrix K with respect to θ_s as ∂K_{θ_s} $(s = 1, 2, .., N_\theta)$ which is a $N \times N$ matrix as follow,

$$\partial K_{\theta_s} = \left[\frac{\partial K_{l,k}^{i,j}}{\partial \theta_s}\right]_{\substack{i=1,..,C,j=1,..,N_i \\ l=1,..,C,k=1,..,N_k}} \tag{7}$$

Then we get $\frac{\partial P}{\partial \theta_s}$ as follows,

$$\begin{aligned}\frac{\partial P}{\partial \theta_s} &= \partial K_{\theta_s} \cdot \Lambda_{NC} - \partial K_{\theta_s} \cdot I_{NC} \\ &\quad - 1_{NN} \cdot \partial K_{\theta_s} \cdot \Delta_{NC} + 1_{NN} \cdot \partial K_{\theta_s} \cdot \Gamma_{NC}\end{aligned} \tag{8}$$

Then the gradient of $F(W)$with respect to θ can be formulated as follows,

$$\frac{\partial F}{\partial \theta_s} = tr(G^T \cdot \frac{\partial P}{\partial \theta_s} \cdot P^T \cdot G + G^T \cdot P \cdot \frac{\partial P^T}{\partial \theta_s} \cdot G) \tag{9}$$

3.2 Applying *OKPE* algorithm on *Kernel Direct-LDA*

Based on the derivation of *KDDA* [10] method, the term $tr\left(W^T S_w W\right)$ is also equal to zero. So the objective function $F(W)$ can be reformulated as follows,

$$\begin{aligned}F(W) &= tr\left(W^T S_b W\right) \\ &= tr\left(\tilde{G}^T \Phi_b^T \Phi_b \Phi_b^T \Phi_b \tilde{G}\right) \\ &= tr\left(\tilde{G}^T \tilde{P} \tilde{P}^T \tilde{G}\right)\end{aligned} \tag{1}$$

where $\tilde{G} = \left(E_m \cdot \Lambda_b^{-1/2} \cdot P \cdot \Lambda_w^{-1/2}\right)$, $\tilde{P} = \Phi_b^T \Phi_b$ is a $N \times C$ matrix and can be expressed in terms of kernel matrix K as:

$$\begin{aligned}\tilde{P} &= \frac{1}{N} B \cdot (A_{NC}^T \cdot K \cdot A_{NC} - \frac{1}{N}(A_{NC}^T \cdot K \cdot 1_{NC})) \cdot B \\ &\quad - \frac{1}{N} B \cdot (\frac{1}{N}(1_{NC}^T \cdot K \cdot A_{NC}) + \frac{1}{N^2}(1_{NC}^T \cdot K \cdot 1_{NC})) \cdot B\end{aligned} \tag{11}$$

where $B = diag[\sqrt{N_1}, \ldots \sqrt{N_C}]$, 1_{LC} is a $N \times C$ matrix with terms all equal to one, $A_{NC} = diag[a_{C_1}, \ldots, a_{C_C}]$ is a $N \times C$ block diagonal matrix and a_{C_i} is a $C_i \times 1$ vector with all terms equal to $\frac{1}{C_i}$ (please refer to [10] for detailed derivation on $\tilde{G}$ and $\tilde{P}$).

So the objective function $F(W)$ can be described as an explicit function of kernel parameters. To get the search direction, we need to compute the gradient of $F(W)$ with respect to kernel parameters θ.

We get $\frac{\partial \tilde{P}}{\partial \theta_s}$ as follows,

$$\begin{aligned}\frac{\partial \tilde{P}}{\partial \theta_s} &= \frac{1}{N} B \cdot (A_{NC}^T \cdot \partial K_{\theta_s} \cdot A_{NC} - \frac{1}{N}(A_{NC}^T \cdot \partial K_{\theta_s} \cdot 1_{NC}) \\ &\quad - \frac{1}{N}(1_{NC}^T \cdot \partial K_{\theta_s} \cdot A_{NC}) - \frac{1}{N^2}(1_{NC}^T \cdot \partial K_{\theta_s} \cdot 1_{NC})) \cdot B\end{aligned} \tag{12}$$

Then the gradient of $F(W)$with respect to θ can be formulated as follows,

$$\frac{\partial F}{\partial \theta_s} = tr(\tilde{G}^T \cdot \frac{\partial \tilde{P}}{\partial \theta_s} \cdot \tilde{P}^T \cdot \tilde{G} + \tilde{G}^T \cdot \tilde{P} \cdot \frac{\partial \tilde{P}^T}{\partial \theta_s} \cdot \tilde{G}) \tag{13}$$

4 Experimental results

In this section, two public face databases, namely *Feret* and *YaleB* face database are adopted to evaluate our proposed *OKPE* algorithm applied on *KSLDA* and *KDDA* methods.

4.1 Face Image Databases

In *FERET* database, we select 250 people, 4 frontal-view images for each individual. Face image variations include illumination, facial expression, partial occlusion and aging [11]. All images are aligned by the centers of eyes and mouth and then normalized with resolution 92×112. Images from two individuals are shown in Figure 1.

Figure 1. Images of two persons from FERET database

The Yale Group B face database contains 5850 source images of 10 subjects each captured under 585 viewing conditions (9 poses$\times$ 65 illumination conditions). In our experiments, we use images under 45 illumination conditions. These 4050 images (9 poses$\times$ 45 illumination conditions) are divided into four subsets according to the angle the light source direction makes with the camera axis, namely subset 1 (0° to 25°, 7 images per pose), subset 2 (up to 12°,

Figure 2. Images of one person from *YaleB* database

12 images per pose), subset 3 (up to $50°$, 12 images per pose), and subset 4 (up to $77°$, 14 images per pose) [12]. All frontal pose images are aligned by the centers of eyes and mouth and the other images are aligned by the center points of the faces. Then all images are normalized with the same resolution 92×112. Some images from one individual are shown in Figure 2. To reduce the computational complexity, wavelet transform is applied on all images so that the resolution of all images is 30×25.

4.2 Results on *KSLDA* method

In this part, we will apply the *OKPE* algorithm on *KSLDA* method and evaluate the generalization capability of the algorithm on *Feret* and *YaleB* databases respectively.

It is known that the results will be different with different training and testing images. To avoid this error, the experiments are repeated 10 times. For each person, we randomly pick 2 images (250x2=500) for training and the rest of the 2 images (250x2=500)for testing. Then the average accuracy is calculated and reported. Table 1 shows the comparison results of the *KSLDA* method with and without *OKPE* algorithm. For the *KSLDA* method without *OKPE* algorithm, we will consider $\theta = \theta_1 = \theta_2 = \ldots = \theta_d$ and manually select one relatively better value for θ in all our experiments. Here, $2\theta^2$ is set to $4e5$ for the *KSLDA* method without *OKPE* algorithm. For the *KSLDA* method with *OKPE* algorithm, the initial value of the eigenvalue stability bound R^0 in our experiments is set to $5e-3$. To balance the performance and the computational load, we use 30 kernel parameters in *Gaussian RBF* kernel function for face recognition application. An image will be divided into 30 blocks and all pixels in one block will share the same parameter.

We can see from Table 1 that *KSLDA* has more than 4 percents improvement in *Rank-1 Accuracy* with the use of *OKPE* algorithm. The generalization capability of *KSLDA* method with *OKPE* algorithm is better than that of original *KSLDA* method.

Table 1. Performance comparison on *Feret* database

Method	Rank 1	Rank 2	Rank 3
KSLDA	80.36%	82.58%	83.68%
KSLDA with *OKPE*	84.44%	85.86%	86.74%

To evaluate the generalization capability with more complicated image variations, *YaleB* face database is used to evaluate the generalization capability of *KSLDA* method with *OKPE* algorithm along pose and illumination dimensions. The experiment settings are as follows. For each pose, we will select 2 images from each illumination subset (out of 4 subsets). This is to say that we will randomly select 720 images (10 persons$\times$9 poses$\times$4 subsets $\times$2 images) for training and the rest of 3330 (10 persons$\times$9 poses$\times$37 images) images for testing. The experiments are repeated 10 times and the average rank 1 to rank 3 accuracies are recorded and shown in Table 2. It can be seen from Table 2 that *KSLDA* method with *OKPE* algorithm has better generalization performance than *KSLDA* method. There are more than 3 percents improvement in *Rank-1 Accuracy*.

Table 2. Performance comparison on *YaleB* database

Method	Rank 1	Rank 2	Rank 3
KSLDA	88.48%	92.18%	94.86%
KSLDA with *OKPE*	91.92%	94.68%	96.13%

4.3 Results on *KDDA* method

Similarly, in this part, we will apply the *OKPE* algorithm on *KDDA* method and evaluate the generalization performance of the algorithm on *Feret* and *YaleB* database respectively. The experiment settings are the same with that for applying the *OKPE* algorithm on the *KSLDA* method.The experiments are repeated 10 times with randomly picked samples for training and the other samples for testing. Table 3 and talbe 4 show the comparison results between *KDDA* method and *KDDA* method with *OKPE* algorithm. As *KDDA* consists of two parameters, namely kernel parameter for *Gaussian RBF* function θ and regularization parameter η for ill-posed within-class scatter matrix. The parameter settings for *KDDA* method without *OKPE* algorithm are $2\theta^2 = 5e5$ and $\eta = 1e-2$. For the *KDDA* method with *OKPE* algorithm, the initial value of the eigenvalue stability bound R^0 in our experiments is set to $1e2$.

Table 3. Performance comparison on *Feret* database

Method	Rank 1	Rank 2	Rank 3
KDDA	78.86%	80.86%	82.10%
KDDA with *OKPE*	79.94%	81.24%	82.16%

Table 4. Performance comparison on *YaleB* database

Method	Rank 1	Rank 2	Rank 3
KDDA	75.20%	85.85%	90.54%
KDDA with *OKPE*	77.10%	86.75%	92.38%

The results from Table 3 and Table 4 both show that *KDDA* method with *OKPE* algorithm has better generalization performance than *KDDA* method.

5 Conclusions

This paper discusses the importance of the concept of generalization capability of kernel-based LDA methods and proposes a new optimized kernel parameter estimation (OKPE) algorithm to improve the existing kernel-based LDA methods for the applications on face recognition technology. The proposed method is developed based on the concept of eigenvalue stability bound and estimate the multiple kernel parameters automatically by maximizing the margin while preserving the eigenvalue stability. The proposed OKPE algorithm has been applied to two existing kernel-based LDA methods, namely *Kernel Subspace-LDA* and *Kernel Direct-LDA*. Two public available face databases, namely *Feret* face database and *YaleB* face database, have been selected to evaluate the proposed algorithm. Experiments results show that after applying the OKPE algorithm, the generalization capability of the two methods are improved and the recognition performance are also improved.

Acknowledgments

This project was supported by the Science Faculty Research grant of Hong Kong Baptist University RGC Earmarked Research Grant HKBU-2119/03E and NSFC (60144001, 10101013). The authors would like to thank the US Army Research Laboratory for contribution of the *FERET* database, and thank Yale University for providing the *YaleB* database. Also, the author would like to thank Dr. Lu for providing the matlab code of *KDDA*.

References

[1] R. Chellappa, C. Wilson, and S. Sirohey, "Human and machine recognition of faces: a survey," *Proceedings of the IEEE*, vol. 83, no. 5, pp. 705–740, 1995.

[2] W. Zhao, R. Chellappa, A. Rosenfeld, and P. Phillips, "Face recognition: A literature survey," *ACM Computing Survey*, vol. 35, pp. 399–458, 2003.

[3] A. M. Martinez and A. C. Kak, "PCA versus LDA," *IEEE Transactions on Pattern Analysis and Machine Intelligence*, vol. 23, no. 2, pp. 228–233, 2001.

[4] P. N. Belhumeur, J. P. Hespanha, and D. J. Kriegman, "Eigenfaces vs. fisherfaces: Recognition using class specific linear projection," *IEEE Transactions on Pattern Analysis and Machine Intelligence*, vol. 19, no. 7, pp. 711–720, 1997.

[5] W. j. Wang, Z. B. Xu, W. Z. Lu, and X. Y. Zhang, "Determination of the spread parameter in the gaussian kernel for classification and regression," *Neurocomputing*, vol. 55, no. 1, pp. 643–663, 2003.

[6] O. Chapelle, V. Vapnik, O. Bousquet, and S. Mukherjee, "Choosing multiple parameters for support vector machines," *Machine Learning*, vol. 46, no. 1, pp. 131–159, 2002.

[7] Mika, "Kernel fisher discriminants," Ph.D. Thesis, Technical University of Berlin, Technical University of Berlin , School of Electrical Engineering and Computer Sciences, 12 2002.

[8] H. Li, T. Jiang, and K. Zhang, "Efficient and robust feature extraction by maximum margin criterion," in *Advances in Neural Information Processing Systems 16*.

[9] J. Huang, P. C. Yuen, W. S. Chen, and J. H. Lai, "Face recognition using kernel Subspace-LDA algorithm," *Proceeding of Asian Conference on Computer Vision*, vol. 1, no. 10, pp. 61–66, Jan. 2004.

[10] J. W. Lu, K. Plataniotis, and A. N. Venetsanopoulos, "Face recognition using kernel direct discriminant analysis algorithms," *IEEE Transactions on Neural Networks*, vol. 14, no. 1, pp. 117–126, Jan. 2003.

[11] P. J. Phillips, H. Moon, S. A. Rizvi, and P. J. Rauss, "The FERET evaluation methodology for face-recognition algorithms," *IEEE Transactions on Pattern Analysis and Machine Intelligence*, vol. 22, no. 10, pp. 1090–1104, 2000.

[12] A. S. Georghiades, P. N. Belhumeur, and D. J. Kriegman, “From few to many: Illumination cone models for face recognition under variable lighting and pose,” *IEEE Transactions on Pattern Analysis and Machine Intelligence*, vol. 23, no. 6, pp. 643–660, 2001.

Handwriting-based Writer Identification

HE Zhenyu

Abstract

Handwriting-based writer identification is a hot research field in pattern recognition. Nowadays, on-line Handwriting-based writer identification is steadily growing toward its maturity. As a contrast, off-line handwriting-based writer identification still keeps as a challenging problem because, in off-line case, the writing features only can be extracted from the handwriting image as leads to plenty of valuable writing information is lost. 2D Gabor filter method is wildly acknowledged to be a good method for off-line handwriting identification, nevertheless, it still suffers from some limitations e.g. high computational cost. In our research, we present a novel wavelet-based GGD method to replace the traditional 2D Gabor filters. Shown in our experiments, this novel method not only achieves better experiment results but also greatly reduces the elapsed time.

1 Introduction

Even with fast development of modern society and new techniques, handwriting has continued to persist as a means of communication and recording information in daily life. Given its ubiquity in human transactions, automated writer identification of handwriting has practical significance in postal addresses on envelopes, in legal amounts on bank checks, in handwritten fields in forms, etc.

We can classify handwriting-based writer identification in several ways. However, the most straightforward one is to distinguish between on-line (also called dynamic) and off-line (also called static) writer identification by input method. The former assumes that a transducer device is connected to the computer, which can convert writing movement into a sequence of signals and send the information to the computer. Since information on the time order and dynamics of the writing process which is captured by the transducer device contains many useful writing features of the writer, on-line handwriting-based writer identification, contrasted to off-line handwriting-based writer identification, is easier to do and get higher accuracy. Off-line handwriting-based writer identification usually deals with handwriting materials scanned into computer with certain resolution, so dynamic information of writing is lost. And despite continuous effort, off-line handwriting-based writer identification still remains a difficultly challenging issue.[1] Unfortunately, on-line system is inapplicable in many cases, and thus developing techniques on off-line writer identification is an urgent task.

Further, the off-line writer identification can also be divided into two parts: text-dependent and text-independent.[1] Text-dependent methods matche the same character and so the writer is required to write the fixed text. Contrastively, given that the handwritings of different people are often visually distinctive, text-independent methods do not require fixed matching characters but extract writing style features from the global writing text. Generally, text-dependent methods have good performances in writer identification, however it is inapplicable in many practical applications because of its requirement on same character. Though owning a wide applicability, while at present, text-independent methods don't obtain as high accuracy as text-dependent methods do. Thus, more research works should be done in text-independent writer identification.

2 Relative work

The Writer identification is the process of confirming a writer's identity by comparing some specific attributes of his handwriting with those of all the writers enrolled in a reference database. Commonly, writer identification is regarded as a typical problem of pattern recognition and contains basically 3 steps: pre-processing, feature extraction, feature matching.

Nowadays, it is an active research field in academia because it is a combination of traditional pattern recognition with jumped-up biometric Authentication. Recently, more and more researchers have touched on this field and some attempts have been presented.[2] But most previous research works are about text-dependent writer identification, especially on signature verification. Even so, there still are some papers on text-independent writer identification, here we introduce these relative works in short. Duverony has reported that the most important variation of the writers transfer is reflected in the low-frequency band of Fourier

spectrum of the handwriting images,[3] as points out that the writing feature in frequency domain is very valuable for writer identification. Similarly, Kuckuck has used Fourier transform techniques to process handwritten text as texture. [4] Inspired by the idea of multichannel spatial filtering technique, Said, Tan and Baker proposed a texture analysis approach.[1] In this method, they regards the handwriting as an image containing some special textures and applied a well-established 2-D Gabor filtering technique to extract features of such textures. Schrihari and Cha extracted twelve shape features from the handwriting text lines to represent personal handwriting style. The features mainly contain visible characteristics of the handwriting, such as width, slant and height of the main writing zones. [5] To improve the accuracy and enhance the robustness, some other papers adopted multiple features integration to writer identification. [5][6].

3 Traditional Gabor method

The Gabor function is the name given to a Gaussian weighted sinusoid. The function is named after Dennis Gabor who used this function in the 1940s. Later, Daugman proposed the function to describe the spatial response of cells in visual stimuli experiments.[8] The preprocessing of images by Gabor function is chosen for its biological relevance and technical properties. The Gabor function is of similar shape as the receptive fields of simple cells in the primary visual cortex. It is localized in both space and frequency domains and has the shape of plane waves restricted by a Gaussian function.

Nowadays, the academia widely acknowledge the 2D Gabor method is an effective method on text-independent writer identification. The computational models of the 2D Gabor filters proposed in reference [1][2] is as follows:

$$h_e(x,y) = g(x,y)\cos[2\pi f(x\cos\theta + y\sin\theta)] \quad (1)$$

$$h_o(x,y) = g(x,y)\sin[2\pi f(x\cos\theta + y\sin\theta)] \quad (2)$$

where h_e and h_o denote the so-called even- and odd- symetric Gabor filters, and $g(x,y)$ is an isotropic Gaussian function.

The spatial frequency responses of the Gabor functions are

$$H_e(u,v) = \frac{[H_1(u,v) + H_2(u,v)]}{2} \quad (3)$$

$$H_o(u,v) = \frac{[H_1(u,v) - H_2(u,v)]}{2} \quad (4)$$

where $j = \sqrt{-1}$ and

$$H_1(u,v) = \exp\{-2\pi^2\sigma^2[(u - f\cos\theta)^2 + (v - f\sin\theta)^2]\}$$

$$H_2(u,v) = \exp\{-2\pi^2\sigma^2[(u + f\cos\theta)^2 + (v + f\cos\theta)^2]\}$$

f, θ, σ are the spatial frequency, orientation, and space constant of the Gabor envelope. For a given input image, $h_e(x,y)$ and $h_o(x,y)$ will combine to provied different channel out of the input image with different f, θ and σ.

The mean values(M) and the standard deviation(S) of the channel output images are used to represent writer global feature for writer identification.

4 New wavelet-based GGD method

Though 2D Gabor filters achieve success in handwriting-based writer identification, this method still suffers from its disadvantages as greatly limit its practicability. One of the most serious disadvantages is its intensive computationally cost, because the 2D Gabor filters have to convolute the whole image in each orientation and each frequency, .

Contrast to the Gabor filters, 2D wavelet can decompose the image into subbands with different frequency and orientation. So, for each frequency and each orientation, we only need to deal with the specified wavelet subband.

Previous experimental work revealed a particular property of the wavelet coefficients $\{WI_j(x,n,i)\}_{x\in R}$ of almost every natural textured image at a given scale n and the subband number j, that the histogram of these coefficients corresponds to a Generalized Gaussian Density model.[9]

The Generalized Gaussian Density(GGD) model is given as

$$p(x;\alpha,\beta) = \frac{\beta}{2\alpha\Gamma(1/\beta)}\exp^{-1(|x|/\alpha)^\beta} \quad (5)$$

where $\Gamma(\cdot)$ is the Gamma function, i.e.,

$$\Gamma(\cdot) = \int_0^\infty \exp^{-t} t^{Z-1}dt, Z > 0.$$

The parameter $\alpha > 0$, called scale parameter, describes the standard deviation and $\beta > 0$, called shape parameter, is inversely proportional to the decreasing rate of the peak. The basic idea of GGD model is to take the parameter couple $\{\alpha, \beta\}$ as the feature of wavelet subband.

We use Kullback-Leibler distance (KLD) for feature matching. The Kullback-Leibler distance (KLD) between two subbands as

$$D(p(\cdot;\alpha_1,\beta_1)\|p(\cdot;\alpha_2,\beta_2)) = \log(\frac{\beta_1\alpha\Gamma(1/\beta_2)}{\beta_2\alpha_1\Gamma(1/\beta_1)}) + (\frac{\alpha_1}{\alpha_2})^{\beta^2}\frac{\Gamma((\beta_2+1)/\beta_1)}{\Gamma(1/\beta_1)} - \frac{1}{\beta_1}; \quad (6)$$

and the Kullback-Leibler distance (KLD) between two handwriting image is the sum of all the distances across all analysed wavelet subbands.

5 Experiment

To contrast the our GGD method to tranditional Gabor method fully, we make two experiments in this paper.

5.1 Experiment 1

20 Chinese handwritings written by 10 persons have been carried out in this experiment, with one training handwriting and one testing handwriting for each person. We produce one handwriting texture image from each handwriting, and thus a total of 20 handwriting texture image are obtained. The test handwriting texture image consists of 64 Chinese characters with size 512×512, as is shown in fig.1 (b). In Gabor method, we use all means and standard deviations at 32, 64, 128, 256; 0, 45, 90and 135, because both reference [1].

A testing handwriting texture image is matched with all training handwriting texture images. And then the place of real writer of the testing handwriting in the sort list of matching results is regarded as the experiment result which can evaluate our algorithm. (For example, if the matching value between the training handwriting and testing handwriting, both of which are written by the same writer, is minimum in the sort list, we say the place of real writer is top 1; in other words, the topper the place of one writer is, the more possibility of being the real writer of the testing handwriting the writer has). The experiment result is in the table 1.

Table 1. IDENTIFICATION ACCURACY OF EXPERIMENT 1

Method name	Top 1	Top 2
GGD	80%	20%
Gabor	70%	30%

Not only contrast the identification accuracy, we also measure the average elapsed time of the two methods. We run and record the average elapsed time of GGD and Gabor methods in Matlab 7.0. The operation system of our computer is Window XP, and the hardware environment of our computer is: Intel Pentium IV 2.66GHZ CPU, 512MB RAM. The experiment result is in the table 2.

5.2 Experiment 2

In this experiment, we divide each handwriting texture image with size = 512 into 4 non-overlap subimages with size = 256. All 4 subimages of training handwriting texture image are used for training, and all 4 subimages of testing handwriting texture image are used for testing. But different from the experiment 1, only when the matching result is top 1, we regard the identification is correct. The experiment result is in the table 3.

Table 2. ELASTED TIME of THE GGD AND GABOR METHOD

Method name	Average elapsed time (second)
GGD	19.338
Gabor	124.812

Table 3. IDENTIFICATION ACCURACY OF EXPERIMENT 2

Method name	Identification accuracy
GGD	92.5%
Gabor	87.5%

References

[1] H.E.S.Said, T.N.Tan, K.D.Baker, *Personal identification based on handwriting* Pattern Recognition, vol.33, no.1, pp.149-160, 2000.

[2] Y. Zhu, Y. Wang and T. Tan, *Biometric Personal Identification Based on Handwriting* Proc. 15th International Conference on Pattern Recognition , volume 2, Barcelona, Spain, Sep3-7, 2000, pp.801–804.

[3] J.Duvernoy, *Handwriting synthesis and classification by means of space-variant transform and Karhunen-Loeve analysis* J.Opt.Soc.Am.65(1975), pp.1331-1336.

[4] W.Kuckuck, *Writer identifcation by spectra analysis* Processdings of the international Conference On Security Through Science Engineering, West Berling, Geranу, 1980, pp.1-3.

[5] S.Cha, S.N.Srihari, *Multiple Feature Integration for writer Verification* the Precddings of 7th IWFHR2000, amstredam, Netherland, September 2000, pp.333-342.

[6] E.N.Zois, V.anastassopousls, *Fusion of Correlated Decisions for Writer Verification* Pattern Recognition, vol.33, no.10, pp.1821-1829, 1999.

[7] Yasushi Yamazaki and Naohisa Komatsu, *A proposal for text-indicated writer verification method* the 4th In-

ternational Conference Document Analysis and Recognition, Ulm, German, August 18 - 20, 1997, pp.333-342.

[8] J.G.Daugman, *Uncertainty relation for resolution in space, spatial frequency, and orientation optimized by two-dimensional visual cortical filters* J.Opt.Soc.Am. A2, pp.1160-1169, 1985.

[9] G. Van de Wouwer, P. Scheunders, D. Van Dyck, *Statistical Texture Characterization from Discrete Wavelet Representations* IEEE transactions on image processing, 8:4, pp. 592-598, 1999.

[10] M. N. Do and M. Vetterli, *Wavelet-based texture retrieval using generalized Gaussian density and Kullback-Leibler distance* IEEE Transactions on Image Processing, vol. 11, pp. 146-158, Feb. 2002.

A New Approach for Locating Mobile Stations under the Statistical Directional Propagation Model

Kenneth M.K. Chu

Abstract

Recently, mobile location estimation is drawing considerable attention in the field of wireless communications. Among different mobile location estimation methods, the one which estimates the location of mobile stations with reference to the wave propagation model is drawing much attention on the grounds that it is applicable to different kinds of cellular network. However the estimation accuracy of the signal propagation model deteriorates as the distance between the mobile station and the receiving base station increases. In view of this, we have designed a New Location Estimation Approach which has divided the location estimation into two phases, the Data Collection Phase and the Location Estimation Phase. We tested the approach with real life data collected from a major mobile operator of Hong Kong. Results show that the New Location Estimation Approach has improved the existing statistical signal propagation model by 30.94%.

1 Introduction

Wireless location has received considerable interest over the past few years due to its great potential in different kind of applications such as logistics, tourism and entertainment. Since cellular radio networks have good coverage in most of the populated areas. Hence, using existing cellular network for location estimation is a more economical solution compared with the Global Positioning System (GPS). Many mobile location methods have been proposed. Basically, these methods are making use of the Time-Of-Arrival (TOA), Angle-Of-Arrival (AOA), Time-Different of Arrival (TDOA) and Received Signal Strength (RSS) for estimating the location of the mobile station (MS). Most of the proposed methods are developed for CDMA cellular system [5, 1]. Hence, these methods are not applicable to all kinds of cellular systems. On the other hand, Received Signal Strength (RSS) is a common attribute in all cellular radio system. Therefore, using RSS to estimate the location of MS is a more general approach.

The Location Fingerprinting is one of the approaches that make use of the RSS. Although the Location Fingerprinting has been widely used in indoor positioning and has been proven for its great accuracy, it is difficult to be implemented in the outdoor due to the scale up problem arise from the large amount of data collection and storage. Moreover, the Location Fingerprint approach is very sensitive to the surrounding environment. It requires re-calibration when the environment changes [4].

The signal propagation model is one of the promising methods for location estimation which utilizes the RSS. The distance between the transmitter and the receiver [1] can be predicted by the mean signal strength with reference to a signal propagation model. However, many factors, such as signal fading, would affect the accuracy of the estimation.

Our new approach has divided the location estimation into two phases. In the first phase, estimation points will be collected using the Directional Propagation Model (DPM) which is designed by our group in previous stage [6]. And in the second phase, we will perform an estimation with the Adaptive Weighted FingerPrinting (AWFP). The AWFP is similar to the Location Fingerprinting, it assumes location with similar RSSs are closed to each other. Experiment has been conducted using this new approach with 195,160 sets of real life data. Results show that the new approach yields good performance even when the MS-BTS separation is large.

2 The New Location Estimation Approach

Our proposed approach has divided the location estimation into two phases, the *Data Collection Phase* and the *Location Estimation Phase* as illustrated in the Figure 1. In Figure 1, M_T is the target MS that is requesting the location estimation service while $M_1, M_2, ...M_n$ are the neighboring MSs. RSS_Vector_i contains the RSSs, $(s_{i0}, s_{i1}, ...s_{iN})$ with their corresponding receiving BTS denoted by $(\mathrm{CID}_{i0}, \mathrm{CID}_{i1}, ...\mathrm{CID}_{iN})$ of the i^{th} MS, where N is the maximum number of BTSs that can be received by MS. (x_{Di}, y_{Di}) and ε_{Di} is the estimation and the expected

[1] Both MS and BTS can be transmitter and receiver at the same time.

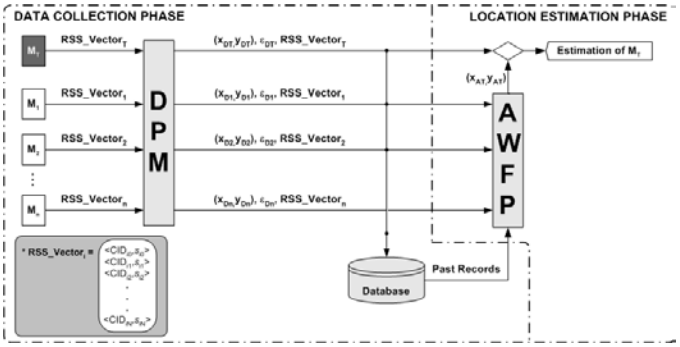

Figure 1. Structure of the new location estimation approach

error of the i^{th} MS with the DPM model respectively, and the (x_{AT}, y_{AT}) is the estimation position of the target MS using the AWFP location estimation algorithm.

2.1 Data Collection Phase

In normal circumstance, a radio cellular network involves many MSs and the position of these MSs should be able to estimate by the operator. On the other hand, when a MS requesting for location service, operator should be able to find neighboring MSs which has similar RSS vector as the target MS at the same time. While the estimation error of these neighboring MSs may be differ due to the signal fading and the separation between the MS and the BTS. In order to determine the estimation error, the statistical DPM model has been chosen in this phase. Using a statistical model in the first phase is on the grounds that the location estimated by the statistical model will come with a probability and this probability can reflect the confidence of the estimation to a certain extent.

In addition to using the probability to determine the estimation accuracy, one can make used of the range estimation. We assume that the posterior p.d.f of the actual location of the target MS is larger than zero. Thus, by finding the maximum distance difference between the estimated location, l, and every possible locations, we will have the upper bound of the estimation error. With the error estimation, we could filter out the *Bad* estimations. On the other hand, the *Good* estimations will be passed to the next phase and store in the database also.

2.2 Location Estimation Phase

When the *Good* estimations has passed to the Location Estimation Phase, the position of the target MS will be estimated by using the AWFP. The basic idea of the AWFP is similar to the Location Fingerprinting. It is defined as,

$$\begin{cases} x_{AT} = \frac{\sum_{i=1}^{n} w_i x_{Di}}{\sum_{i=1}^{n} w_i} \\ y_{AT} = \frac{\sum_{i=1}^{n} w_i y_{Di}}{\sum_{i=1}^{n} w_i} \end{cases} \quad (1)$$

where w_i is the weighting factor of the i^th neighboring MS and is given as follows,

$$w_i = \frac{M^p}{\sum_{j=1}^{N} |s_{Tj} - s_{ij}|} \quad (2)$$

In Eq 2, p is the power factor that needs to be adjusted. M is the number of common receiving BTSs between the target MS and the i^{th} neighbor MS.

After calculating the position of the target MS using the AWFP, the results of the DPM and the AWFP will be compared. The comparison is based on the error estimation of the DPM. If the error estimation of the position estimated by the DPM does not exceeded a pre-defined bound, the DPM estimation will be selected. Otherwise, the AWFP will be selected.

3 Experiments and Results

Table 1. Comparison between the *Bad* set and the New Location Estimation Approach

Method	Avg. Err.	Min. Err.	Max. Err.	Variance
New Approach	360.44 m	31.25 m	1135.34 m	41946.44
DPM - *Bad* Set	521.96 m	202.44 m	3370.21 m	168179.28

A comparisons between the *Bad* set and the the results using the new location estimation approach is showed in Table 1. As observed from Table 1, the New Location Estimation Approach enhanced the *Bad* set in a great extent. The average error of the *Bad* set using the New Location Estimation Approach has improved up to 30.94%.

References

[1] A. Tarighat, N. Khajehnouri and A. H. Sayed. Cdma location using multiple antennas and interference cancellation. In *Proceedings of VTC2003-Spring*, volume 4, Jeju, Korea, April 2003.

[2] A. Tarighat, N. Khajehnouri and A. H. Sayed. Improved wireless location accuracy using antenna arrays with interference cancellation. In *Proceedings IEEE International Conference on Acoustics, Speech, and Signal Processing (ICASSP)*, Hong Kong, April 2003.

[3] Federal Communications Commission. Revision of the commission's rules to ensure compatibility with enhanced 911 emergency calling systems. Technical Report CC Docket No.94-102, Report and Order and Further Notice of Proposed Rulemaking, July 1996.

[4] Heikki Laitinen, Suvi Ahonen, Sofoklis Kyriazakos, Jaakko Lahteenmaki, Raffaele Menolascino, Seppo Parkkila. Cellular location technology. Technical Report 007, VTT Information Technology, November 2001.

[5] J. J.J. Caffery. *Wireless Location in CDMA Cellular Systems*. Kluwer Academic Publisher, Boston, 2000.

[6] Kenneth M.K. Chu, Karl R.P.H. Leung, Joseph Kee-Yin Ng, Chun Hung Li. Locating mobile stations with statistical directional propagation model. In *Proceedings of the 17th International Conference on Advanced Information Networking and Applications (AINA2004)*, pages 230–235, Fukuoka, Japan, March 29-31 2004.

[7] Masato Aso, Manabu Kawabata and Takeshi Hattori. A New Location Estimation Method Based on Maximum Likelihood Function in Cellular Systems. In *Proceedings of VTC2001-Fall*, Atlantic City, NJ USA, October 7-11 2001.

[8] Masato Aso, Takahiko Saikawa, Takeshi Hattori. Mobile Station Location Estimation using the Maximum Likelihood Method in Sector Cell Systems. In *Proceedings of VTC2002-Fall*, Vancouver, British Columbia, Canada, September 24-28 2002.

[9] T. S. G. G. R. A. Network. *3GPP TS 05.08 v8.16.0*. 3rd Generation Partnership Project (3GPP), 2003-04. Radio subsystem link control.

[10] T. Rappaport. *Wireless Communications: Principles & Practice*. Prentice Hall PTR, Upper Saddle River, New Jersey, 2002.

[11] Teemu Roos, Petri Myllymaki, Henry Tirri. A statistical modeling approach to location estimation. In *IEEE Transactions on Mobile Computing*, volume 1, pages 59–69, January-March 2002.

[12] W. Burgard, D. Fox, D. Hennig, and T. Schmidt. Estimating the absolute position of a mobile robot using position probability grids. In *Proceedings 13th National Conf. on Artificial Intelligence (AAAI-1996)*, Portland, 1996.

Wireless LAN Positioning with Mobile Devices in a Library Environment

William H., Wong

Abstract

This paper describes the issues involved in performing location tracking in a library environment using existing Wireless LAN infrastructure and Personal Digital Assistants. Limitations on computation power and operating systems support are considered in the experiment design and four mainstream location estimation algorithms: Center of Gravity, Triangulation, Smallest M-vertex Polygon and Fingerprinting, are being compared to facilitate location-aware computing.

1 Introduction

Many research work had been proposed for office environment, which could be dynamic and need frequent re-profiling. Researchers have concentrated on minimizing profiling effort by using sniffers [2] and performs environmental profiling [1].

In this paper, we propose an interesting location-aware application, book finding within a library, which requires high precision of estimation. Our site, the library, is a static environment and the need of re-profiling is minimal. But in other perspective, obstacle in library brings unseen challenges to many existing location estimation techniques. This blockage includes crowded metal bookshelves and books which act like a wall and effective blocks radio signal. When compared to other studies, the environment we conducted the experiment resembles a small building with 20 tiny offices which are 1.5m $\times$ 6m big and each of them are separated by walls as thick as 2 feet.

Here, we present four algorithms of two different streams and evaluate their performance at static location estimation. Improvements had been made to increase accuracy for each of the algorithm. In addition, fusion between algorithms were introduced to stabilize the system.

2 Algorithms

We will study two different approaches, antenna-centric and location-centric, including four different algorithms, and their performance on location estimation. We will study antenna-centric algorithms: Weighted Center-of-Gravity (CG) [3] and Triangulation, and location-centric algorithm: Smallest M-vertex Polygon (SMP) [4] and Fingerprint using Nearest Neighbors in Signal Space (NNSS).

2.1 Antenna-centric approach

2.1.1 Weighted Center-of-Gravity algorithm

The idea of weighted Center-of-Gravity (CG) is based on natural competition. A strength value (RSS) was assigned to every participating node (active AP). Competition rule is very simple, given n elastic cords connected between the actual position and every AP. AP with higher strength value will increase the tension on the particular elastic cord, which will move the estimated position closer to the AP.

2.1.2 Triangulation algorithm

Another antenna-centric method is triangulation algorithm. For each neighbor AP, a circle is formed and centered at the position of the AP. Depends on the signal strength value, radius of the circle is estimated by a principal formula which was trained at the data preparation phase. The circle illustrates locus of positions which the user may lies on. Intersection points between all circles are collected and triangles are formed. The estimated position is the centroid of the smallest area triangle. On the other hand, if number of candidates is insufficient to form any triangle, the estimated location would be the averaged result.

2.2 Location-centric approach

2.2.1 Smallest M-vertex Polygon algorithm

Smallest M-vertex Polygon (SMP) method is similar to triangulation. But instead of performing space transformation (or propagation model training) between signal space and world space, SMP performs estimation with a discrete approach. Similarly, a number of candidate locations were promoted by each neighbor AP. The idea of SMP is to find a common candidate amongst all promoted locations.

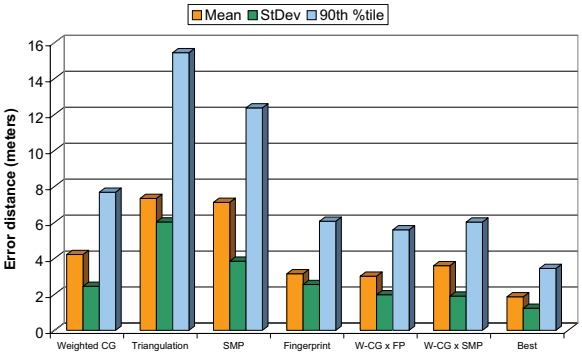

Figure 1. Overall result (bold value indicates best performer)

2.2.2 Fingerprint algorithm

The basic of fingerprint algorithm is to remember different radio characteristics at different locations (or markers). Radio characteristics (or snapshot) includes unique network address and RSS of nearby APs. In preparation phase, these information along with the marker location, which served as primary key, will be stored in a characteristics database

$$db_n = \langle \underline{x, y}, (addr_1, rss_{addr_1}), \ldots, (addr_i, rss_{addr_i}) \rangle \quad (1)$$

where x, y denotes the marker location of the snapshot, and $(addr_i, rss_i)$ represent unique network address and receive signal strength of one of the nearby APs respectively.

In positioning, the current snapshot will be matched against every snapshot in the characteristics database. Euclidean displacement in signal space will be used to determine location probability and the best location is given by smallest signal displacement.

3 Result and Discussion

The objective of the paper is to compare performance between four fore-mentioned algorithms. Figure 1 shows the results achieved by each algorithms, fusion between algorithms and the best result by an ideal algorithm selector.

3.1 AP-centric Result

The result of AP-centric algorithms clearly show that weighted CG outperforms triangulation method by more than 3.1 meters in average. We concluded the reason in two categories. First, the solution space of triangulation is larger than weighted CG. Estimation made by weighted CG was always bounded within convex hull of neighbor AP. Moreover, if the global signal level fluctuates, triangulation could not adapts to the new level. Therefore, the estimation from weighted CG were more accurate than triangulation 65.36% of the time.

	W-CG	FP	SMP	Fusion
W-CG × FP	27.68%	44.29%	-	28.04%
W-CG × SMP	39.76%	-	19.05%	41.19%

Figure 2. Winning ratio of individual algorithm in fusion

3.2 Location-centric Result

On the other hand, location-centric algorithms can generally achieves better result than AP-centric approach. It was because space conversion does not exists in location-centric approach. Comparing SMP and fingerprint result, fingerprint outperforms SMP and is the best performer amongst all algorithms. Although both SMP and fingerprint use lookup function to gather list of candidates, since fingerprint use signal displacement to score candidates, global signal fading would not seriously affects the overall ranking.

3.3 Fusion Result

Apart from individual algorithm, we introduced fusion between different approaches. For each selected algorithm, a normalized weighting is chosen and the final result is given by interpolation between algorithms according to their weighting.

Both fusion surpassed all of their ancestors by 7.0 - 98.1%. But surprisingly, Figure 2 showed the winning rate of the W-CG × FP fusion result was only 28.04%. Compares to individual performance, the ratio is not significant. That means winning locations from fusion algorithm usually outruns those from individual algorithm. Nonetheless, the winner of the fusion is weighted CG fused with fingerprint. On the average, the error distance is 3 meters, which equals to width of 2 grids in our sample data.

References

[1] P. Bahl, A. Balachandran, and V. Padmanabhan. Enhancements to the RADAR user location and tracking system. Technical report, Microsoft Corporation, February 2000.

[2] S. Ganu, A.S.Krishnakumar, and P.Krishnan. Infrastructure-based location estimation in wlan networks. In *Proceedings of the IEEE Wireless Communications and Networking Conference (WCNC 2004)*, 2004.

[3] K. K.-H. Kan, S. K.-C. Chan, and J. K.-Y. Ng. A dual-channel location estimation system for providing location services based on the gps and gsm networks. In *Proceedings of the 17th International Conference on Advanced Information Networking and Applications*, pages 7–12. IEEE Computer Society, March 2003.

[4] D. Pandya. A hierarchical location tracking system project report. Technical report, Imperial College, London, 2002.

Locating Mobile Station with Ellipse Propagation Model Based on the GSM Networks

Junyang Zhou

Abstract

Mobile location estimation is drawing considerable attention in the field of wireless communications. In this report, we proposed a location estimation model that is based on the GSM mobile phone Network. A directional propagation model - Ellipse Propagation Model (EPM) is designed. The EPM assumes the contour line of signal strength resembles an ellipse with the base station at one of focus. By mapping the distance with the received signal strength using the EPM, the mobile station can be estimated. And we present two algorithms to find out the estimation of mobile station based on the Ellipse Propagation Model. We also provide a statistical estimation based on the EPM and extend the EPM into three dimension space. We have tested the EPM with real data taken in Hong Kong and it is proved that the EPM yields higher accuracy when compare with other existing location estimation algorithms in different kinds of environments.

1 Introduction

Recently, mobile location estimation is receiving considerable attention in the field of wireless communications. Many positioning technologies have been developed. The most famous location system is the Global Positioning System (GPS) [10, 12].

There are many existing positioning algorithms that is based on signal strength like [1, 2, 8, 9, 11, 14, 15]. Our group has also proposed several location estimation approaches that is based on the received signal strength (RSS) [3, 4, 7]. However, these methods have not included the directional properties. From our observations, we have found that BSs have directional property. The BSs always transmit signal in a direction. And [6, 13] present two models which consider the transmission direction, which computed the mobile location estimation based on the directional propagation model. But the algorithms mentioned above all have no self-modification property.

In this report, we present a directional propagation model – the Ellipse Propagation Model (EPM). The EPM was derived from the original propagation model [5]. We observed that the antenna transmits the signal in a direction. Thus, the contour line of signal strength is not a circle. We modify the original propagation model by considering the contour line as an ellipse with the BS at the focus. Since the RSS is the only attribute we have which is not the distances between the MS and the BS, thus, the EPM is focus on the relationship between the distance and the RSS. We present two new methods called the Geometric Algorithm and Iterative Algorithm. The Geometric Algorithm is a new method for finding out the location of mobile estimation with the propagation model. The results show that the EPM with the Geometric Algorithm is simple and accurate for different types of terrains. while the Iterative Algorithm has self-modification property, which is different with all other algorithms mentioned above, and it chooses the convergence value as the estimation. And the Iterative Algorithm has improved the Geometric Algorithm. But it needs more computational cost. And we also present a Statistical Estimation based on EPM, and extend the EPM into three dimension space.

2 The Ellipse Propagation Model

We modify the original signal propagation model as an ellipse instead of a circle. On the ellipse, it has the same signal strength in the contour line. We can get the relationship between the MS-BS distance and RSS as,

$$d = k(s_0/s)^{1/\alpha}(1-e)/(1-e\cos(\theta)) \qquad (2.1)$$

where

θ is the deviation;
s is the signal power received;
s_0 is the transmitting power of the BS;
k and α are constants.

We call this relationship as the Ellipse Propagation Model (EPM), which the contour line of the signal strength is an ellipse as illustrated in Figure 1.

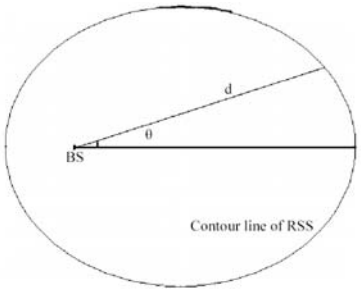

Figure 1. The Ellipse Propagation Model(EPM)

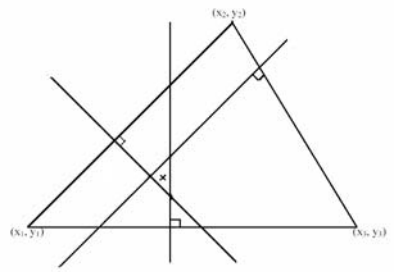

Figure 2. The geometric interpretation of the Geometric Algorithm.

3 The Geometric Algorithm based on EPM

Suppose a MS received RSS, s_1, s_2, s_3 from three BSs with locations, (x_1, y_1), (x_2, y_2), (x_3, y_3) respectively. In addition, the distance between the MS and the BSs are denoted by $d(s_1)$, $d(s_2)$, $d(s_3)$, sometimes, they are simply denoted by d_1,d_2 and d_3. Thus, by the formula of the two points distance in the 2-D Euclidian space, we can form three circles formulas which are shown as follows,

$$\begin{cases} d_1^2 = (x - x_1)^2 + (y - y_1)^2 \\ d_2^2 = (x - x_2)^2 + (y - y_2)^2 \\ d_3^2 = (x - x_3)^2 + (y - y_3)^2 \end{cases} \tag{3.1}$$

In order to give a location estimation every time, the Geometric Algorithm derive another three equation group based on the equation group 3.1. As each new equation group can find out a solution, thus, we will have three solutions. The estimation of the MS will then be the center of these three solutions. Figure 2 demonstrates the Geometric Algorithm graphically. As illustrated by Figure 2, the three points on the vertex marked by (x_1, y_1),(x_2, y_2) and (x_3, y_3) are the locations of the 3BSs, and the "cross" point is the location estimation of the MS by the Geometric Algorithm, which is the center of the three intersections.

By setting,

$$A = \begin{pmatrix} 2(x_2 - x_1), & 2(y_2 - y_1) \\ 2(x_3 - x_1), & 2(y_3 - y_1) \end{pmatrix}$$

and

$$b = \begin{pmatrix} d_1^2 - d_2^2 - (x_1^2 + y_1^2) + (x_2^2 + y_2^2) \\ d_1^2 - d_3^2 - (x_1^2 + y_1^2) + (x_3^2 + y_3^2) \end{pmatrix}$$

$$X = \begin{pmatrix} x \\ y \end{pmatrix}$$

If $|A| \neq 0$, the only solution of the matrix equation is,

$$X = A^{-1} b \tag{3.2}$$

If $|A|$ does not equal to zero, then the equation group 3.2 has a real root. As we will have three equation group similar to the equation group 3.2, thus, we will have three solutions. By calculating the center of these three solutions, we can have an estimation of the MS location.

4 The Iterative Algorithm Based on EPM

4.1 Structure of the Iterative Algorithm

By rewriting x and y as two parts, we have,

$$\begin{cases} x = f(x_0, y_0; s; l) + \epsilon \\ y = g(x_0, y_0; s; l) + \eta \end{cases} \tag{4.1}$$

where

$f(x_0, y_0; s, l)$ and $g(x_0, y_0; s, l)$ are the certain terms;
x_0 and y_0 are the estimations of x and y;
ϵ and η are random variables;
f and g are some function structures;
which have first order and second order derivatives.

Furthermore, assumed that $E(\epsilon) = 0$, $E(\eta) = 0$, $var(\epsilon) = \sigma_\epsilon^2$, $var(\eta) = \sigma_\eta^2$, $cov(\epsilon, \eta) = 0$, x_0 and y_0 are unbiased estimations. Thus, $E(x - x_0) = 0$,$E(y - y_0) = 0$.

We choose the certain terms as the estimation:

$$\begin{cases} x_0 = f(x_0, y_0; s_1, s_2, ..., s_m; l_1, l_2, ..., l_m) \\ y_0 = g(x_0, y_0; s_1, s_2, ..., s_m; l_1, l_2, ..., l_m) \end{cases} \tag{4.2}$$

Since x_0 and y_0 appear in both sides of the two equations, one can use the iterative method to find out the solution.

4.2 Using Geometric Algorithm with the Iterative Algorithm

From the Iterative Algorithm, we have,

$$x_{n+1} = f(x_n, y_n; s_1, s_2, s_3; l_1, l_2, l_3),$$
$$y_{n+1} = g(x_n, y_n; s_1, s_2, s_3; l_1, l_2, l_3).$$

So the iterative formulas become,

$$\begin{aligned} x_{n+1} &= 2[(\beta_3-\beta_2)(d_1^2(n)-(\alpha_1^2+\beta_1^2)) \\ &\quad +(\beta_1-\beta_3)((d_2^2(n))-(\alpha_2^2+\beta_2^2)) \\ &\quad +\beta_2-\beta_1)(d_3^2(n)-(\alpha_3^2+\beta_3^2))]/|A| \\ y_{n+1} &= 2[(\alpha_2-\alpha_3)(d_1^2(n)-(\alpha_1^2+\beta_1^2)) \\ &\quad +(\alpha_3-\alpha_1)((d_2^2(n))-(\alpha_2^2+\beta_2^2)) \\ &\quad +(\alpha_1-\alpha_2)(d_3^2(n)-(\alpha_3^2+\beta_3^2))]/|A| \end{aligned}$$

If (x_n, y_n) converges to one point $(\hat{x}, \hat{y})$, then $(\hat{x}, \hat{y})$ is considered to be the location estimation of the MS.

4.3 Convergence of the Iterative algorithm

The Iterative Algorithm is convergence under some conditions, and we present these conditions as a theory.

Define,

$$d(x, y, \alpha_l, \beta_l, \alpha, s, e) = (s_0/s)^{1/\alpha}(1-e)/(1-e\cos(\theta)) \quad (4.3)$$

$$de(x, y, \alpha_l, \beta_l) = \sqrt{(x-\alpha_l)^2+(y-\beta_l)^2} \quad (4.4)$$

If three circles intersected at one point, then $d(x, y) = de(x, y)$. Otherwise, we suppose that $d(x, y) \leq de(x, y)$.

Theorem 4.1 *If (α_1, β_1), (α_2, β_2), (α_3, β_3) are not in the same line, and suppose that*

$$|\frac{d_i^2(x,y)}{de_i^2(x,y)} \cdot \frac{(y-\beta_i)}{de_i(x,y)} \cdot \frac{e_i\sin(\theta_i)}{1-e_i\cos(\theta_i)}| \leq 1,$$

and

$$|\alpha_i - \alpha_i| \geq 4, if |\alpha_i - \alpha_i| \neq 0;$$
$$|\beta_i - \beta_i| \geq 4, if |\beta_i - \beta_i| \neq 0;$$

where $i \neq j$ and $i, j = 1, 2, 3$.

Then the iterative formula $\{x_n\}$ and $\{y_n\}$ have convergence.

5 The Statistical Estimation based on EPM

5.1 Introduction of the Statistical Estimation

Suppose we have two random variables x,y, which are independent to each other. They are used to describe the east and north coordinates, and their exact distributions can be known or unknown to us, for example, the value of the two variables can be distributed under the normal distribution. So the estimation can be seen as a conditional expectation of the signal and location information, denoted by,

$$x_1 = E(x|x_0, y_0), \text{ and } y_1 = E(y|x_0, y_0)$$

where (x_0, y_0) is the initial information.

We consider the second row of signal strength: s_{21},s_{22},$\cdots$, s_{2m_2}, and the corresponding location information,l_{21},l_{22},$\cdots$, l_{2m_2}. And the second estimation should have some relationship with the first one. And it can be written as

$$x_2 = E(x|x_1, y_1, x_0, y_0),\ y_2 = E(y|x_1, y_1, x_0, y_0).$$

Since we have n snapshots, so the n-th estimation can be written as

$$x_n = E(x|x_{n-1}, y_{n-1}, \cdots, x_1, y_1, x_0, y_0)$$

$$y_n = E(y|x_{n-1}, y_{n-1}, \cdots, x_1, y_1, x_0, y_0).$$

Set $D_t = \{x_t, y_t, D_{t-1}\}$, and $D_0 = \{x_0, y_0\}$, we have a series of the estimation by the above formula:

$$\begin{aligned} &x_1 = E(x|D_0), y_1 = E(y|D_0); \\ &x_2 = E(x|D_1), y_2 = E(y|D_1); \\ &\cdots \\ &x_n = E(x|D_{n-1}), y_n = E(y|D_{n-1}). \end{aligned}$$

That is, $x_n = E(x|D_{n-1})$, $y_n = E(y|D_{n-1})$ and $D_n = \{x_n, y_n, D_{n-1}\}$,for $n \geq 1$, where $D_0 = \{x_0, y_0\}$.

we call the estimation of (x_n, y_n) the statistical estimation.

5.2 Good Feature of the Statistical Estimation

Suppose $E(x_n) = x_0$ and $E(y_n) = y_0$ for $n \geq 1$.

Set $Error(n) = \sqrt{(x_n - x_0)^2 + (y_n - y_0)^2}$, and we use it as the estimation measuring criteria. Since we know that x_n and y_n are random variables from their definitions, $Error(n)$ is also a random variable. So we should compare them with their expectations.

And we have a conclusion about the error criteria as Lemma.

Lemma: If $E(x_n) = x_0, E(y_n) = y_0$, and $var(x_n) < +\infty, var(y_n) < +\infty$, then

$$E(Error(n)) \leq E(Error(n-1)).$$

So we can draw a conclusion that if n increases, then the expectation of $Error(n)$ will not increase. If we have n snapshots, then choose (x_n, y_n) where $x_n = E(x|D_{n-1}), y_n = E(y|D_{n-1})$ as the estimation will produce the best result in terms of stability.

5.3 Structure of the Statistical Estimation

We can rewrite the series of estimations mentioned in the previous section as

$$\begin{aligned}
&x^1 = f^1(x_0, y_0; s_{11}, \cdots, s_{1m_1}; l_{11}, \cdots, l_{1m_1}) + \epsilon^1,\\
&y^1 = g^1(x_0, y_0; s_{11}, \cdots, s_{1m_1}; l_{11}, \cdots, l_{1m_1}) + \eta^1,\\
&\cdots\\
&x^n = f^n(x_0, y_0; s_{n1}, \cdots, s_{nm_n}; l_{n1}, \cdots, l_{nm_n}) + \epsilon^n,\\
&y^n = g^n(x_0, y_0; s_{n1}, \cdots, s_{nm_n}; l_{n1}, \cdots, l_{nm_n}) + \eta^n,
\end{aligned}$$

We present two structures for the Statistical Estimation: one for the common average, and one for a special weighted average structure.

The average structure

$$x_n = \tfrac{1}{n}\sum_{i=1}^{n} x^i, y_n = \tfrac{1}{n}\sum_{i=1}^{n} y^i.$$

$$\begin{aligned}
f_n &= (f^1 + f^2 + \cdots + f^n)/n,\\
g_n &= (g^1 + g^2 + \cdots + g^n)/n,\\
\epsilon_n &= (\epsilon^1 + \epsilon^2 + \cdots + \epsilon^n)/n,\\
\eta_n &= (\eta^1 + \eta^2 + \cdots + \eta^n)/n,
\end{aligned}$$

The Special weighted average structure

$$\begin{aligned}
&x_1 = x^1, y_1 = y^1,\\
&x_2 = (x^2 + x_1)/2, y_2 = (y^2 + y_2)/2\ ,\\
&\cdots\\
&x_n = (x^n + x_{n-1})/2, y_n = (y^n + y_{n-1})/2
\end{aligned}$$

where

$$\begin{aligned}
&f_1 = f^1, g_1 = g^1, \epsilon_1 = \epsilon^1, \eta_1 = \eta^1;\\
&\cdots\\
&f_n = (f^n + f_{n-1})/2,\ g_n = (g^n + g_{n-1})/2,\\
&\epsilon_n = (\epsilon^n + \epsilon_{n-1})/2,\ \eta_n = (\eta^n + \eta_{n-1})/2.
\end{aligned}$$

6 Mobile Location Estimation in Three Dimension Space

6.1 the 3-D Space Ellipse Propagation Model

Suppose the location of four BS locations are known, denoted by $A(\alpha_1, \beta_1, \gamma_1)$, $B(\alpha_2, \beta_2, \gamma_2)$, $C(\alpha_3, \beta_3, \gamma_3)$ and $D(\alpha_4, \beta_4, \gamma_4)$. The RSS from them are denoted by s_1, s_2, s_3 and s_4 with the transmission powers of these BSs are s_1^0, s_2^0, s_3^0 and s_4^0,respectively. Then the attenuation powers of transmission are $s_1^0 - s_1$, $s_2^0 - s_2$, $s_3^0 - s_3$, $s_4^0 - s_4$. Let the MS location be $M(x, y, z)$, which is unknown now and it will be estimated by the above information. Given the distances between the BSs and the MS are d_1,d_2,d_3 and d_4.

We rewrite the ellipse-sphere for the three dimension polar coordinates, which can be determined by three factors: distance, horizontal angle and vertical angle, denoted by (r, θ, δ), and the transform formulas of the polar coordinates and the rectangular coordinates are:

$$\begin{cases} x = rcos(\theta)cos(\delta)\\ y = rsin(\theta)cos(\delta)\\ z = rsin(\delta) \end{cases} \tag{6.1}$$

where $\theta \in [0, 2\pi)$ and $\delta \in [-\pi/2, \pi/2)$.

We have a model:

$$r = k(s^0/s)^{1/\alpha}\frac{frac1 + frac2}{1 + \frac{e_1^2}{1-e_1^2}sin^2(\theta)cos^2(\delta) + \frac{e_2^2}{1-e_2^2}sin^2(\delta)} \tag{6.2}$$

where

$frac1 = \frac{e_1}{1+e_1}cos(\theta)cos(\delta)$;
$frac2 = \frac{1}{1+e_1}\sqrt{1 - \frac{e_1^2(1-e_2^2) - e_2^2(1-e_1^2)}{1-e_2^2}sin^2(\delta)}$;
k is proportion constant;
s^0 is the transmitting power of the BS;
s is the received signal power from the BS;
α is the path loss exponent;
$\theta \in [0, 2\pi)$ is the horizontal angle;
$\delta \in [-\pi/2, \pi/2)$ is the vertical angle;
e_1 is the eccentricity of the horizontal ellipse;
e_2 is the eccentricity of the vertical ellipse;
r is the distance between the MS and BS.

We call this relationship as the 3-D Ellipse Propagation Model (3DEPM), in which the contour surface of the signal strength is an ellipse-sphere.

If $\delta = 0$, then Eq.(6.2) can be rewritten as:

$$r = k(s^0/s)^{1/\alpha}(1 - e_1)/(1 - e_1cos(\theta)). \tag{6.3}$$

This becomes the 2-D Ellipse Propagation Model.

6.2 Structure of the 3-D Geometric Algorithm

By the formula of the two points distance in the 3-D Euclidian space, we can form four spheres formulas which are shown as follows,

$$\begin{cases} d_1^2 = (x - x_1)^2 + (y - y_1)^2 + (z - z_1)^2\\ d_2^2 = (x - x_2)^2 + (y - y_2)^2 + (z - z_2)^2\\ d_3^2 = (x - x_3)^2 + (y - y_3)^2 + (z - z_3)^2\\ d_4^2 = (x - x_4)^2 + (y - y_4)^2 + (z - z_4)^2 \end{cases} \tag{6.4}$$

For the convenience of our discussion, we just discuss one of the equation groups in detail.

By setting,

$$A = \begin{pmatrix} 2(x_2 - x_1), & 2(y_2 - y_1), & 2(z_2 - z_1)\\ 2(x_3 - x_1), & 2(y_3 - y_1), & 2(z_3 - z_1)\\ 2(x_4 - x_1), & 2(y_4 - y_1), & 2(z_4 - z_1) \end{pmatrix} \tag{6.5}$$

and

$$b = \begin{pmatrix} (d_1^2 - d_2^2) - (x_1^2 + y_1^2 + z_1^2) + (x_2^2 + y_2^2 + z_2^2) \\ (d_1^2 - d_3^2) - (x_1^2 + y_1^2 + z_1^2) + (x_3^2 + y_3^2 + z_3^2) \\ (d_1^2 - d_4^2) - (x_1^2 + y_1^2 + z_1^2) + (x_4^2 + y_4^2 + z_4^2) \end{pmatrix} \quad (6.6)$$

and

$$X = \begin{pmatrix} x \\ y \\ z \end{pmatrix} \quad (6.7)$$

If $|A| \neq 0$, the only solution of the matrix equation is,

$$X = A^{-1}b \quad (6.8)$$

We will have 20 solutions. By calculating the centroid of these solutions, we can have an estimation of the MS location.

7 Simulation Results

We compare the results of CG and CT algorithms with the algorithms we present above: The Geometric Algorithm ,the Iterative Algorithm and the Statistical estimation. And we give the mean and the standard deviation of the erros to see their estimation effect. And the results are in Table 1.

Model	Average Error	Std.	successful %
CG	335.35	319.61	92.6%
CT	321.62	229.06	81.5%
Geometric Algorithm	285.27	309.80	98.3%
Iterative Algorithm	282.68	309.05	98.3%
SE of GEPM	260.26	285.64	98.3%
SE of IGEPM	257.94	288.53	98.3%

Table 1. Compare with CG, CT Algorithm (Unit: meter)

References

[1] G.Chen and D.Kotz. A Survey of Context-Aware Mobile Computing Research. Technical report, Dept. of Computer Science, Dartmouth College, November 2000. Technical Report TR2000-381.

[2] J.Hightower and G.Borriello. Location Systems for Ubiquitous Computing. In *Computer, special issue on location-aware computing*, 8, pages 57–66, 2001.

[3] Joseph K. Ng, Stephan K. Chan, And Kenny K. Kan. Location Estimation Algorithms for Providing Location Services within a Metropolitan area based on a Mobile Phone Network. In *Proceedings of The 5th International Workshop on Mobility Databases and Distributed Systems(MDDS 2002)*, pages 710–715, Aix-en-Provence, France, September 2002.

[4] Joseph Kee-Yin Ng, Stephen Ka Chun Chan, and Shibin Song. A Study on the Sensitivity of the Center of Gravity Algorithm for Location Estimation. Technical report, Hong Kong Baptist University, May 2003. http://www.comp.hkbu.edu.hk/tech-report/tr03014f.pdf.

[5] Kaveh Pahlavan, Prashant Krishnamurthy. *Principles of Wireless Networks a Unified Approach*. Pearson Education, Inc., 2002.

[6] Kenneth M. Chu, Karl R.P.H. Leung, Joseph K. Ng, and Chun H. Li. Locating Mobile Stations with Statistical Directional Propagation Model. In *Proceedings of the 18th International Conference on Advanced Information Networking and Applications (AINA 2004)*, pages 230–235, Fukuoka, Japan, March 2004.

[7] Kenny K.H. Kan, Stephen K,C. Chan, and Joseph K. Ng. A Dual-Channel Location Estimation System for providing Location Services based on the GPS and GSM Networks. In *Proceedings of The 17th International Conference on Advanced Information Networking and Applications(AINA 2003)*, pages 7–12, Xi'an, China, March 2003.

[8] N.Bulusu, J.Heidemann, and D.Estrin. GPS-Less Low Cost Outdoor Localization for Very Small Devices. In *IEEE Personal Comm.*, 5, pages 28–34, 2000.

[9] P.Bahl, V.N. Padmanabhan, A. Balachandran. Enhancements to the RADAR User Location and Tracking System. Technical report, Microsoft Research, February 2000. Technical Report MSR-TR-00-12.

[10] Peter H. Dana. Global Positioning System Overview.

[11] P.J.Brown, J.D. Bovey, and X.Chen. Context-Aware Applications:From the Laboratory to the Marketplace. In *IEEE Personal Comm.*, 5, pages 58–64, 1997.

[12] Richard Walter Klukas, Gerard Lachapelle, and Michel Fattouche. Cellular Telephone Positioning Using GPS Time Synchronization.

[13] Teemu Roos, Petri Myllymaki, Herry Tirri. A Statistical Modeling Approach to Location Estimation. In *IEEE Transactions on Mobile Computing*, volume 1 of *1*, pages 59–69, January-March 2002.

[14] T.S.Rappaport, J.H.Reed, B.D.Woerner. Position Location Using Wireless Communications on Highways of the Future. *IEEE Comm. Magazine*, 34:33–41, 1996.

[15] U.Leonhardt. *Supporting Location-Awareness in Open Distributed Systems*. PhD thesis, Dept. of Computing, Imperial College, London, May 1998.